UNIVERSITÀ DEGLI STUDI DI MILANO
FACOLTÀ DI FARMACIA

Dottorato in chimica del farmaco (XXV ciclo)

Proteomic Approaches in Drugs and Biomarkers Discovery

Coordinatore: Chiar.mo Prof. Ermanno VALOTI
Tutor: Prof.ssa Marina CARINI
Co-tutor: Prof. Sergio ROMEO

Dr. Andrea PANCOTTI
Matricola n°: R08811

Index

Preface

Proteomics is the high-throughput characterization of the global complement of proteins in a biological system using cutting-edge technology (robotics and mass spectrometry) and bioinformatics tools (Internet-based search engines and databases).

In the early 1990s, the world of the protein biochemist was transformed by a series of technological development such as: new mass spectrometers (MS) , available bio-information and database containing protein and DNA sequences on the Internet, engines that enable MS data content to be rapidly compared with *in silico* versions to provide a protein identification.

Now it is possible to analyze thousands of proteins with minimum sample preparation in automated high-throughput workflows. This revolution became known as proteomics which, in 1994, was defined by Marc Wilkins as " the examination of a complete set of proteins synthesized by a cell under a given set of physiological or developmental conditions"[1].

Nowadays various range of proteomics strategies have evolved to answer specific problems.

In particular, during my PhD studies, I focused my attention on the development and applications of proteomic approaches in two fundamental research areas.

The first part of this thesis, is about proteomic applications in drug discovery (chemical proteomics). It is a useful tool to identify the target of a new class of antimalarial compounds that I have synthesized during my undergraduate thesis. Chemical proteomics is a currently emerging field with the mission to identify and validate target protein that directly binds with a binder such as a bioactive small molecule in a rapid, systematic and comprehensive manner by design, synthesis and application of relevant chemical probes. As a multidisciplinary science, chemical proteomics proposes the integration of tools and technologies from a variety of disciplines (chemistry, biochemistry, biology, proteomics and informatics). Thus, an integrated strategy in chemical proteomics can provide the information about the binding site of a bioactive small molecule in its target protein and, importantly, it could be the starting point to develop the drug screening system based on the structure of target protein[2].

The second part of this thesis, is about proteomic approach in biomarker discovery that could be an useful tool for biomarker identification, that can be used as measurements within clinical studies and for the purpose of predictive diagnosis. In particular the aim of my research will be the detection and quantization of post-translational modifications of proteins caused by oxidative and carbonyl stress. While the development of specific antibodies against modified proteins has made possible to confirm the occurrence of oxidative stress in vivo and

its involvement in several physio-pathological conditions, the resultant chemical modifications of proteins has not yet been explored. Hence we need proteomic tools, which can sensitively detect oxidative damage on peptides and proteins: these tools would be helpful to understand exactly when, how, and where the damage occurred, and to explore the mechanism of onset, progression, and/or complications of the diseases.

Part I

Proteomic approaches in drug discovery

1. Introduction

1.1 Malaria

Malaria has a massive impact on human health, being one of the major disease in the world causing in 2010 approximately 655,000 deaths[3].

It is an infectious disease caused by the protozoa of the genus *Plasmodium*. There are at least 150 species of malarial *plasmodia* which parasitize vertebrate hosts, such as reptiles, birds, primates and humans, but every kind with his own specific parasite. The species of *Plasmodium* which cause malaria in humans are four: *P. vivax, P. ovale, P. malariae* and *P. falciparum*.

It is estimated that every year 243 millions of people have been affected by this disease, with 93% of cases due to *P. falciparum*, the agent that causes the most severe form of malaria[4]. In recent years, the progress made to fight the spread of malaria has been remarkable, especially through the use of mosquito nets and new treatments, despite that about half of the global population risks the infection. Moreover in 108 countries the disease is endemic (Figure 1)[4].

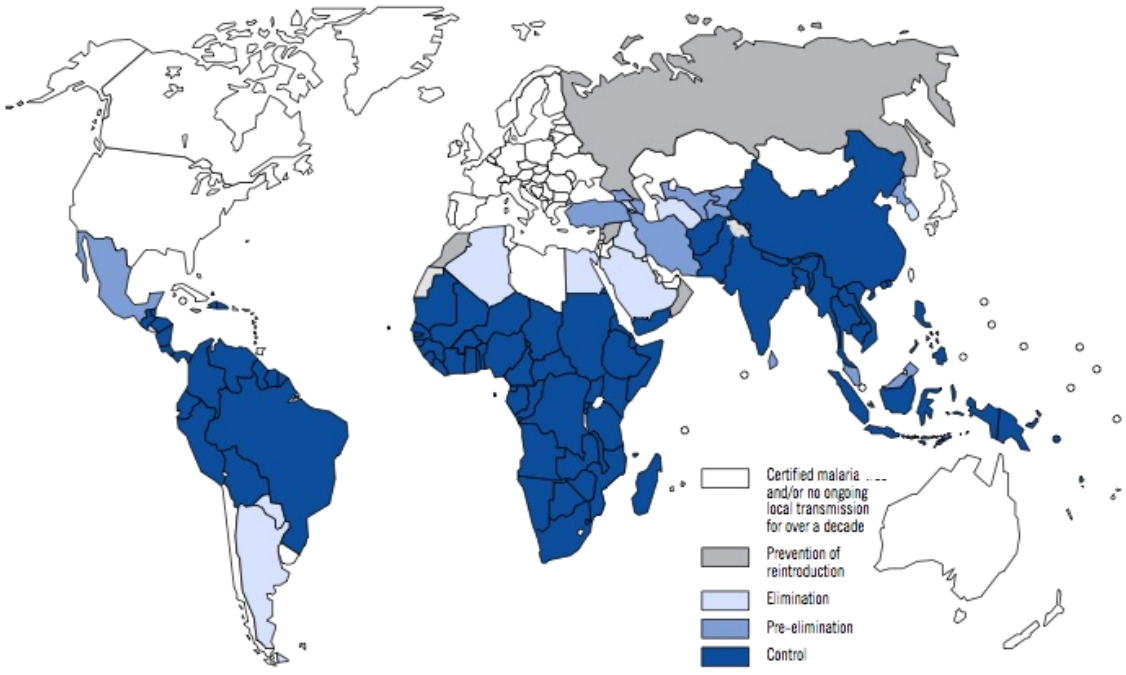

Figure 1: Countries where malaria is endemic under control, pre-elimination, elimination and prevention against reintroduction.

According to the World Health Organization's data, 91% of the deaths due to malaria involved the regions of Africa (particularly sub-Saharan Africa), where the most affected people were children under 5 years and pregnant women[3].

Although malaria is the first cause of death in Africa, also Asia, (limited to West Asia and Middle East) and Latin America are considered high-risk areas[5].

Malaria has been defeated in many countries as United States of America and European Union, but even in these areas are reported cases related mainly to immigrants or tourists coming back from infection risk areas[4].

The geographical distribution of the disease is linked to climatic factors such as temperature, humidity and rain, in fact the ideal places for mosquito breeding are the tropical and subtropical regions.

Malaria is considered one of the "poverty diseases" because it shows epidemiology associated with poor economic, social and health conditions typical of the countries in development. The population at risk of malaria infection lives in the poorest countries of the planet, where the annual per capita income is less than $ 400 USA[6].

The disease is also a real cause of impoverishment: in countries with high transmission, malaria causes an average loss of 1,3% economic annual growth [7]. Over time, this loss leads to substantial differences between the PIL of the countries in which malaria is endemic and those where it has been defeated[7].

The direct costs of malaria include public and private spending for prevention and treatment of the disease. In some countries, malaria is the cause of 40% of public health expenditure, 39-50% of hospital admissions and 60% of day care consults.

In the most affected regions, the infection has a direct impact on human resources because hinders social development and decreases school attendance and so the learning attitude[4]. The majority of imported malaria cases are reported in the European Union, in particular in France, the United Kingdom, Germany and Italy. Every year between 10,000 and 12,000 cases of imported malaria are reported[4].

For over 50 years alkaloids of *cinchona* and their derivatives have been used to control malaria. Chloroquine has been one of the most effective anti-malarial drugs ever produced. However, resistance to chloroquine by *Plasmodium falciparum* was manifested for the first time in South East Asia and South America, and now has spread to Africa and Asia. This has led to a global resurgence of malaria.

Currently these alkaloids are replaced by terpene *Artemisia Annua*.

The Artemisinin, a very effective antimalarial and expensive compound, quickly became the first drug to be used when other therapeutic approaches were unsuccessful. Unfortunately, in some regions, the parasite is developing resistance even against Artemisinin[8]. Therefore, there is a huge need to develop new antimalarial agents that, compared to traditional drugs, will be active against these resistant strains with improved pharmacokinetic properties, fewer side effects and lower costs.

1.2 Life cycle of the parasite

Malaria is usually transmitted from person to person almost exclusively by a female mosquito of the genus *Anopheles*, while there are rare cases of accidental transmission due to blood transfusions or use of contaminated syringes.

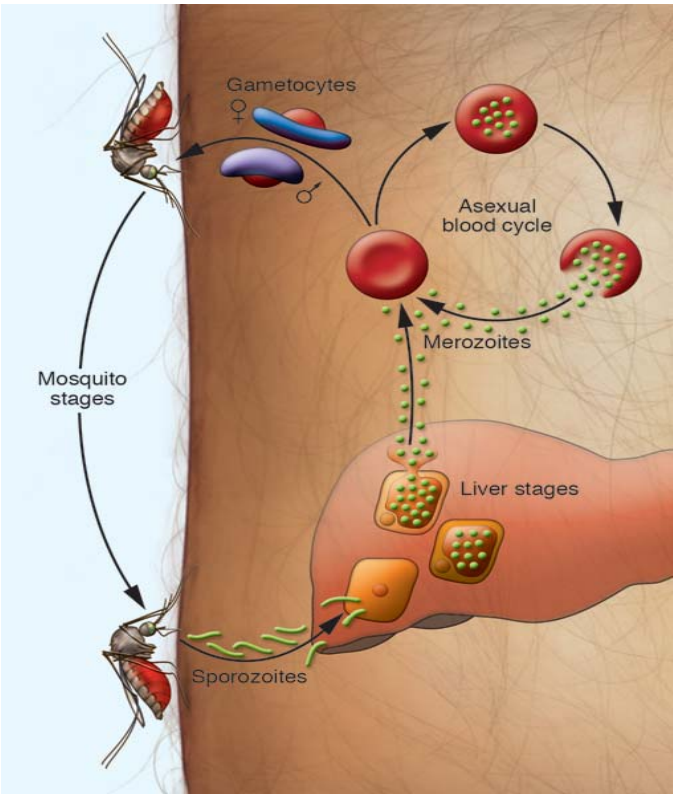

Figure 2: *Plasmodium* life cycle

The infected mosquito transmits malaria to everyone who can bite during its life cycle, inoculating, along with saliva, the infectious forms of the parasite named sporozoites. The sporozoites remain in circulation for less than half an hour, then move into the liver, in the parenchymal cells. This phase is called "hepatic phase". During this phase the sporozoites undergo a first cycle of asexual multiplication with the production of plurinuclear schizonts which are divided into many intracellular mononuclear merozoites. After that the infected hepatocytes break and release merozoites into the blood stream. The merozoites stick together to the red blood cell membrane starting a new phase called "red cell cycle", the second asexual cycle. The merozoite turn in trophozoite and it is recognizable under the microscope due to typical ring shape of the trophozoite. The trophozoites initially grow feeding on the hemoglobin, then split up itself and reach the stage of schizont. After a series of nuclear

divisions, the erythrocytes are broken and release numerous merozoites (from 6 to 36 per schizont) which start a new invasion cycle in other red blood cells.

The symptoms of malaria are characterized by febrile (coinciding with the breakdown of red blood cells and the subsequent invasion of new erythrocytes), chills, splenomegaly and anemia.

Depending on the *plasmodium* kind infecting, the cycle repeats at regular intervals: in cases of *P. falciparum* (malignant tertian malaria), *P. ovale* and *P. vivax* (benign tertian malaria) every 48 hours, while in the case of *P. malariae* (malaria quart) every 72 hours. The destruction of the red blood cells causes anemia, while their aggregation and adhesion in several vital organs microvasculature leads to a blockage of blood vessels, causing a decrease of oxygenation of organs such as liver, kidneys or, in the case of *P. falciparum*, brain (cerebral malaria), causing the death[7].

In *P. vivax* and *P. ovale* hepatic parasites persist in the form of hypnozoites to generate, after months or years, new infections of red blood cells, known as "malarial relapse." Some trophozoites transform into male and female gametocytes (erythrocyte gendered forms). When a mosquito bites an infected person, ingests these sexual forms that, in the stomach mate (cycle "sexed" or "sporogonic") to produce numerous oocyst. The oocyst become sporozoites and accumulate in the salivary glands of the vector. When the *Anopheles* mosquito bites a new individual, it is capable of transmitting malaria to the subject.

1.3 Pathogenesis

The growth of the parasite causes significative changes in the host red blood cell (RBC), that have been studied for many years and are the most apparent cause of pathogenic events. On the erythrocyte membrane there are protuberances called "Knobs", consisting in specific proteins of the parasite (HRP-"histidin rich protein"), and red blood cell that mediate adhesion of parasitized RBCs on vascular endothelium causing the formation of so-called "rosettes" (aggregates composed by a parasitized red blood cell surrounded by RBC not parasitized and 4-hydroxynonenal [4-HNE]) [9]. The phenomenon of adhesion and occlusion of capillaries together with the high production of inflammatory factors, such as NO and TNF, is responsible of tissue damage, hypoxia and metabolic acidosis that characterize cerebral malaria and cause seizures, coma and death[10].

Anemia, that can be established in cases of severe malaria (SMA), is a frequent complication of malaria caused by *P. falciparum* due to the loss of parasitized or not parasitized erythrocytes and erythropoiesis inhibition[11].

The RBC loss is a process not yet fully understood and may be affected by the formation of rosettes.

The inhibition of erythropoiesis can be characterized by: a reduction of the number of circulating reticulocytes, a normal or increased production of erythropoietin (EPO) and the altered morphology of erythroid precursors[12, 13].

The erythropoiesis takes place in the eritroblaste islands that have inside a macrophage which supplies iron, cytokines, chemokines and grow factors to the erythroblasts that surround it[14].

The analysis of the bone marrow (BM) of individuals died for anemia caused by severe malaria, showed that macrophages of eritroblaste islands contain the malarial pigment called hemozoin (HZ), that derives from the crystallization of heme molecules (β-hematin) together with a substantial amount of polyunsaturated fatty acids (such as arachidonic acid), which are not enzymatically peroxidized and split up to form the complex HZ-Fe and the terminal hydroxyaldehyde such as 4-hydroxynonenal (4-HNE) [15].

It has been observed that there is a relationship between the large number of BM macrophages loaded of hemozoin, the morphological abnormalities of the RBC, the reduction of reticulocytes and the severity of malaria.

HNE is a highly bioactive molecule able to bind covalently with nucleophilic portions of macromolecules such as proteins and DNA, generating cell damage and subsequent death due to necrosis and apoptosis.

Recently it has been demonstrated that monocytes containing hemozoin inhibit the growth of surrounding erythroid cells and produce HNE that, spreading to adjacent cells, generates protein adducts able to interact with the cell cycle without causing apoptosis, in particular by modifying the proteins p53 and p21[15].

Furthermore, hemozoin and HNE are able to inhibit the expression of certain key proteins of normal erythropoiesis, such as transferrin receptors, interleukin-3 and erythropoietin[16].

1.4 Degradation of hemoglobin

The degradation of human hemoglobin is one of the metabolic processes essential for parasite's survival. In the intraerythrocytic phase of its life cycle, the merozoite reproduces itself asexually in red blood cells, requiring a significant amount of nutrients to survive and to proliferate[17]. The parasite does not possess the ability to synthesize amino acids *de novo*, thus the host hemoglobin's catabolism becomes the main source of amino acids. The parasite uses these mechanisms not only for protein synthesis, but also to ballast the intracellular osmolarity during its replication and its development into erythrocytes[18;19]. Inside the parasite digestive vacuole, a lysosomal specialized organelle which presents a pH between 5.2 and 5.6[20], occurs the hemoglobin degradation process. Many proteolityc enzymes[21] are involved in the degradation process, including aspartic proteases (plasmepsin), cysteinic proteases (falcipain), metallo proteases (falcilysine), a dipeptidyl aminopeptidase1 (DPAT1) and histo-aspartic protease (HAP) [22,23] **(Figure 3)**.

Studies show that Plasmepsins (Plm I; Plm II) perform the first cleavage of hemoglobin between Phe33-Leu34 producing large peptide fragments. These fragments are then cut by a cysteinic protease called falcipain. Falcilisine and DPAP1 degrade these new peptides into smaller fragments which are subsequently hydrolyzed to amino acids by aminopeptidase. During the degradation of hemoglobin, the heme is released [Fe (II)] and is oxidized to hematin [Fe (III)].

In mammals, the hematin is degraded by the heme oxygenase/reductase and the biliverdin. The malaria parasite has developed its own way of hematin detoxification by the conversion into a black substance, insoluble and crystalline, known as "malaria pigment" or hemozoin. It has been shown that at least 95% of the heme released from hemoglobin is converted into hemozoin.

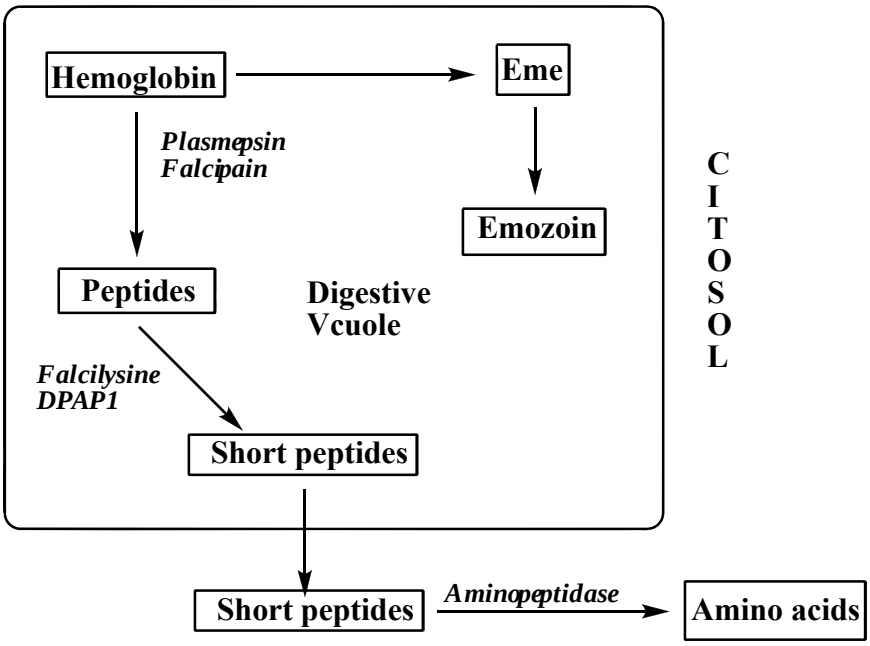

Figure 3: Hemoglobin degradation

Plasmepsin

Into the *P. falciparum* digestive vacuole have been identified 3 different aspartic proteases: the plasmepsin I (Plm I), the plasmepsin II (Plm II) and the plasmepsin IV (PlmIV) and a histo-aspartic protease (HAP), which are all involved in the degradation of hemoglobin. The four plasmepsins are highly homologous to each other, sharing more than 60% amino acid identity. On the contrary HAP is unique in its kind, because it has histidine in place of the first canonical aspartic acid, but it is still an active protease that may function like an aspartic or serine protease mechanism[17].

It has been proved in vitro the importance of aspartic proteases during the erythrocytic stage: inhibiting these enzymes with plasmepsin inhibitors, the parasite growth can be blocked. Observing the growth of plasmodia knock-out for plasmepsin genes, either in culture rich of nutrient or with a limited availability of amino acids, was detected a decrease in parasites growth[17].

Thanks to these observations, plasmepsins are considered interesting targets, suitable for the development of drugs able to overcome the problem of resistance. The research focused mainly on the identification of new plasmepsin II inhibitors, because the enzyme can be produced in large quantities by *E. coli* and, after purification, reported in enzymatically active conformation.

Each plasmepsin has a different cleavage specificity and it demonstrates the existence of a

synergistic mechanism[17]. So the use of selective agents is restricted, requiring the development of inhibitors active against each one of the four plasmepsins[24]. A different approach could be to obtain inhibitors of the enzyme responsible for the maturation of the pro-plasmepsin. As matter of fact recent studies demonstrated that only one enzyme is responsible for the cleavage of all pro-plasmepsins[17].

Falcipain

Using inhibitors of proteases cysteinic, such as Leupetina and E-64[25;26], it has been demonstrated that these proteases have a fundamental role in the hemoglobin degradation, because their inhibition causes the block of the catabolic process.

The most studied family of cysteine proteases in *P. falciparum* is falcipain. The genomic sequence shows that there are four types of falcipain: falcipain-1, falcipain-2, falcipain-2 ' and falcipain-3. There is little homology between the falcipain-1 gene and the other three falcipaines (about 40%), while falcipaine-2 and 3 have a sequence much more similar (about 80%).

Recently falcipain-2 has been isolated and it has been demonstrated that it is responsible for more than 90% of the activity of proteases cysteinic identified in the trophozoites lysate[27]. Every falcipain is expressed at different stages of the parasite life cycle, in fact falcipain-2 and falcipain-3 are expressed into the trophozoite stage, while falcipain-1 is expressed into the merozoite stage[28].

Falcipain-2, being able to hydrolyse the proteins of the cytoskeleton of erythrocyte, is necessary for the release of merozoites that rapidly invade other red blood cells to repeat the asexual cycle. It has been demonstrated that the inhibition of protease cysteineynic involves the failure of the erythrocyte lysis, which completes the erythrocytic cycle of *Plasmodium*.

1.5 Antimalarial therapy

The first active drug used for the treatment of malaria was the bark of the *Cinchona* plant, discovered in Perù in 1600 and imported to Europe by the Jesuits. In 1800 in France, chemists Pelletier and Caventou isolated in pure form quinine from the *Cinchona* bark. The Dutch cultivated *Cinchona ledgeriana* in large plantations in their colonies in Indonesia. The bark of *Cinchona* alkaloids contains other anti-malarial drugs (quinidine, cinchonine, cinchonidine) but the most used was quinine. For centuries, despite of its side effects, quinine remained the only anti-malarial drug used. During the World War I, the blockade of ports and submarine attacks hindered the supply of quinine, so it was necessary to synthesize new antimalarial drugs, such as pamaquine, primaquine and mepacrine. The need to protect the American troops in the Pacific during the World War II, encouraged the development of new antimalarial drugs. In fact after World War II it has been discovered chloroquine, amodiaquine, pyrimethamine and proguanil (used for prophylaxis).

As chloroquine resistance appeared in South America and South East Asia in 1960, associations of sulfonamide with pyrimethamine and quinine with tetracycline were then used. During the Vietnam War at the U.S. Army Research Institute "Walter Reed" was discovered mefloquine, but unfortunately mefloquine resistance appeared soon in Thailand. Thus was observed that in traditional Chinese medicine for many years was used an extract of *Artemisia annua* for the treatment of fevers. So in 1971 it was extracted from this plant artemisinin, a drug with no resemblance to the previous antimalarials, and were subsequently synthesized the artemether, artesunate and arteetere. Currently there are continuous studies in order to discover and synthesize antimalarial drugs more effective and safe. The set of compounds is shown in **Table 1.1** In the second half of the 20th century, the most used drug for the treatment of malaria was chloroquine (CQ). In recent years, the widespread and indiscriminate use of all antimalarials has prompted the development of parasites with high levels of resistance to all classes of drugs.

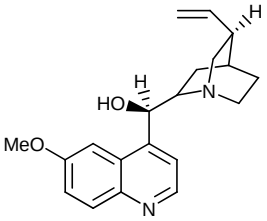

Quinine

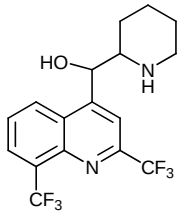

Mefloquine

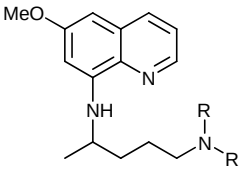

R= C_2H_5 : **Pamaquine**
R= H : **Primaquine**

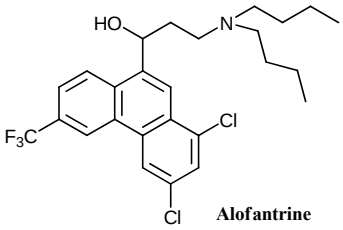

Alofantrine

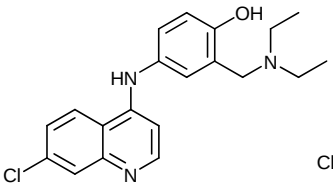

Amodiaquine

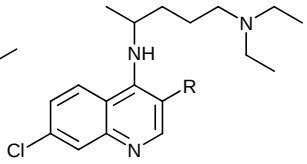

R= CH_3 : **Sontoquine**
R= H : **Cloroquine**

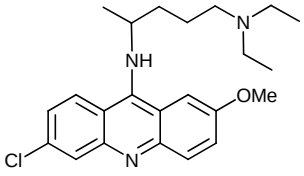

Mepacrine

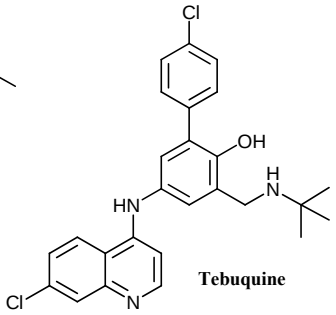

Tebuquine

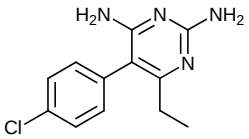

Pyrimethamine

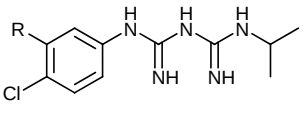

R= H : **Proguanil**
R= Cl : **Cloroproguanil**

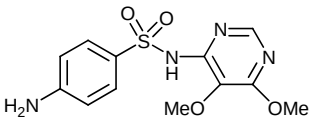

Sulfadoxine

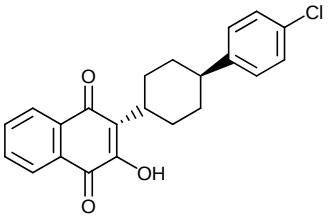

Atovaquone

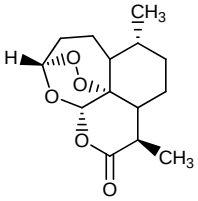

Artemisinin

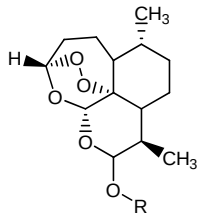

R= CH_3 : **Artemetere**
R= $COCH_2CH_2COONa$: **Artesunate**

Table 1.1

1.6 Action mechanism of the main antimalarial agents

Chloroquine

A selective accumulation of chloroquine was observed in the digestive vacuole of the parasite, where the degradation of the hemoglobin takes place.

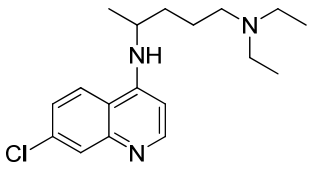

Cloroquine
IC_{50}: 39-49 nM (D10); 965-1536 nM (W2)

The weak basic properties of chloroquine can explain this accumulation: at neutral pH chloroquine diffuses easily through the membranes as free base, but at the acidic pH of the digestive vacuole chloroquine is protonated and can no longer diffuse outwards. The chloroquine prevents the polymerization of hematin (H_2O/HO-Fe (III) PPIX) to hemozoin or β-hematin ([Fe (III) PPIX] 2) through the formation of an adduct π – π with the hematin that is toxic for the plasmodium. The toxicity of this complex leads to oxidative stress due to the peroxidation of membrane lipids of the parasite and subsequent death of the parassite.

Artemisinin

Artemisinin is an endoperoxide sesquiterpene isolated from *Artemisia Annua* which is characterized by a high activity against *P. falciparum*.
The compound was already known and well documented in medical treatises such as the "Compendium of Materia Medica" written in 1596[29].
The dihydroartemisinin is an antimalarial compound characterized by a seven times higher activity against *Plasmodium* that has been obtained by the reduction of artemisinin[30].

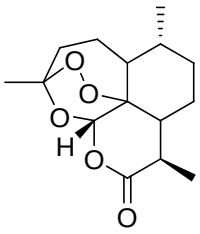

Artemisinin IC_{50}: 13 nM (D10); 9nM (W2)

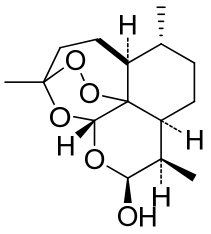

Dihydroartemisinin

Changing the lactone system it has been developed the first generation of artemisinin, including artemeter[31], arteeter[32, 33] and artesunate[34, 35].

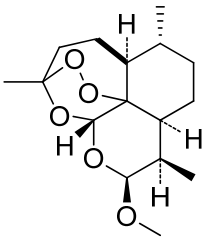

Artemeter

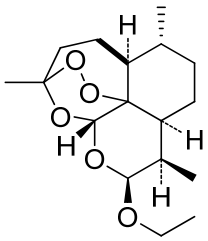

Arteeter

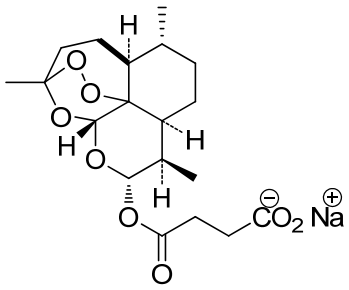

Na Artesunate

Artemeter and arteeter are lipophilic compounds and have a higher intramuscular bioavailability, while the artesunate is soluble in water and generally is administered intravenously. These analogs are safe, able to rapidly reach active blood concentrations and active towards the *P. falciparum*. They are generally administered in combination with a long-term antimalarial drug[36].

The mechanism of artemisinin has not been clarified yet, but it could be due to an interaction of the molecule endoperoxydase function with the heme group (resulting in the degradation of hemoglobin), followed by the formation of free radicals capable of alkylating various biological targets[37,38].

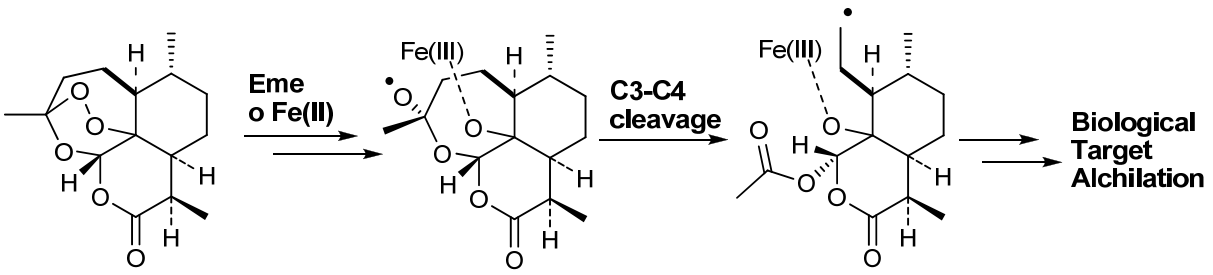

The possible presence of multiple targets can explain the delay in the resistance diffusion.

Atovaquone

Atovaquone is a derivative hydroxy-1,4-naftochinonico, that is a highly lipophilic molecule, with a very low water solubility and high metabolic stability.

Usually is associated with proguanil (Malarone) against chloroquine-resistant strains of *Plasmodium*, while the resistance against *P. falciparum* rapidly occurs if used alone[39].

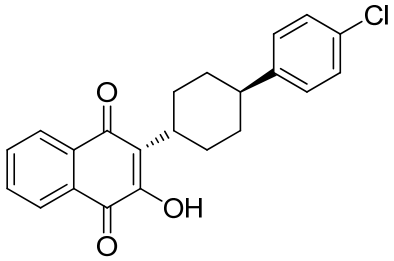

Atovaquone IC_{50}: 0.3 nM (D10); 0.43 nM (W2)

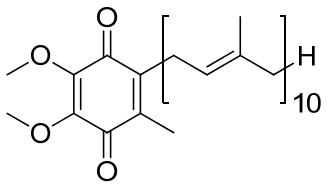

Ubiquinone

Atovaquone is characterized by a mechanism that could explain why its resistance may arise quickly in malaria parasites[40]. The drug acts by inhibiting mitochondrial electron transport at the level of cytochrome *bc*1 complex in malaria parasites at 100-fold lower concentrations than effective for the mammalian mitochondria. In fact, this molecule has a similar structure to ubiquinone (also called coenzyme Q), an essential component of the electron flow in the aerobic respiration; ubiquinone accepts electrons from the enzyme dehydrogenase and donates them to cytochromes involved in the electronic transport chain[40;41]. The passage of electrons from ubiquinone to cytochrome *bc*1 (complex III) requires binding of coenzyme Q complex III at the Qo cytochrome domain; this step is inhibited by atovaquone. The structure of the Qo cytochrome binding site has been defined and explains the selective toxicity of atovaquone to parasitic mitochondria[40;42].

Several parasite enzymes are linked to the mitochondrial electron transport system and are inhibited. Among these enzymes, there is the dihydroorotate dehydrogenase (DHOD), which is required in the biosynthesis of pyrimidines. As plasmodia is unable to scavenge pyrimidines for DNA synthesis and it is required to synthesize them de novo, inhibition of DHOD results in parasite death[40;43].

1.7 Combination therapy

Since parasites developed resistance to most of the existing drugs, it is considered a new therapeutic strategy to fight morbility and mortality due to infection by *P. falciparum*: the combination of two or more antimalarial drugs against different targets, with additive or synergistic action. The ultimate goal is the effective elimination of the parasite in the shortest time, considering that two drugs in combination may have different characteristics.

The half-life is an important parameter to be considered, in fact if the component with a low half-life can eliminate most of the parasites (such as artemisinin and its derivatives) and have a short effect, the second compound, with a long half-life (eg. mefloquine and lumefantrine) is able to eliminate few parasites, should have a low risk of developing resistance[44]. Although the combination sulfadoxine-pyrimethamine is excellent and has good activity against *P. falciparum*, the long half-life of the active ingredients involves the development of resistance, especially in areas of high transmission, such as in eastern Africa[44]. Studies demonstrated that the synergistic interaction between atovaquone and proguanil (Malarone), is also active against *P. falciparum* chloroquine resistant strains. The association between cicloproguanile and dapsone (Lapdap) is another combination used in clinical study.

The artemisinin and its analogues are frequently used in combination therapy due to their excellent chemical-physical properties like rapid-action, short half-life, limited toxicity, activity towards multi-drug resistant strains.

Artemeter and lumefantrine in combination (Coartem) are effective against *P. falciparum* multidrug resistance and present no serious side effects. Other interesting combinations are artesunate (similar to artemisinin), with mefloquine, sulfadoxine-pyrimethamine or dapson-cloroproguanile[36;45]. However in 2006, it has been reported the first case of resistance to artemisinin on the border between Thailand and Cambodia[46].

In 2011, the European Medicines Agency has approved Eurartisim, association of Diidroartemisin-piperaquine, developed by Italian Sigma-Tau in collaboration with Medicines for Malaria Venture.

1.8 Resistance

The number of deaths caused by malaria have increased due to the resistance of *P. falciparum* against quinolines and in particular chloroquine [47]. The areas characterized by the presence of parasites resistant to chloroquine or mefloquine are represented in **Figure 4**.

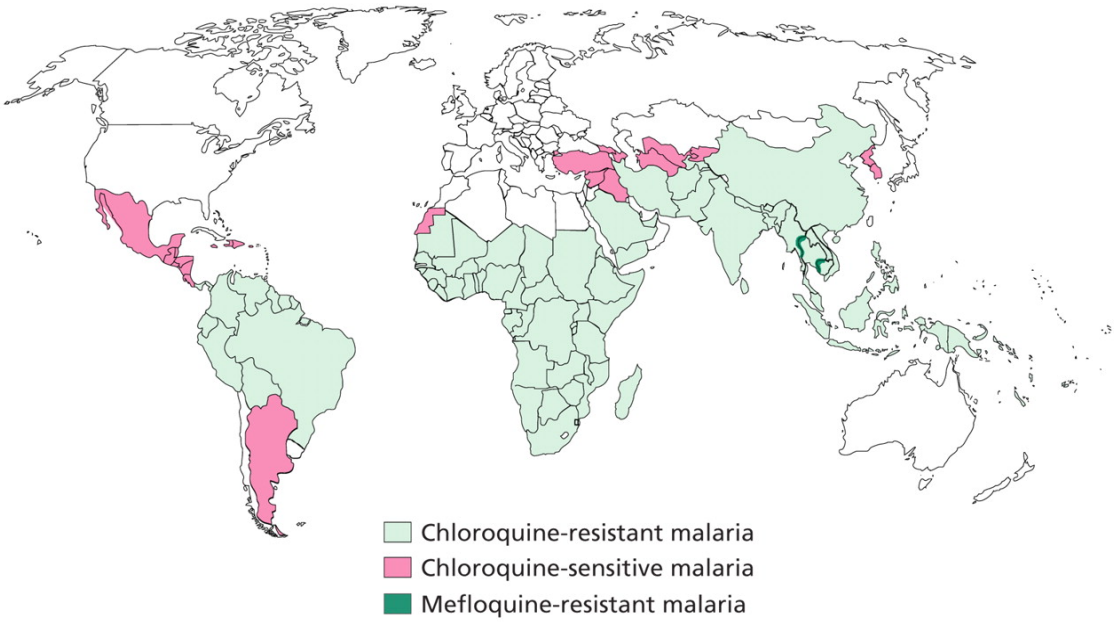

Figure 4: Zone of resistance

Chloroquine resistance is associated with the reduction of its accumulation inside the digestive vacuole[47].

Both genetic and biochemical studies have attempted to explain why parasites become resistant to chloroquine.

These theories include:

- the alteration of the Na^+/H^+ pump which causes an increase of the cytoplasmic pH and a reduction of the uptake of chloroquine[48];
- the gene Pfmdr amplification that involves overexpression of the protein Pgh-1, causing the drug loss;
- digestive vacuole membrane mutations: *P. falciparum* cloroquine resistance transporter (PfCRT).

However only the mutation of Pgh-1It is not enough to confer resistance to the parasite but other mutations are necessary.

Rowena E. Martin et al. in their recent studies showed the correlation between the PfCRT mutations and the chloroquine resistance[49]. This protein is localized in the digestive vacuole membrane and has 10 transmembrane domains.

When the mutation of this protein occurs, in particular at Lys76 and Thr (K76T), it causes the modification of the first transmembrane domain and significant increase of chloroquine resistance is observed. *Reed et al.* have shown that the mutation of the protein Pgh-1 contributes not only to the chloroquine resistance but also to a modulation of the resistance to other compounds such as mefloquine, alonfantrine and quinine[50].

Compounds strictly analogous to chloroquine are active on chloroquine-resistant strains, thus demonstrating that the resistance is not attributable to target changes, but is compound-specific.

Therefore, the chloroquine resistance can be overcome, realizing compounds able to act on drug outgo protein, or developing quinoline derivatives, agents with the same mechanism of chloroquine, which are not recognized by the transport protein.

Mitochondrial DNA (mtDNA), with 6 kb of length, is quite unusual in malaria parasites and is the shortest mtDNA known[40;51]; it is also highly conserved. It encodes for only three proteins (subunits I and II of cytochrome oxidase c and cytochrome b).

It has been observed that the resistance to various cytochrome bc1 complex inhibitors is characterized by mutations in a defined region coding for the cytochrome b sequence and diversity in these positions may concern the different toxicity of antimalarial idroxyinaftoquinonic[40;51].

The region of the cytochrome b implicated in the mechanism of resistance is part of the catalytic domain, the site Qo, in which ubiquinol is oxidized by the complex bc; in particular, the mutations observed in *P. yoelii* resistant covers a region of 15 amino acids surrounding the highly conserved sequence of the cytochrome PEWY B[40;41;52]. Mutations alter the hydrophobicity and the volume of the part of the binding cavity: therefore even slight variations can affect the affinity of atovaquone towards cytochrome bc1[40]. The resistance to atovaquone rapidly onset in malaria by *P. falciparum* when it is used as a single agent and experimental evidence have shown that parasites that become resistant to atovaquone are also resistant to the synergistic effects of proguanil, thus making the association weak[40].

Even combinations of two or more drugs may present resistance, especially combinations with long half-life drugs such as sulfadoxine and pyrimethamine.

1.9 Resistance to Artemisinin

Combination therapy based on derivatives of artemisinin or ACT (artemisinin combination therapy) provides an important alternative to quinoline derivatives.

The resistance to quinoline compounds has emerged on the border between Thailand and Cambodia and later spread worldwide. This has seriously affected their employment and has contributed to a dramatic increase in mortality due to malaria before the introduction of ACTs at the end of the last century[53].

In the last decade almost all countries with endemic malaria have adopted a combination therapy of artemisinin derivatives for the treatment of *P. falciparum* malaria. The artemisinin has a very short half-life and is rapidly eliminated from the body due to glucuronidation by CYP 2B6[8]. For this reason, this molecule is usually associated with long half-life antimalarial drugs such as piperaquine and amodiaquine[8]. In 2006 was registered the first case of resistance to artemisinin in Ta Sanhal, a small city near the border between Thailand and Cambodia.

The cause of resistance to artemisinin in South-East Asia has been assigned to the widespread use of this drug in monotherapy[53].

The 'World Health Organization' (WHO), even before the artemisinin resistance has been reported, banned artemisinin monotherapy to delay the development of resistance and protect these important derivatives for antimalarial therapy.

Although Vietnam has been the country that used artemisinin monotherapy in South East Asia for the longest time, surprisingly it was not the first country to develop resistance.

In fact, in Vietnam, artemisinin is used to control malaria since 1989, and although current national guidelines recommend to use ACT, artemisinin and artesunate monotherapy are still widely available through the private sector (pharmacies and shops). Vietnam is also one of the few countries where artemisinin monotherapy leaded to a highly successful program for the malaria control.

The cases of malaria in the country fell sharply from 1,672,000 with 4,650 deaths in 1991, 91,635 clinical cases with 43 deaths in 2006[53].

Current data suggest that resistance to artemisinin is simply a natural consequence of the massive use of ACTs in South East Asia[46].

Since when the resistance to artemisinin has been observed for the first time in 2006, the WHO started an ambitious campaign to contain the problem of resistance along the border

between Thailand and Cambodia. These efforts included detection and early treatment of all malarial infections on both borders, preferably with a therapy that is not based on ACTs.
Thus follows the distribution of insecticide-treated nets to reduce malaria transmission and a more detailed mapping of the spread of resistance to artemisinin.
History teaches us that the border between Thailand and Cambodia has always been a hot spot for the development of resistance to antimalarial drugs and that it can emerge independently in other parts of the world[53].
The possibility that the parasite can develop resistance to artemisinins could be a catastrophe for overall health, because currently there are no drugs that can replace artemisinin, and it may take five or more years to find drugs equally effective and safe[8].

1.10 Chemical proteomics

Chemical proteomics is a currently emerging field with the mission to identify and validate target protein that directly links with a binder such as a bioactive small molecule in a rapid, systematic and comprehensive manner by design, synthesis and application of relevant chemical probes. As a multidisciplinary science, chemical proteomics proposes the integration of tools and technologies from a variety of disciplines (chemistry, biochemistry, biology, proteomics and informatics). Thus, an integrated strategy in chemical proteomics can provide the information about the binding site of a bioactive small molecule in its target protein and, importantly, it could be the starting point to develop the drug screening system based on the structure of target protein[2].

Chemical proteomics comes in two different methods: (i) activity based probe profiling (ABPP), which focuses on the enzymatic activity of a particular protein family, and (ii) a compound-centric approach, which focuses on characterizing the molecular mechanism of action of an individual bioactive small molecule. Thus, they also serve different purposes. ABPP detects members of a defined class of enzymes that are active under certain conditions for example, in a disease. This method can lead to the identification of new proteins with the respective biochemical activity, or it can be applied to determine the selectivity profile of drugs targeting an enzyme family via pretreatment of the lysate with the drug of interest and subsequent labeling and identification of the remaining enzymes using appropriate reactive probes.

Compound-centric chemical proteomics consists of classical drug affinity chromatography that is similar to the method used for decades but that is now performed in combination with modern high-resolution mass spectrometry (MS) analysis and statistics or bioinformatics for subsequent identification of binding proteins. This approach benefits from the tremendous technological developments in the MS field during recent years, particularly with regard to sensitivity and throughput. The development of nano-electrospray ionization (ESI) and methods for quantification such as stable isotope labeling and the analysis of important post-translational modifications (for example, phosphorylation) were major breakthroughs and deserve special mention in this context. The emergence of highly sensitive, high-resolution instrumentation such as quadrupole time-of-flight or linear ion trap (LTQ)/Fourier transform ion cyclotron resonance (FT-ICR) and LTQ/orbitrap mass spectrometers has opened up new possibilities. It is important to note that the technology requires access to purpose-fitted

laboratory information management systems, statistical evaluation and database management necessities that are not to be underestimated by those considering adopting the technology.

A typical chemical proteomics experiment (**Figure 5**) starts with immobilizing a bioactive compound on a matrix, such as sepharose or agarose.

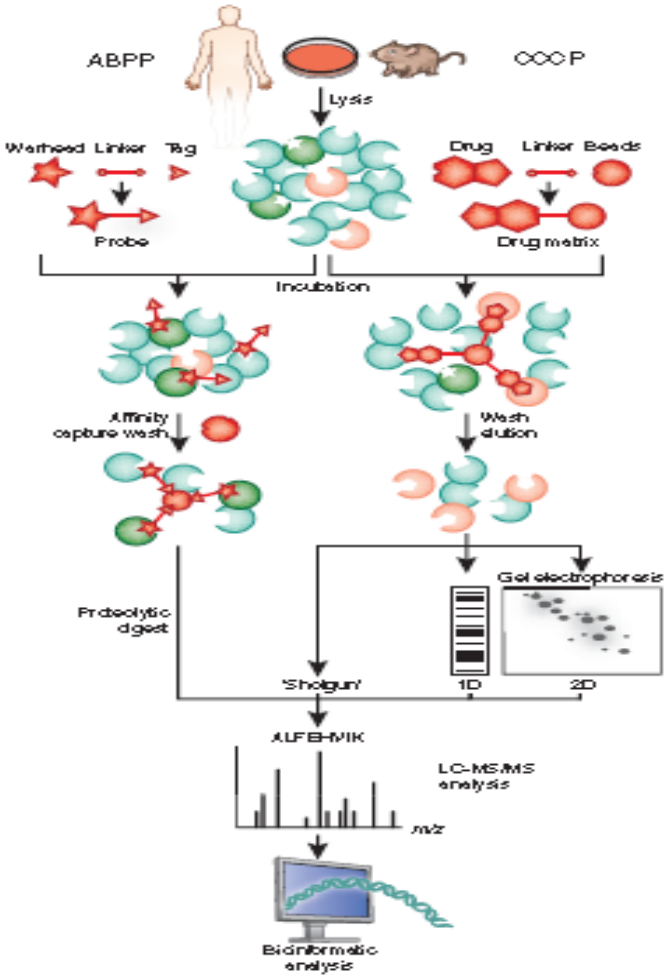

Figura 5: Chemical proteomic approach

There are various commercially available activated resins that allow for the attachment of specific chemical groups (for example, sulfhydryl, amino, hydroxyl or carboxyl groups). When a compound needs to be modified for immobilization, it is important to follow up this modification chemistry with an appropriate biochemical or cell-based assay to ensure that activity is retained.

In parallel, a cell extract is prepared either from cells or tissue. Subsequently, this lysate is incubated with the affinity matrix and washed extensively before elution. Depending on the experimental strategy, washes of different stringencies are used. Detergents, salts or denaturing agents can be used for nonspecific elution. More specific elution can be achieved

by competition with an excess of soluble compound or via specific cleavage of an engineered linker.

Processing by SDS-PAGE (one- or two-dimensional) or a gel-free method ('shotgun proteomics') and subsequent digest of the proteins with a protease, typically trypsin, generates a complex peptide mixture that is then analyzed by nano-HPLC coupled to nano-ESI-MS/MS. The results are searched against an appropriate protein database (for example, SwissProt or the US National Center for Biotechnology Information) with a search engine (for example, Mascot or Sequest) before being submitted to a more in-depth bioinformatic analysis.

2. Purpose of research

Currently about 40% of the world population is at risk of malaria infection. 90% of malaria deaths occur in sub Saharian regions[4]. The WHO estimates that the clinical cases of malaria are 300/500 millions every year, with more than one million deaths every 10 seconds. There are many children that, suffering from an acute attack of malaria, undergoes to a cerebral form, with coma and fatal outcome. In Africa, malaria causes 20% of infant mortality, 30-50% of outpatient visits and 50% of admissions. In endemic areas, pregnant women are four times more susceptible to malaria attacks[4].

Malaria mainly affects the poorest people of the World, but the low-cost drugs available, such as chloroquine, are those for which the parasite has developed resistance. In addition, in some regions of South East Asia, the phenomenon is spreading towards more effective therapies based on the use of artemisinin derivatives[54]. Therefore it is necessary to discover new antimalarial agents that present low cost and capability to overcome the resistance problem, acting on new targets.

In the digestive vacuole of *P. falciparum* there are plasmepsines I, II and IV and an hysto aspartic protease that are involved in the hemoglobin degradation cascade, an essential process for the *Plasmodium* survival[19]. Therefore they represent a very promising target for the design of new antimalarial agents. However, it is known that the four proteases have acquired complementary roles that increase their catalytic efficiencies. Recent studies have demonstrated that parasites stay alive even if they have lost one or two enzymes as a result of a genic deletion[17]. Therefore it is necessary to develop non-specific inhibitors of plasmepsins. This may explain why the molecules synthesized shown little effect on the growth of *P. falciparum* even if they inhibit plasmepsins at nanomolar range.

The Professor Romeo's laboratory has obtained interesting results[55] by applying the approach called "double drugs". It consists in the synthesis of a compound characterized by the presence of two molecules able to interact with two different drug targets. This molecules are linked through a binder.

In particular have been synthesized compounds that may present antimalarial activity, characterized by a β-hydroxy-γ-amino acid (statin), as a potent inhibitor of nonspecific plasmepsine, primaquine, atovaquone or the 4-amminoquinolinic core, characteristic of chloroquine. The statin acts by mimicking the tetrahedral intermediate transition which is formed during the hydrolysis of the peptide bond by the plasmepsine.

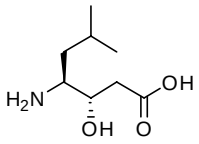

Statine

The most active compound of each series are shown in **Table 2.1**.

		D10 IC50 (nM)	W2 IC50 (nM)
RV97	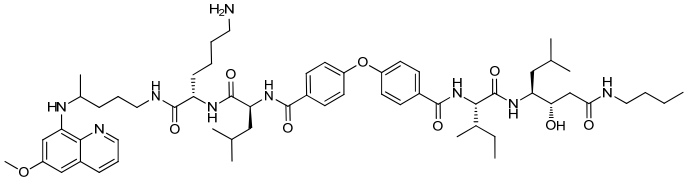	400	700
PM47	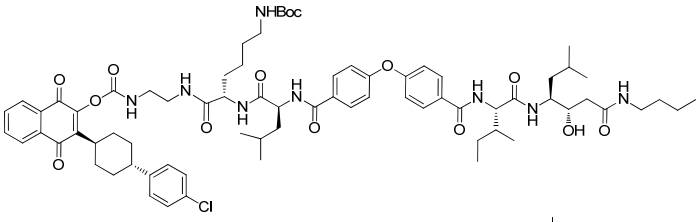	4.8	5.3
FP37	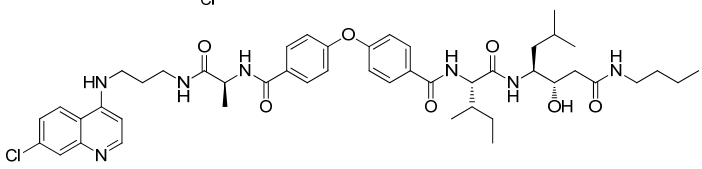	114.2	63.7

Table 2.1

RV97 belongs to the first series synthesized and it is characterized by a dipeptide linked to primaquine, 4,4'-oxybisbenzoic acid, an aromatic linker optimized from a previous study, and the statin containing the dipeptide Ile-Leu functionalized with the butilammide. The primaquine is one liver schizonticide and therefore does not interfere with the statin mechanism of action. Recently it has been demonstrated that the serious side effects due to primaquine can be reduced by binding the drug to a peptidic component[56]. The quinolinic structure acts as a carrier of the "double drugs" because it promotes the membrane cross. The compound inhibits the growth of *P. falciparum* at the intraheritrocitic stage on both chloroquine-sensitive strains (D10) and chloroquine-resistant strains (W2).

It showed a good in vivo activity (ED_{50} = 6.11 mg/Kg) comparable to that of chloroquine and a good plasmepsine I, II and IV inhibition (Plm I: 110 nM; Plm II: 0.4 nM; Plm IV: 0.5 nM).

The development of the "double drugs" continued with the replacement of primaquine with a prodrug of atovaquone, described in earlier studies,[57] characterized by a carbamate, allowing the improvement of solubility in water and the increas release of atovaquone with a pH-dipendent mechanism [58]. **PM47** presents a good *P. falciparum* growth inhibitory activity in vitro (IC_{50} = 5.3 nM) against *plasmodia* chloroquine resistant strains (W2).

Considering the promising results obtained with the approach called "double drugs", it has been designed a series of inhibitors using a new pharmacophore: the 4-amminoquinolinic core, characteristic of chloroquine.

The chloroquine combined with an inhibitor of Plasmepsine, should not lead to an improvement of the *P. falciparum* growth inhibitory activity because the heme group, obtained from the hydrolysis of hemoglobin by plasmepsins, is essential for the pharmacological action of chloroquine. Recent studies have demonstrated that plasmepsins are not the unique enzymes family capable to cleavage hemoglobin, but in the digestive vacuole there are other proteases with same function: the falcipain. Therefore it is possible that, despite the plasmepsine are effectively inhibited, there could be a constant heme group release. Thus the presence of chloroquine, combined with the statin in the same molecule, could lead to a marked improvement of the *P . falciparum* growth inhibitory activity.

Different 4-amminoquinolinic derivatives have been synthesized. They are characterized by the 4-amminoquinolinic system linked to 4,4'-oxybisbenzoic acid as linker using different spacer containing amino acids or not.

FP37 was the most active product in this series.

During the "double drugs" SAR studies has it been demonstrated that in spite of some derivatives were characterized by excellent plasmepsin inhibition, they showed no antimalarial activity. This observation has led us to examine if the plasmepsins were actually the target of the "double drugs" synthesized.

Starting from **IM43** (**Table 2.2**) was undertaken a study that led to the replacement of the amino acid statin with leucine, obtaining **NV165**. Unespectantly, an increase in malaria activity has been observed, demonstrating that the "double drugs" were acting on a different target and that statin was not essentianl for the "double drugs" antimalarial activity.

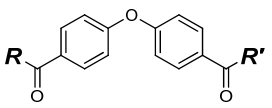

Compound	R	R'	D10 IC_{50} (nM)	W2 IC_{50} (nM)
IM43	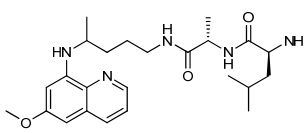	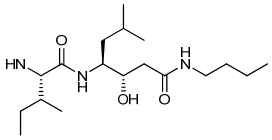	230	280
NV165	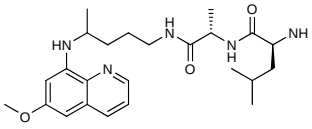	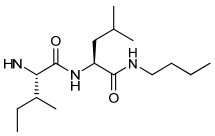	36.8	103.9
FG30	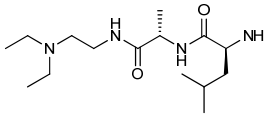	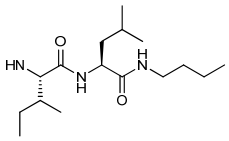	345	143
NV197	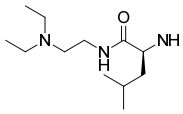	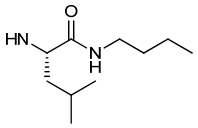	357	314

Table 2.2

The Professor Romeo's laboratory decided to continue the SAR studies considering **NV165** as the new lead compound.

For the SAR studies **NV165** has been divided into three parts: the oxybisbenzoic system in the center and the two residues R and R' on the sides of the aromatic system. The aromatic system derived by 4,4'-oxybisbenzoic acid has not been modified since considered essential for the activity[59], but have been differentiated in the substituents R and R'.

It was initially varied the substituent R keeping constant the two amino acids and varying the quinoline system in order to verify its activity **(FG30)**.

The replacement of the quinoline system with an aliphatic diamine resulted in a reduction of the antimalarial activity, in particular against D10 strain. Anyway, it has allowed us to demonstrate that quinoline is not essential for the parasite growth inhibition. Subsequently the number and type of amino acids were varied, in order to obtain molecules with lower molecular weight and reduced peptidic character.

NV197, which was obtained removing two amino acids, one from the substituent R' and one from the substituent R, has a molecular weight reduced by one third compared to **NV165**

while maintaining a good antimalarial activity. This compound has been considered for further SAR studies of the substituent R'.

From the subsequent SAR studies (**Table 2.3**) it was demonstrated that only one amino acid at the sides of the oxybisbenzoic system is sufficient to have a good antimalarial activity. In particular it has been descovered that leucine methylester group in R' gave the best results **(AN12)**.

Compound	R	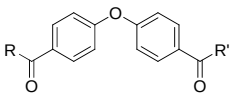	R'	D10 IC50 (nM)	W2 IC50 (nM)
AN12	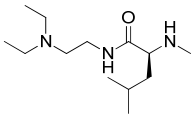		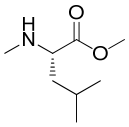	12.97	8.46
AO7	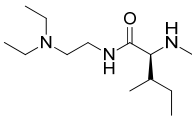		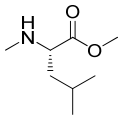	5.83	2.76

Table 2.3

AN12 presents a lower molecular weight than **NV165** and the antimalarial activity is approximately 3 times higher against D10 strains and about 10 times higher agaist W2 strains. Considering the **AN12** high activity, in subsequent studies the substituent R' was maintained. The substituent R was varied, applying the strategy already described. The substituent R was divided into two portions: the amino acid and the terminal group that were varied alternately. The substitution of leucine with isoleucine residue **AO7** has led to an increase of antimalarial activity of about 2 times.

AO7 presents an higher activity than **IM43** 40 times against D10 strains and 100 times higher against W2 strain.

The SAR studies performed in the Professor Romeo's laboratory have led to very good results, but the molecular target of these compounds is unknown. In order to improve the antimalarial activity of this new class of potent compounds it is necessary to know the molecular target. So, chemical proteomics, as previously described, could be a useful tool in order to reach this goal.

Thus the purpose of this first part of my PhD thesis is the identification of the molecular target of this new class of potent antimalarial compounds using a chemical proteomics approach.

In order to reach this goal, first of all different fluorescent lead compound derivatives would be synthesized in order to identify the target localization into *P. falciparum* and thus facilitate LC-MS analysis and subsequent database target identification.

Subsequently a chemical proteomics approach would be performed. There are several limitations in chemical proteomics approach that can affect the results. For example, it is necessary to use tag compounds that present high activity and affinity for the protein target. Moreover considering that LC-MS analysis is a very sensitive methodology that can be used for protein target identification, the high background noise caused by non specific protein binding could greatly complicate the proteomic analysis.

Thus in order to overcome these problems we have considered that it is necessary to use a chemical proteomics methodology that would allow us to recognize target protein with high selectivity. In particular, we have considered that could be useful for us to use a cleavable linker between the tag compound and the generally used biotin unit in order to confer high selectivity as previously described by Ki Duk Park[60].

In particular we decided to follow the experimental procedure represented in the scheme below (**Figure 6**):

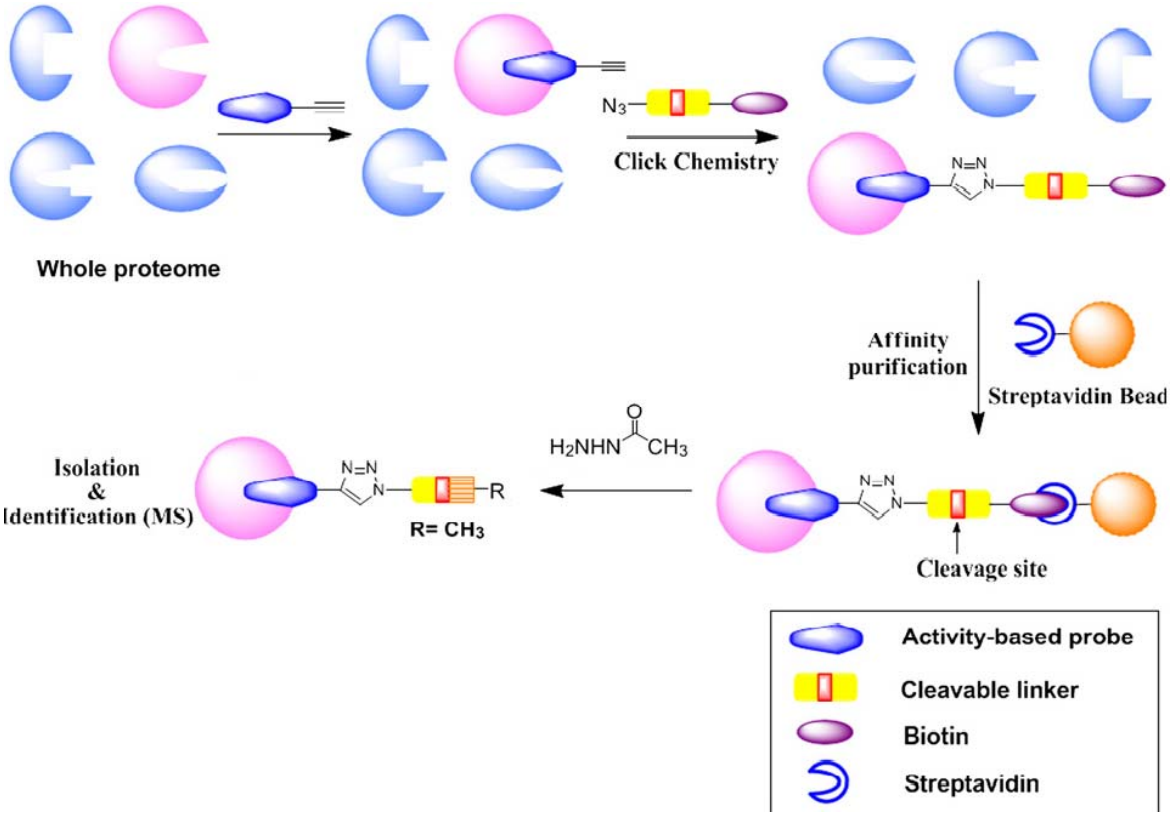

Figure 6: Experimental procedure

According to this procedure an active alkyne derivate will be incubated into a *P. falciparum* lysate. After that, a suitable cleavable linker will be designed and synthesized in order to fish the incubated tag compound with high selectivity using click chemistry. This cleavable linker is characterized by a biotin unit, an acylhydrazon cleavable linker and a terminal azide.

Then the lysate will be purified through an affinity purification column characterized by agarose streptavidin beads.

During the cleavage step, the tag compound will be released with high selectivity thanks to the acylhydrazone exchange with acethylhydrazide that belongs only to the incubated compound; while the naturally biotinilated proteins, that could be attached to the agarose streptavidin beads, will be held into the column.

Finally LC-MS and databases analysis will be performed in order to identify the protein primary sequence or the target protein of this new class of antimalarial compounds.

3. Results and Discussion

3.1 Fluorescent studies:

The target identification of this new class of potent antimalarial compounds, starts from the synthesis of different florescent lead compound derivates in order to identify the target localization into *P. falciparum* and thus facilitate LC-MS and databases analysis.

The lead compound of this class of antimalarial agents is **AN 12**, represented below:

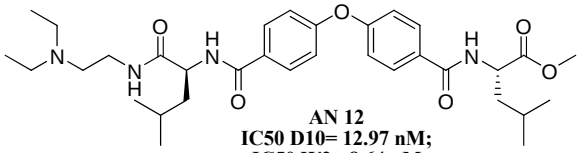

AN 12
IC50 D10= 12.97 nM;
IC50 W2= 8.64 nM

It is characterized by a high in vitro activity against *P. falciparum* (IC_{50} D10= 12.97 nM; IC_{50} W2= 8.64 nM). We considered the possibility to introduce three different fluorescent groups replacing the N,N-diethylethylendiammine with an ethylendiammine, as spacer, and carboxyfluorescein **1**, carboxy-coumarine **2** or dansyl **3** as fluorescent tags.

The antimalarial activity against *P. falciparum* D10 and W2 strains has been tested in the Professor Taramelli's laboratory. Compound **1** resulted to be inactive, while compounds **2** and **3** were characterized by antimalarial activity but elicted only in a micromolar range (**table 3.1**), not sufficient to perform fluorescent studies.

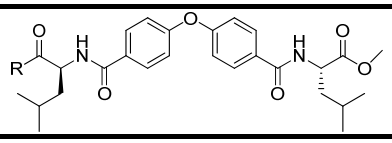

COMPOUND	R	D10 IC_{50}(nM)	W2 IC_{50}(nM)
1	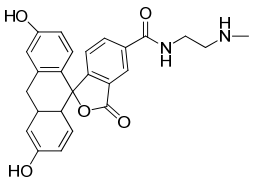	Inactive	Inactive
2	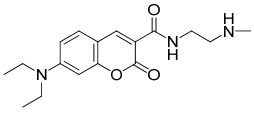	1462	1699
3	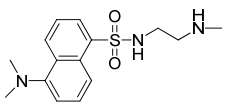	4166	4219
AN 12	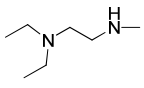	12.97	8.64

Table 3.1

Considering the SAR studies of these fluorescent molecules, the high antimalarial activity decrease could be caused by the substitution of the basic nitrogen group (tertiary amine), presented in the lead compound, with an amidic nitrogen.

Among the three fluorescent substituents, the carboxy-coumarine derivative **2** resulted the most accepted fluorescent group.

In parallel studies performed in Professor Romeo's laboratory, enduring the lead compound SAR studies, **AO 26**, a new lead compound, has been identified:

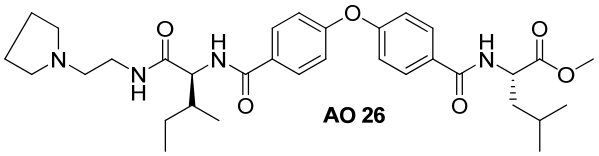

AO 26

This compound is characterized by an higher antimalarial activity against D10 and W2 strains than **AN 12** as represented in **table 3.2**

COMPOUND	STRUCTURE	D10 IC_{50}(nM)	W2 IC_{50}(nM)
AN 12	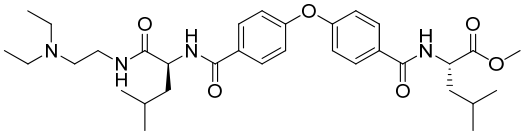	12.97	8.64
AO 26	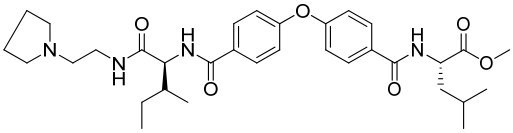	0.49	0.34

Table 3.2

Thus a new fluorescent compound starting from **AO 26** has been synthesized. Considering the SAR studies of the previous series of fluorescent compounds, we substituted the methyl ester group with a carboxy-coumarine linked to a propylendiamine as spacer obtaining compound **4**.

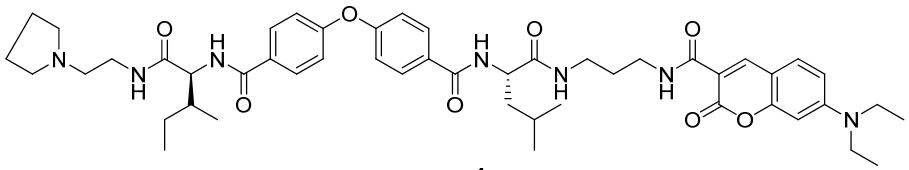

4
D10;W2 IC_{50} = 13nM

In this case we maintained in the same position the basic tertiary amine group bound to isoleucine, that from **AO 26** SAR studies seems to be the most accepted aminoacid in that position.

Compound **4** obtained was characterized by a good antimalarial activity (D10; W2 IC_{50}= 13nM) sufficient to perform fluorescent studies in Professor Taramelli's laboratory.

These studies are still in progress and would facilitate LC-MS and database analysis.

3.2 Chemical proteomics studies:

Considering that several limitations can affect chemical proteomics, we decided to follow the procedure previously described by Ki Duk Park[60]. In fact it permits us to identify the target with high selectivity and sensitivity.

This procedure consist in five steps:

1. the incubation of an alkyne modified lead compound into a cellular lysate;
2. the capture of this tag compound linked to the target protein, using a suitable probe characterized by the presence of a cleavable linker, a biotin unit and a terminal azide to permit capture with the alkyne modified lead compound using click chemistry;
3. purification using affinity chromatography (agarose streptavidin beads);
4. selective cleavage
5. LC-MS analysis in order to identify protein target.

Thus we focused our attention on the synthesis of a suitable tag compound characterized by the presence of a terminal alkyne group. Considering the previous fluorescent SAR studies, it was well evident that, starting from **AO 26**, the substitution of the lead compound basic nitrogen group would have led to inactive compounds. Thus we considered the possibility to substitute the methylester group on the other side of the molecule with a propargyl amine, analogously to the synthesis of compound **4**.

This substitution led to the synthesis of compound **5** which was less active than **AO 26** but equal to **AN 12** (**Table 3.3**). Considering the high antimalarial activity of compound **5** we presume that it would recognize with high affinity the protein target thus limiting aspecific protein binding.

COMPOUND	STRUCTURE	D10 IC_{50}(nM)	W2 IC_{50}(nM)
AO 26	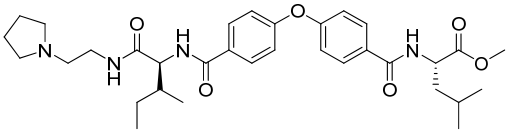	0.49	0.34
AN 12	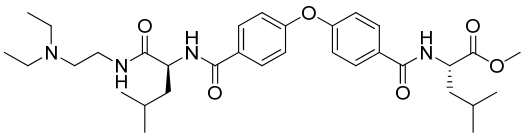	12.97	8.64
5	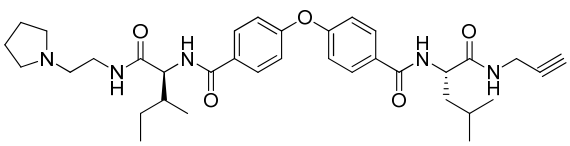	8	12

Table 3.3

Accordingly to chemical proteomic procedure that we aimed to follow, we have designed and synthesized a suitable probe, compound **6**, in order to recognize and release the alkyne tag compound linked to the protein target with high selectivity.

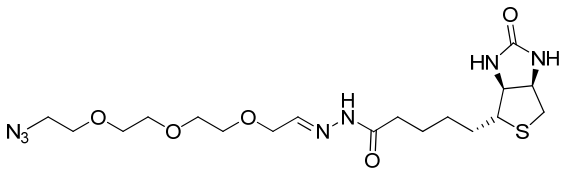

6

The chemical structure of the cleavable linker allow us to recognize the protein target with high selectivity and sensitivity, thus limiting the background noise that usually affects the chemical proteomics procedures.

It is characterized by a terminal azide that permits to capture the alkyne modified lead compound through click chemistry. We can capture the alkyne tag compound with high selectivity because it is the only compound in the whole proteome that can react with compound **6**.

The presence of a poliethylenglycol linker increases the water solubility. Moreover achylhydrazon cleavable linker provides selectivity during the cleavage step from the resin. Considering that in the *P. falciparum* lysate there could be other proteins naturally biotinilated that could be attached to the resin due to the biotin streptavidin recognition, only the tag compound is released from the resin, as it is the only compound characterized by the cleavable linker.

Finally the biotin unit links the streptavidin beads during the affinity chromatography purification step.

In order to verify if compounds **5** and **6** could be useful tools for chemical proteomics procedure, first of all we focused our attention on click chemistry reactions.

We performed this reaction with different conditions (**Table 3.4**):

	5/6 ratio	Reaction time	Conditions	Yield of compound 7
1	1/1	24 h	• $CuSO_4$ • Na ascorbate • H_2O/t-BuOH (1:1)	No reaction
2	1/1	12 h	• $CuSO_4$ • Na ascorbate • THF/H_2O (1:1)	15%
3	1/1	1 h	• CuBr • HEPES pH 7.4	30%

Table 3.4

In case 1 we didn't observe product formation probably because the two reagents haven't been completely dissolved. Thus in case 2 we introduced THF. In this case we obtained compound **7** in 15% yield. Better results have been obtained in case 3 using HEPES solution (pH 7.4) and CuBr.

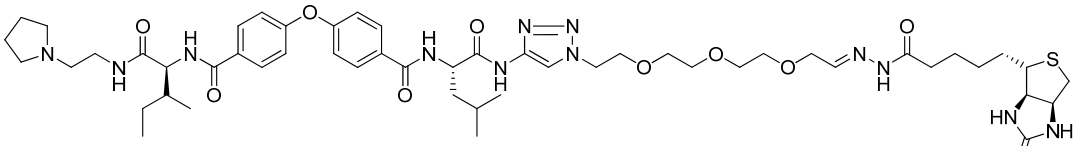

7

The expected compound has been obtained in 30% yield. Moreover these are also the best conditions to perform the click chemistry reaction in a biological media.

Before starting the chemical proteomics procedure we considered the possibility to verify if the acylhydrazon/acyldrazide exchange occurs. Thus we synthesized again compound **7** and then we immobilized it on strptavidin agarose beads. After the exchange step and ESI-Ms direct infusion analysis we confirmed that compound **8** was formed.

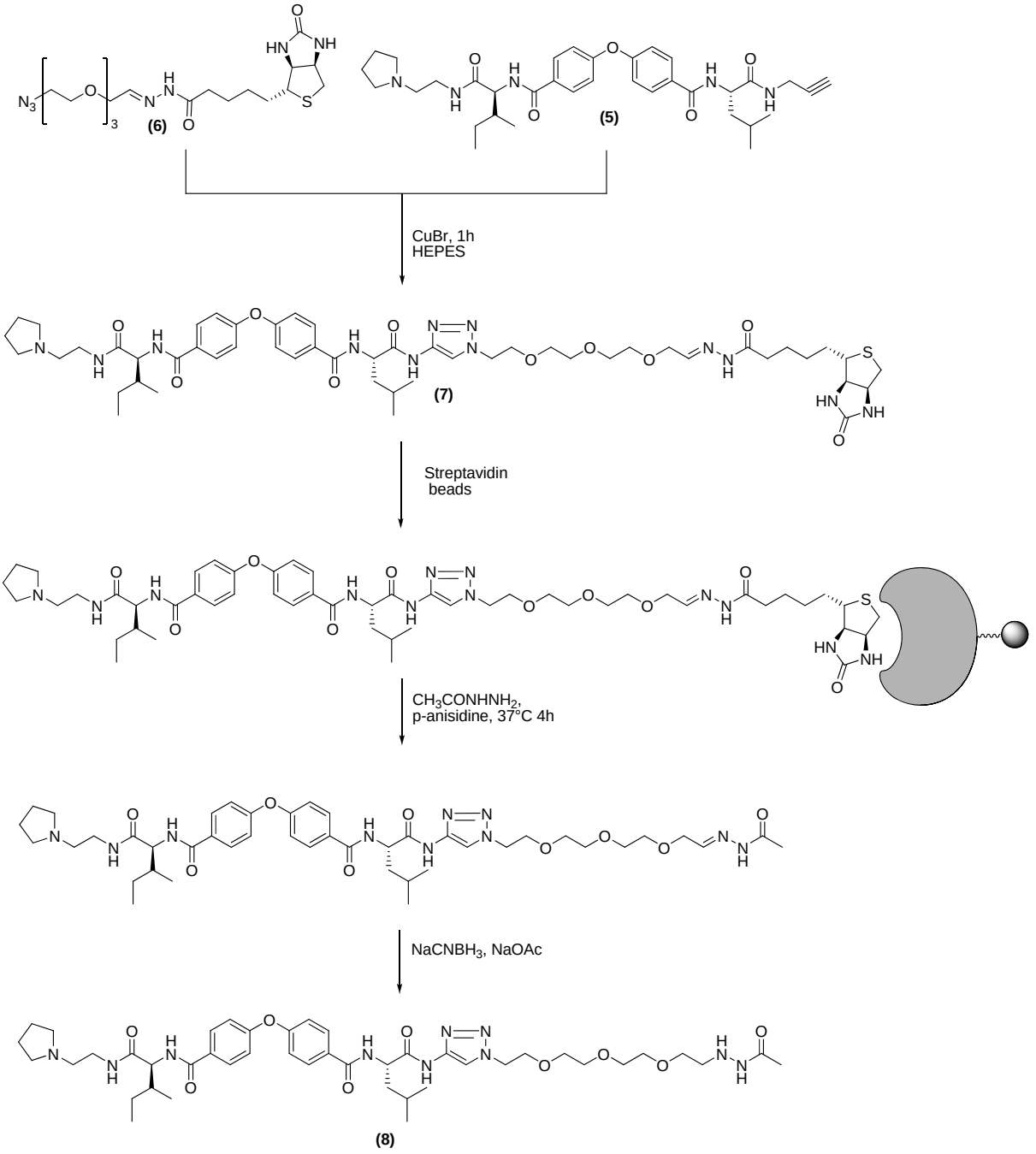

At the moment we are waiting for *P. falciparum* lysate from Professor Taramelli's laboratory. Future studies will be focused on the application of this chemical proteomics techniques in order to identified the biological target of this new class of potent antimalarial compounds

4. Synthesis

Compounds **(1-3)** are characterized by a common fragment (ethylendiamine-leucine-oxibisbenzoic acid-leucinemethylester) linked to three different fluorescent groups using ethylendiamine as linker.

As shown in table 1, compound **1** is characterized by the common fragment linked to carboxyfluoresceine; compound **2** by the common fragment linked to carboxy-coumarine and compound **3** by the common fragment linked to dansyl.

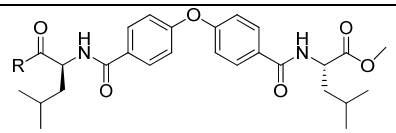

COMPOUND	R
1	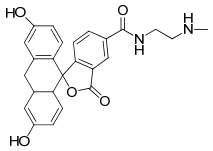
2	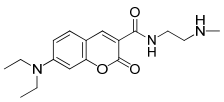
3	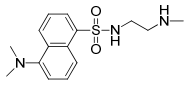

Table 1

Compound **4** is characterized by 1-(2-aminoethyl)pyrrolidine-Isoleucine fragment linked to one acid group of 4,4'-oxibisbenzoic acid. The other acid portion is substituted by Leucine linked to a propilendiamine as spacer and corboxycoumarin group as shown in the figure below.

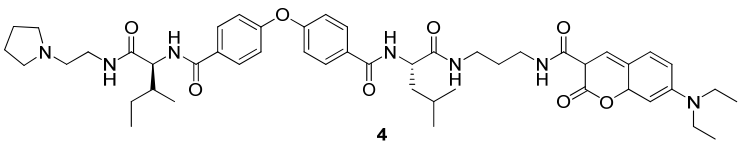

4

Compound **5** is characterized by 1-(2-aminoethyl)pyrrolidine-Isoleucine fragment linked to one acid group of 4,4'oxibisbenzoic acid. The other acid portion is substituted by Leucine linked to propargylamine as shown in the figure below.

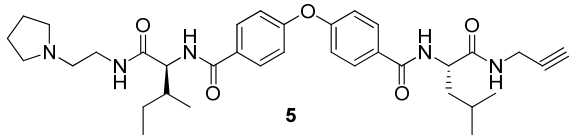

5

Compound **6** is characterized by the biotin unit, acylhydrazon cleavable linker, polietylenglycole linker and terminal azide as shown in the figure below.

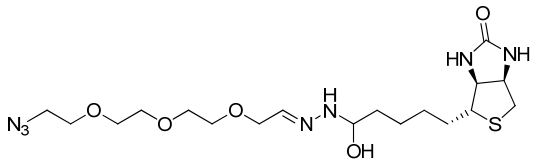

6

Compound **7** is characterized by the 4,4'-oxybisbenzoic acid substituted at one side by a 1-(2-aminoethyl)pyrrolidine-Isoleucine fragment and on the other side by leucine linked to the triazole ring, linked to a polietylenglycole linker-acylhydrazon cleavable linker-biotin unit fragment as shown in the figure below.

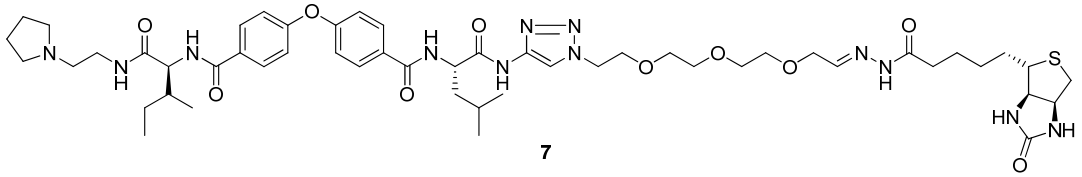

7

Compound **8** is characterized by 4,4'-oxybisbenzoic acid substituted on one side by 1-(2-aminoethyl)pyrrolidine-Isoleucine fragment and on the other side by leucine linked to triazole ring, linked to a polietylenglycole and acetydrazide

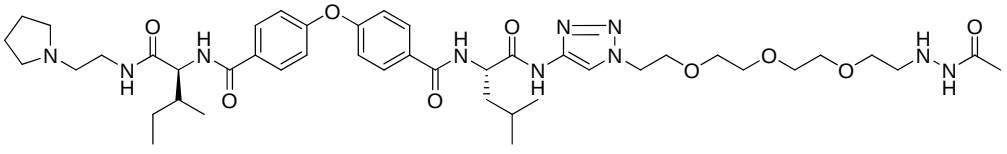

8

4.1 Reactions and mechanisms

Coupling reaction:

This reaction is a key step in the process of production of peptides, and requires activation of the carboxylic acid by means of coupling reagents.

The "peptide coupling reagents" have evolved significantly over the last 10 years: from carbodimmidi salts onium (phosphonium and uronium). The "coupling reagents" **(Figure 7)** can be classified as:

• Carbodiimmide coupling reagent.

• Benzotriazoles.

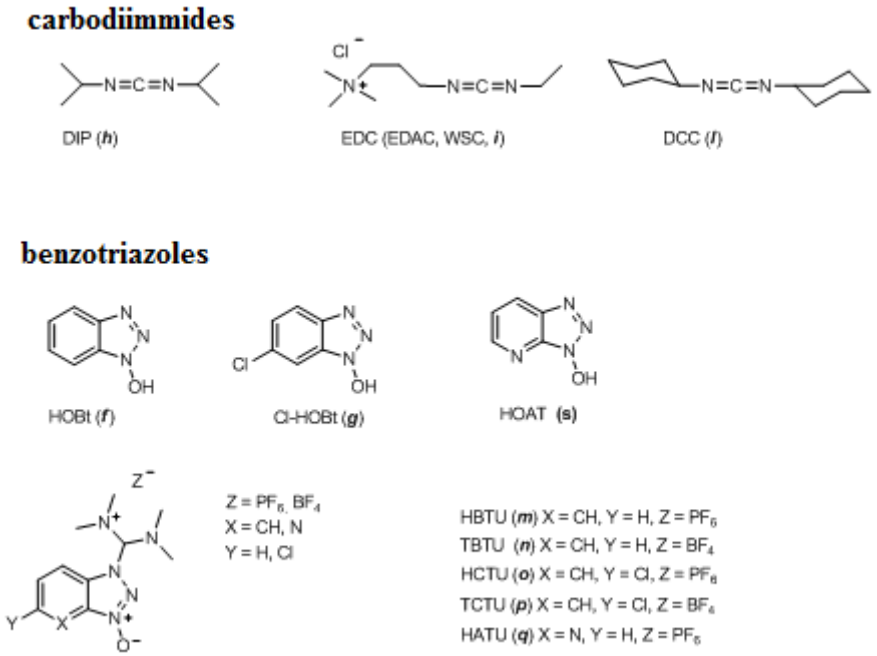

Figure 7

The use of coupling reagents of industrial began in 1955 with the introduction of dicloesilcarbodiimmide (DCC). Unfortunately, the carbodiimmide due to the high reactivity may cause racemization and secondary coupling reactions **(Figure 8)**.

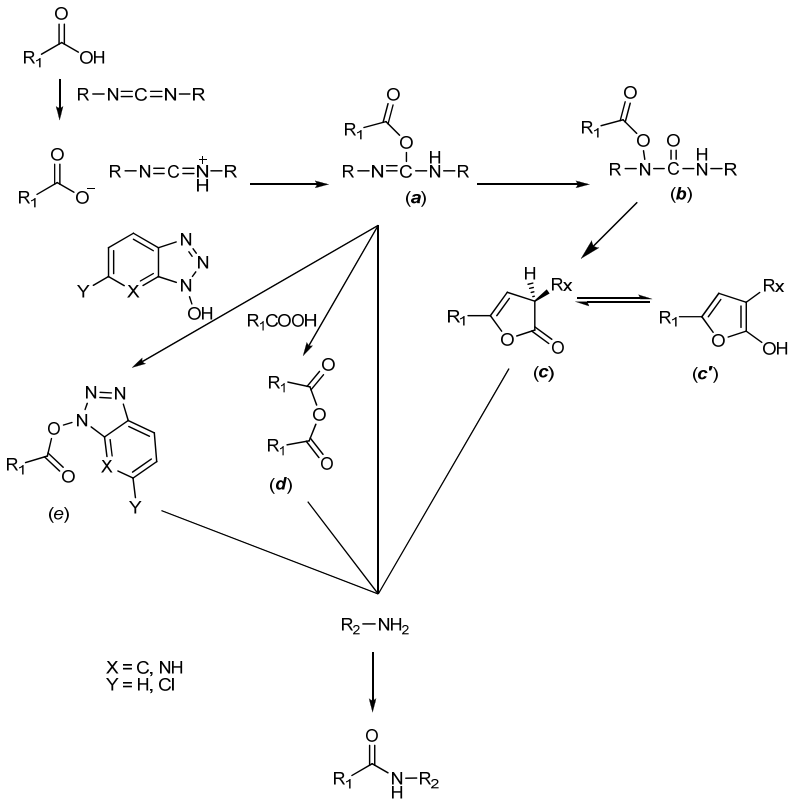

Figure 8

The mechanism of activation of carbodimmide (complex mechanism and solvent dependent) begins by the transfer of a proton carbodimmide, followed by the addition of the carboxylate to form the O-acilisourea (a) **(Figure 8)**. This is the most reactive species that can attack the amine to give the corresponding amide. The O-acilisoura (a) may rearrange to give the N-acyl urea (b), which is not reactive or it may undergo an intramolecular cyclization to give 5 (4H)-ossazolone (c), which is less reactive (as) and can tautomerize with the corresponding loss of chirality (c '). If the activation is conveyed in a solvent with low dielectric constant such as $CHCl_3$ or CH_2Cl_2, the formation of (a) occurs instantaneously and is absent if a nucleophile or a base, can remain stable for several hours. If the activation is carried out in the presence of a more polar solvent such as DMF, no immediate reactions are found, indeed, can form a complex mixture of amino acids initiates as symmetrical anhydrides (d). The 1-hydroxybenzotriazole (HOBt) (f) **(Figure 7)** is used as additive to reduce the DCC for racemization, and has recently developed new derivatives benzotriazoles as 1-hydroxy-5-chlorobenzotriazole (Cl-HOBt) (g) or 1 -hydroxy-7-azabenzotriazolo (HOAT) (s). The HOBt active esters (s) **(Figure 8)** are less reactive intermediate (a), but more stable and less ready to racemize.

The addition of benzotriazoles [HOBt (f) and Cl-HOBt (g)] **(Figure 7)** to the carbodimmide coupling reagent leads to the formation of the active ester of benzotriazole, which is less reactive O-acilisourea (a) **(Figure 8)**, reducing the racemization of the protected amino acids and avoiding the formation of other less reactive derivatives. The Cl-HOBt (g) functions as the HOBt (f) **(Figure 7)**, although it is much more acid (pKa: 3.35 for Cl-HOBt and 4.60 for HOBt), is a better leaving group and the active esters are more reactive than HOBt esters. The Cl-HOBt is used as additive along with the HBTU (m) **(Figure 8)** to suppress racemization during the realization of coupling.

The pyridine derivatives of HOBt (HOAT) are not suitable for industrial use, because the presence of nitrogen in the aromatic ring makes the structure unstable.
In the last decade the salts (phosphonium and uronium) of hydroxybenzotriazole derivatives were introduced in the market (HBTU, TBTU, HATU). The species that reacts with the salt is the carboxylate **(Figure 9)** and therefore it is essential the presence of a minimum amount of base for acid deprotonation. The intermediate species of acyloxy-phosphonium salts, which have not been isolated, they react immediately with the benzotriazolic derivative to give (e) **(Figure 8)**, which reacts with the component Ilino ammonium to give the corresponding amide.

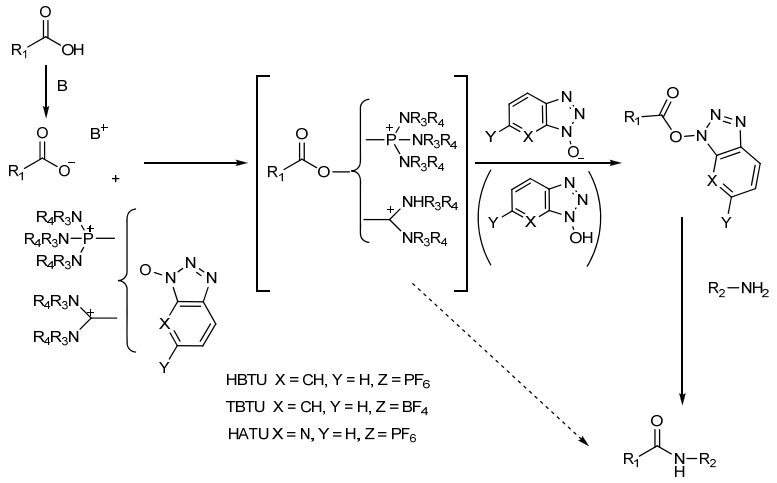

Figure 9

The use of more reactive salt HATU (q) **(Figure 7)** presents the disadvantage of the high price. HCTU (o)\TCTU (p) **(Figure 7)** are a good alternative to HBTU (m)\TBTU (n) **(Figure 7)**, because the presence of Cl-HOBt makes these reagents more reactive.

Click chemistry reaction:

"Click Chemistry" is a term that was introduced by K. B. Sharpless in 2001 to describe reactions that are high yielding, wide in scope, create only byproducts that can be removed without chromatography, are stereospecific, simple to perform, and can be conducted in easily removable or benign solvents. This concept was developed in parallel with the interest within the pharmaceutical, materials, and other industries in capabilities for generating large libraries of compounds for screening in discovery research. Several types of reaction have been identified that fulfill these criteria, thermodynamically-favored reactions that lead specifically to one product, such as nucleophilic ring opening reactions of epoxides and aziridines, non-aldol type carbonyl reactions, such as formation of hydrazones and heterocycles, additions to carbon-carbon multiple bonds, such oxidative formation of epoxides and Michael Additions, and cycloaddition reactions.

As one of the best click reactions to date, the copper-catalyzed azide-alkyne cycloaddition features an enormous rate acceleration of 10^7 to 10^8 compared to the uncatalyzed 1,3-dipolar cycloaddition. It succeeds over a broad temperature range, is insensitive to aqueous conditions and a pH range over 4 to 12, and tolerates a broad range of functional groups. Pure products can be isolated by simple filtration or extraction without the need for chromatography or recrystallization.

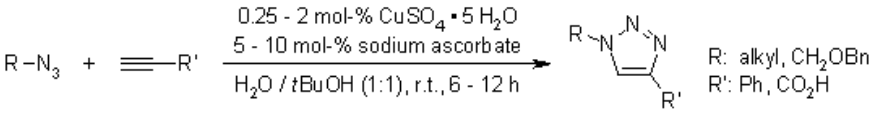

The active Cu(I) catalyst can be generated from Cu(I) salts or Cu(II) salts using sodium ascorbate as the reducing agent. Addition of a slight excess of sodium ascorbate prevents the formation of oxidative homocoupling products. Disproportionation of a Cu(II) salt in presence of a Cu wire can also be used to form active Cu(I).

DFT calculations have shown that coordination of Cu(I) to the alkyne is slightly endothermic in MeCN, but exothermic in water, which is in agreement with an observed rate acceleration in water. However, coordination of Cu to the acetylene does not accelerate a 1,3-dipolar cycloaddition. Such a process has been calculated to be even less favorable than the uncatalyzed 1,3-dipolar cycloaddition. Instead, a copper acetylide forms, after which the azide

displaces another ligand and binds to the copper. Then, an unusual six-membered copper(III) metallacycle is formed. The barrier for this process has been calculated to be considerably lower than the one for the uncatalyzed reaction. The calculated rate at room temperature is $1s^{-1}$, which is quite reasonable. Ring contraction to a triazolyl-copper derivative is followed by protonolysis that delivers the triazole product and closes the catalytic cycle **(Figure 10)**.

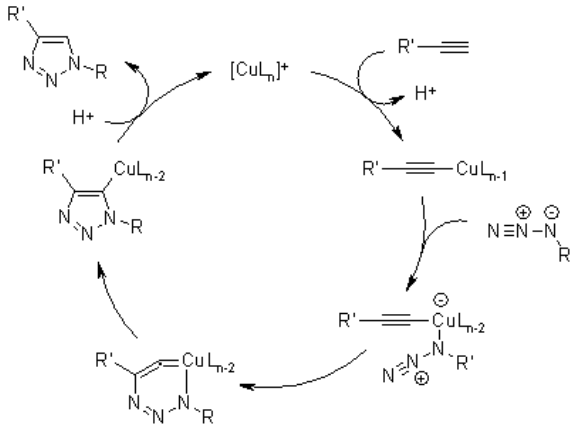

Figure 10: Catalytic cycle

4.2 Schemes of synthesis

Compounds 1-3 synthesis:

The synthesis of compounds **1-3** started from the synthesis of a common fragment, intermediate **12**:

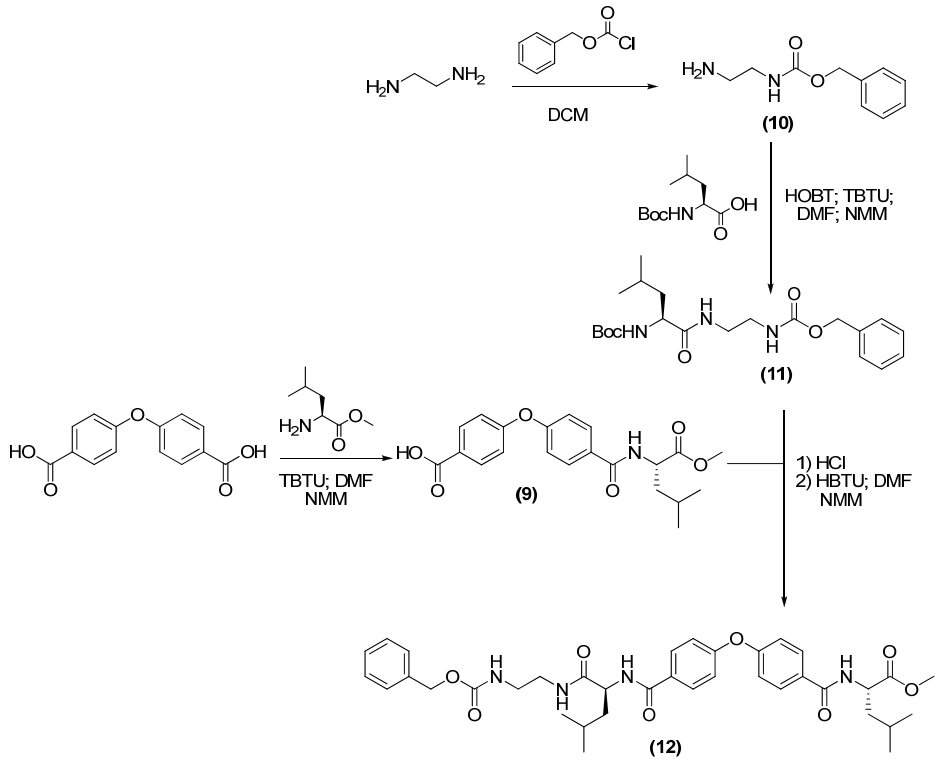

Intermediate **12** has been synthesized using a coupling reaction between intermediate **9** and intermediate **11** deprotected from the Boc group using HCl 4N in dioxane. Intermediate **9** has been obtained from the coupling reaction between Leucine-methylester and 4,4'-oxibisbenzoic acid. Intermediate **11** has been synthesized by coupling Boc-leucine with intermediate **10** obtained from the reaction between etylendiamine and benzylchloroformate.

Then intermediate **12** has been deprotected using catalytic hydrogenation obtaining common **fragment A:**

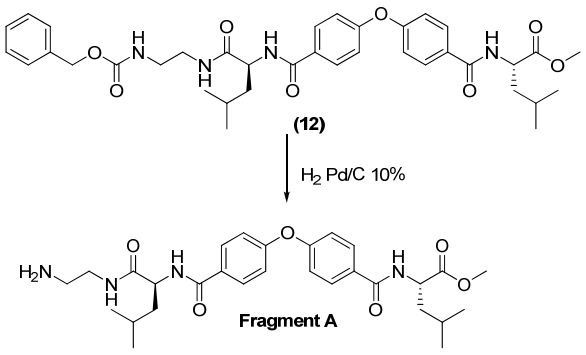

Fragment A was coupled with carboxy-fluoresceine obtaining compound **1**; with carboxy-coumarine obtaining compound **2** and with dansyl obtaining compound **3**

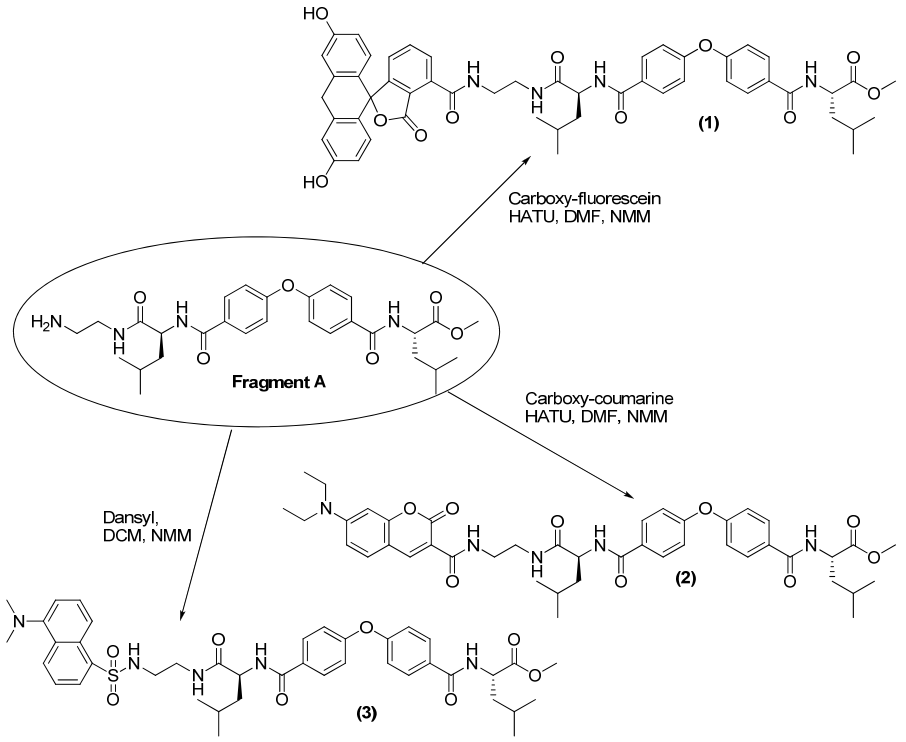

Compound 4 synthesis:

Compound **4** has been synthesized coupling carboxy-coumarine and intermediate **17** previously deprotected using catalytic hydrogenation. Intermediate **17** has been synthesized coupling deprotected intermediate **14** and intermediate **16**.

Intermediate **14** has been synthesized with coupling reaction between Boc-leucine and intermediate **13** obtained thanks to coupling reaction between propilendiamine and benzylchlorophormiate.

Intermediate **16** has been synthesized coupling 4,4'-oxybisbenzoic acid and previously deprotected intermediate **13** obtained thanks to coupling reaction between 1-(2-aminoethyl)pyrrolidine and Boc-isoleucine.

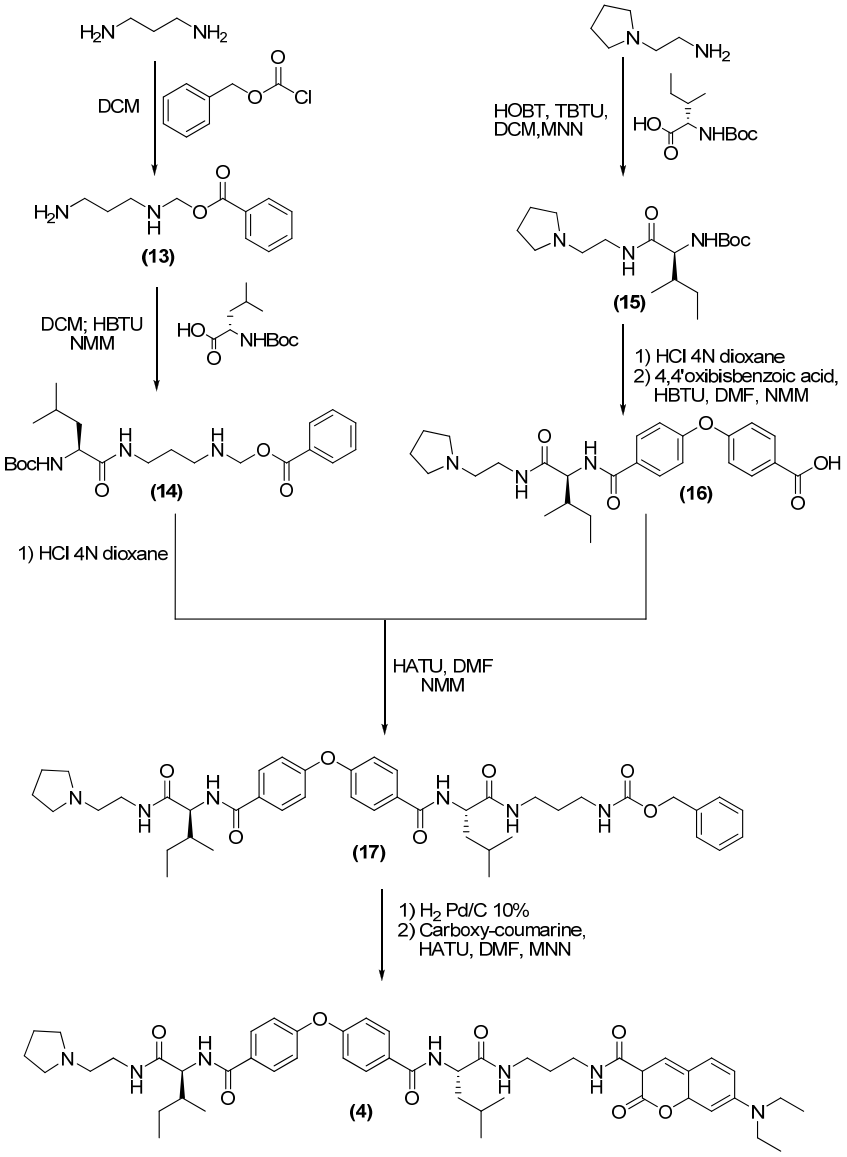

Compound 5 synthesis:

Compound **5** has been synthesized coupling Boc-deprotected intermediate **18**, obtained by coupling reaction between propargilamine and Boc-leucine, with intermediate **20** deprotected using catalytic hydrogenation.

Intermediate **20** has been synthesized coupling Boc-deprotected intermediate **15**, obtained by coupling reaction between 1-(2-aminoethyl)pyrrolidine and Boc-isoleucine, with intermediate **19** obtained by the reaction between 4,4'oxibisbenzoic acid and benzyl bromide.

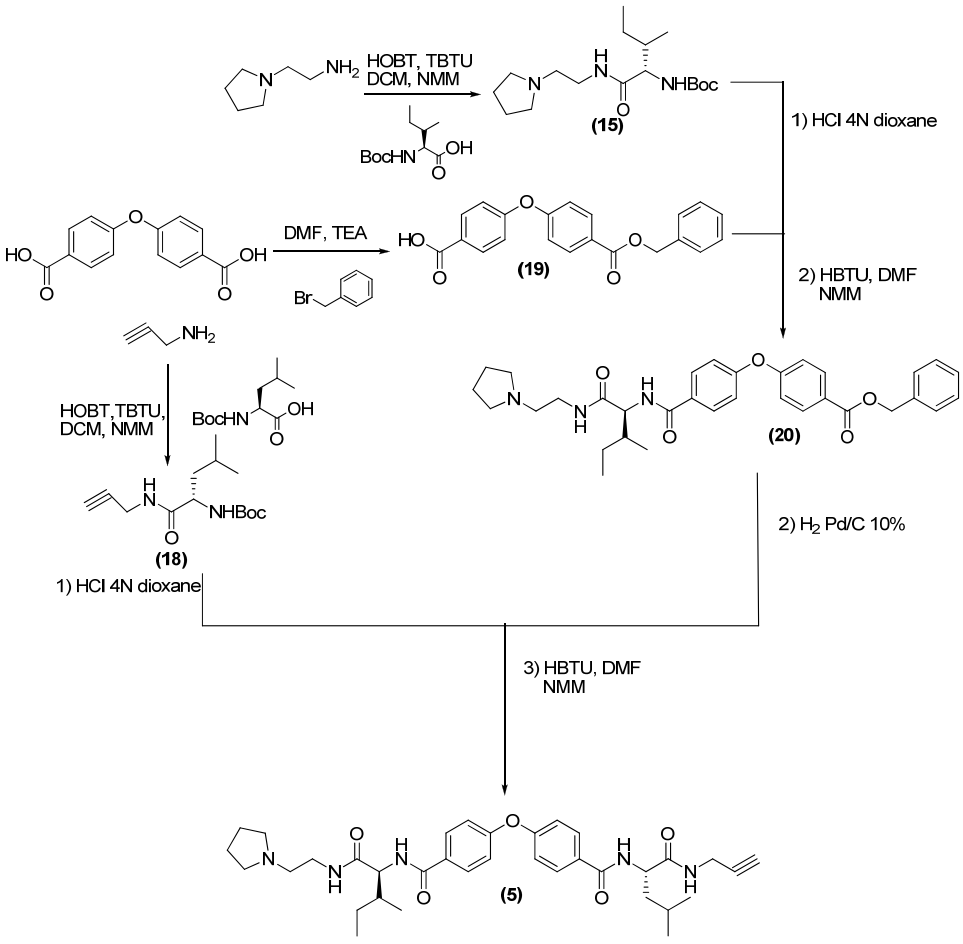

Synthesis of compound 6:

Compound **6** has been synthesized stirring overnight a solution of intermediate **23** in CH_2Cl_2 and a solution of intermediate **25** in THF/H_2O (1:1).

The synthesis of intermediate **23** started from the reaction between tetraethylene glycol and *p*-toluenesulfonyl chloride at 0°C obtaining intermediate **21**. This intermediate has been treated with NaN_3 at 70°C obtaining intermediate **22** that has been oxidized, trough Swern oxidation reaction, obtaining intermediate **23**.

Intermediate **25** has been synthesized treating intermediate **24**, obtained from biotin esterification reaction, with NH_2NH_2 in MeOH.

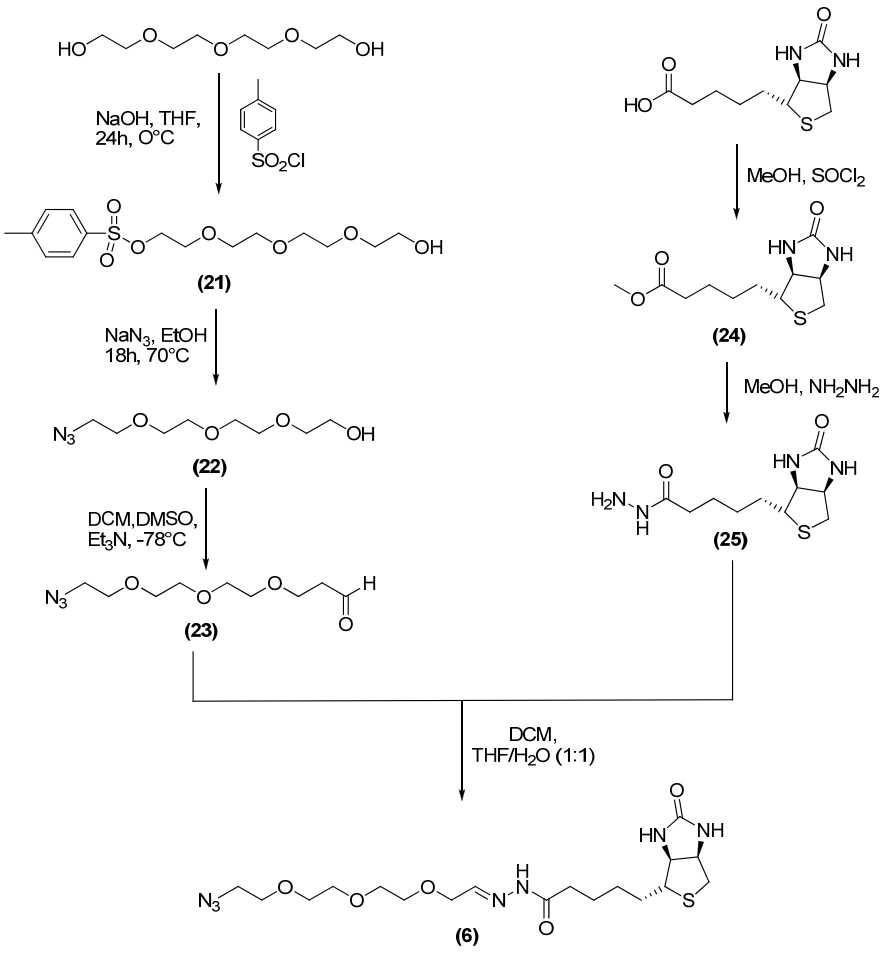

Synthesis of compound 7:

Compound **7** has been synthesized with click chemistry reaction between compound **6** and compound **5**. The synthesis of these compounds has been described above.

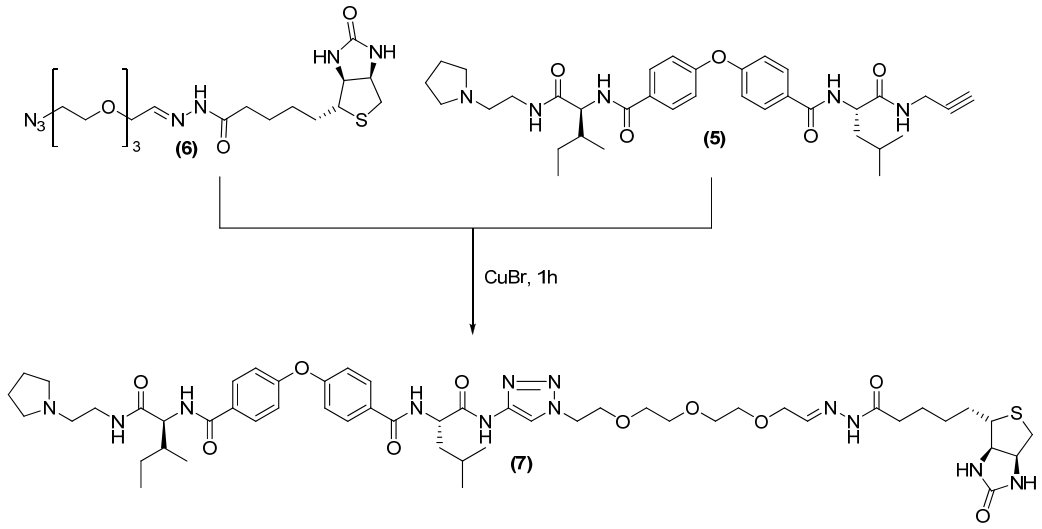

4.3 Proteomic reactions: method

A typical chemical proteomics experiment starts immobilizing a bioactive compound on a matrix, such as sepharose or agarose.

There are various commercially available activated resins that allow the attachment of specific chemical groups (for example, sulfhydryl, amino, hydroxyl or carboxyl groups). When a compound needs to be modified for immobilization, it is important to follow up this modification chemistry with an appropriate biochemical or cell-based assay to ensure that activity is retained.

In parallel, a cell extract is prepared either from cells or tissue. Subsequently, this lysate is incubated with the affinity matrix and washed extensively before elution. Depending on the experimental strategy, washes of different stringencies are used. Detergents, salts or denaturing agents can be used for nonspecific elution. More specific elution can be achieved by competition with an excess of soluble compound or via specific cleavage of an engineered linker.

Processing by SDS-PAGE (one- or two-dimensional) or a gel-free method ('shotgun proteomics') and subsequent digest of the proteins with a protease, typically trypsin, generates a complex peptide mixture that is then analyzed by nano-HPLC coupled to nano-ESI-MS/(MS). The results are searched against an appropriate protein database (for example, SwissProt or the US National Center for Biotechnology Information) with a search engine (for example, Mascot or Sequest) before being submitted to a more in-depth bioinformatic analysis.

4.4 Proteomic reactions: scheme of synthesis

Synthesis of compound 8:

Compound **8** has been synthesized starting from the click chemistry reaction between compound **5** and compound **6** obtaining compound **7**. This compound has been immobilized on agarose strptavidine beads due to selective recognition between compound **7** biotin portion and streptavidin. The final compound has been obtained through the selective cleavage due to acylhydrazone exchange with acetyldrazide and subsequent reduction with $NaCNBH_3$.

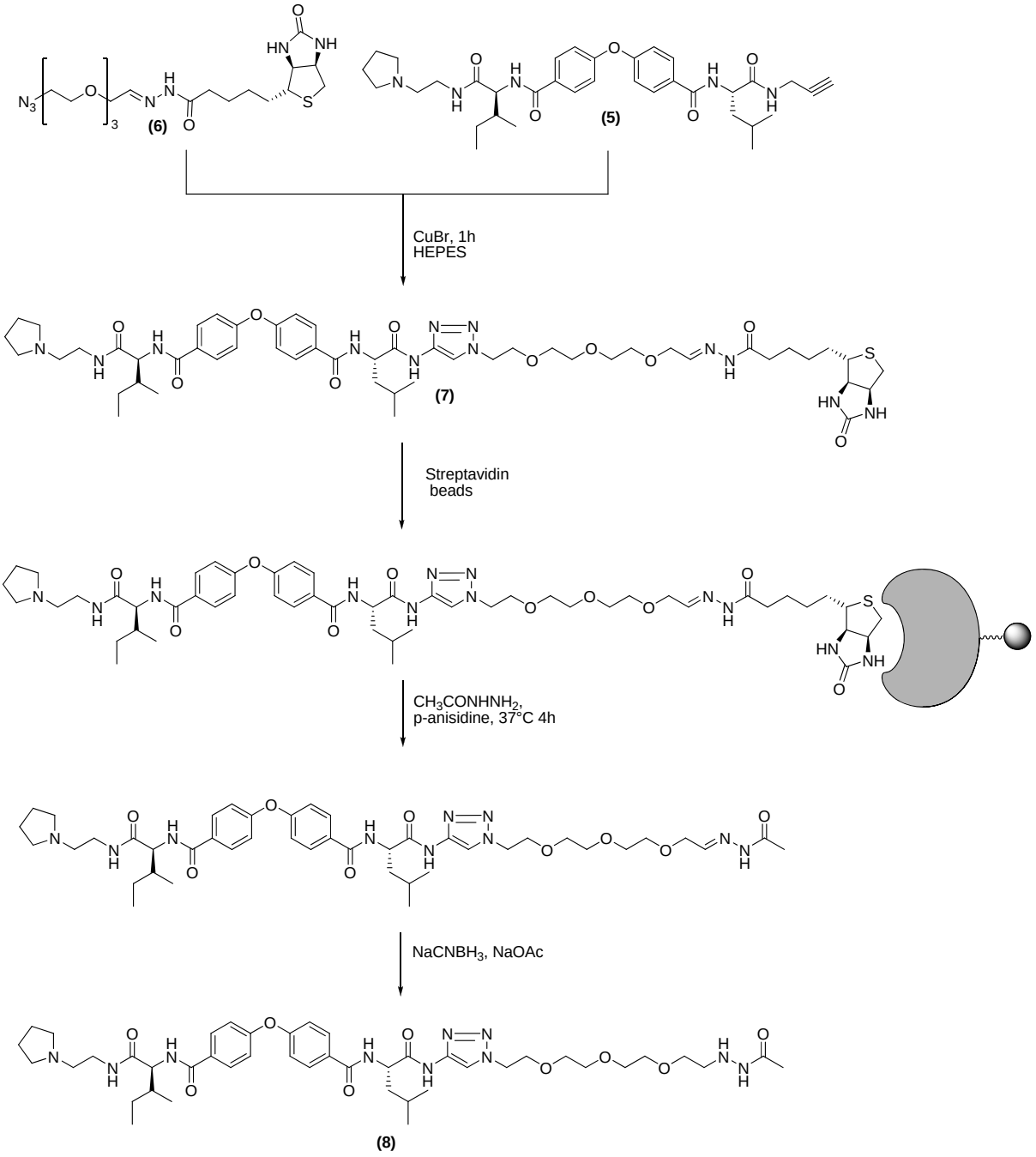
(6)
(5)
CuBr, 1h
HEPES
(7)
Streptavidin
beads
$CH_3CONHNH_2$,
p-anisidine, 37°C 4h
$NaCNBH_3$, NaOAc
(8)

5. Conclusions

In this first part of my PhD thesis I have set up a chemical proteomics methodology in order to identify the biological target of potent antimalarial compounds that were synthesized in Professor Romeo's laboratory.

The identification of the biological target is the first step necessary to start rational SAR studies. Furthermore, this might lead to the identification of a new target for the development of different therapeutics.

In the last decade different approaches have been attempted in order to identify the target of various antimalarial drugs, but has not been obtained any result yet.

As an example, O'Neal *et al* [61] focused their attention on the identification of the target of the antimalarial artemisinin. In particular, within their research, they have focused on the preparation of activity based probes of artemisinin and trioxolane incorporating a biotin moiety for streptavidin affinity "pull down" of covalently tagged target proteins. They have also developed methodology for the integration of a cleavable linker between the biotin tag and the site of attachment to the target protein to permit mild elution of probe labeled proteins and direct identification by HPLC-MS/MS. At the moment it is not yet published any results.

The majority of failures in applying chemical proteomics approaches to malaria can be caused by several factors.

First, the system *Plasmodium*-host red blood cell is a complex biological system characterized by heterogeneous proteins. In addition the parasite is characterized by a complex growth mechanism that develops in several stages and each stage is characterized by different proteins that may or not be expressed. Moreover in the cell lysate there is often the hemozoin, characterized by a core of iron that can cause interference especially when using a proteomic approach characterized by magnetic separations.

In addition proteomic searches using affinity-based chromatography have been severely hampered by low protein recovery yields, protein destruction and denaturation, and the release of background proteins from the support that confound protein identification.

Thus, to identify a protein target in a biologically complex system like *Plasmodium falciparum* could be useful to follow a chemical proteomics approach which is characterized by high selectivity and sensitivity.

The methodology set up during my PhD thesis is characterized by high selectivity and sensitivity as demonstrated by preliminary tests.

In details, the selectivity is due to the presence of an azido cleavable linker, that can recognize with high selectivity the alkyne modified lead compound using click chemistry. Moreover, during the cleavage step, it can release from the streptavidine beads only the proteins that effectively reacted with the modified lead compound.

In addition, the alkyne modified lead compound would recognize with high selectivity the protein targets, thanks to its high activity, limiting aspecific protein binding and thus the presence of background proteins that would greatly complicate the protein identification.

The sensitivity of this method is due to the HPLC-MS/MS analysis that will be performed using an high resolution, high sensitivity mass spectrometer, the LTQ-Orbitrap, able to analyze till 5-10 pM concentrations.

So, future studies will apply this chemical proteomic approach on a *P. falciparum* lysate, prepared by Professor Taramelli's laboratory, in order to identify the protein target or at least its primary sequence, using SDS-PAGE and HPLC-MS/MS analysis.

6. Experimental section

6.1. Abbreviations, materials and methods

Bd: doublet broadened **s**: singlet, **t**: triplet, **bs**: broadened singlet, **d**: doublet, **dd**: double doublet, **m**: multiplet, **bm**: multiplet expanded, **ppm**: parts per million; **Boc**: tert-butoxycarbonyl, **Cbz**: benzyloxycarbonyl ; **Rf**: retention factor; **AcOEt**: ethyl acetate; **DMF**: dimethylformamide; **DMSO**: dimethylsulfoxide **TEA**: triethylamine; **HBTU**: 2 - (1H-benzotriazol-1-yl) -1,1,3,3-tetramethyluronium hexafluorophosphate; **Et_2O**: diethyl ether; **HOBt**: 1-hydroxybenzotriazole; **NMM**: N-methylmorpholine; **TLC**: thin layer Chromatography; **TBTU**: O-(Benzotriazole-1-yl)-N, N, N ', N'-tetramethyluronium tetrafluoroborate; **MeOH**: methanol; Pd / C: palladium on carbon.

For TLC was used silica gel 60 F254 supported on aluminum sheets (Merck). The flash chromatographic columns were carried out using gel silice60 (0040-0063 mm, Merck).
The reagents were purchased from: Sigma Aldrich, Acros, Fluka and Iris Biotech.

The NMR spectra were recorded at 300 MHz NMR Varian Mercury 300 instrument using VX using as solvent DMSO-d_6 or $CDCl_3$. The peaks were assigned by NMR spectroscopy-dimensional (COSY), which is compatible with the structure under examination. The display of TLC was carried out using a UV ray lamp and Camag immersion in 2% phosphomolybdic acid in ethanol.

6.2. General procedures for synthesis

A: Amide bound formation:

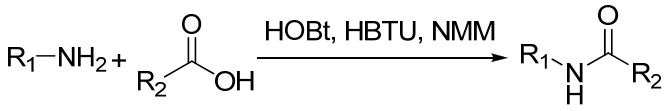

The carboxylic acid (1.1 eq) and the amine (1.0 eq) are dissolved under nitrogen in an appropriate solvent (DMF or dichloromethane) (5mL/mmol), N-methylmorpholine was then added followed by hydroxybenzotriazole solution (HOBt) (1.5 eq). The resulting solution was cooled at 0 °C and *O*-(benzotriazol-1-yl)-*N,N,N′,N′*-tetramethyluronium hexafluorophosphate (HBTU) was added (1.1 eq). The mixture was then stirred at room temperature overnight. Dichloromethane was then added and the organic phase washed with HCl 1N, saturated $NaHCO_3$, water, brine, dried, filtered and concentrated.

B: Removal of the Cbz group by catalytic hydrogenation

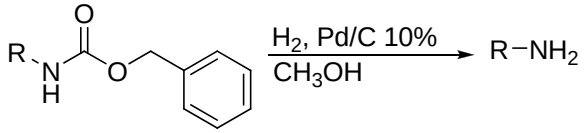

The Cbz protected compound was dissolved in methanol (10 mL/mmol) and then Pd/C (10%) (80 mg/mmol) was added. When the reaction was completed (30-40 min) the mixture was filtrated, washed with methanol and the residue concentrated and used in the next step without any further purification or characterization.

C: Removal of the Boc group

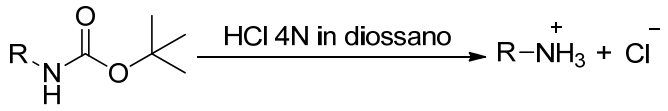

After cooling the Boc protected compound at 0 °C, HCl 4N in dioxane was added (10 mL/g of compound). The mixture was stirred at room temperature for 30 minutes, after this time the

mixture was concentrated and the resi*due washed 3 times with ethyl ether and used in the next step without any further purification or characterization**.**

D: 4,4'oxybisbenzoic acid monosostitution

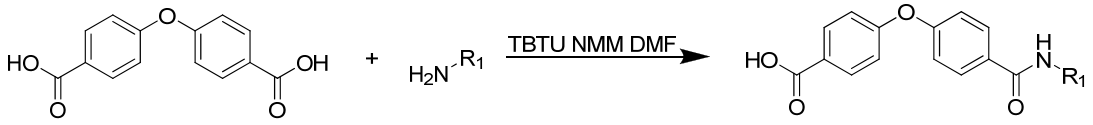

4,4 'oxybisbenzoic acid (1 eq.) and the amino acid (1 eq.) are placed in a flask equipped with a $CaCl_2$ valve. Subsequently they are solubilized in DMF (5 ml for each mmole). The flask is placed in an ice bath to cool the reaction environment before any further additions. TBTU (0.8 eq.) and NMM (3 eq.) are added to pH ≥ 7. The reaction mixture is stirred at room temperature for 1:40 h. The organic phase was then dried and dissolved in CH_2Cl_2. Subsequently the solution was washed with HCl 1N (3 washes) and a saturated solution of NaCl. The organic phase was then dried over Na_2SO_4, filtered and dried under vacuum.

E: Monoamine acylation

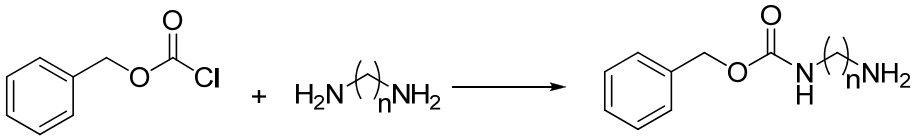

The diamine (1 eq) is dissolved in DCM (8.8 ml/g) and the solution is cooled in a ice bath. A solution of benzilchlorophormiate (3 eq) in DCM is added dropwise over 20 min. The ice bath is removed. The reaction mixture is stirred overnight and extracted with H_2O. The crude product is purified by silica gel flash chromatography.

6.3 General procedures for target identification

F: Click chemistry reaction

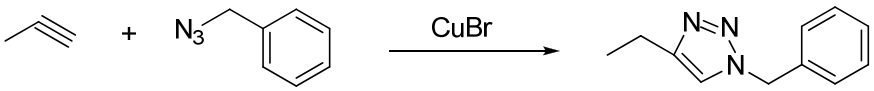

A 5 mM solution (5% CH_3CN/HEPES pH 7.4) of azido-compound is added to a 25 μM solution (HEPES 50 mM ph 7.4) of alkyne compound. Then CuBr is added and the reaction mixture is vigorously stirred at room temperature for 1h. At the end of the reaction the solution appears blu.

G: Immobilization on agarose streptavidin beads

Agarose streptavidin beads is packed into a Pierce Centrifuge column and the column is then placed into a collection tube. The system is centrifuged at 500 rpm for 1 min to remove the storage solution. One column volume (1 ml) of binding buffer (Phosphate-buffer saline) is added on the top of the resin bed. The suspension is centrifuged at 500 rpm for 1 min to remove the buffer. This step is repeated two times discarding buffer from collection tube.

The column is placed in a new collection tube and the sample is added and incubated at room temperature for 10 min. The column is washed with one column volume of binding buffer and centrifuged at 500 rpm for 1 min. This step is repeated four times discarding buffer from the collection tube.

H: Acylhydrazon cleavage

The agarose streptavidin beads are washed with HEPES 15 mM pH 7.4 (10 times, 0.8 ml) centrifuging 1 min at 1000 rpm. HEPES 50 mM is added and the resin is incubated 4h at 37°C with acetyldrazine and p-anisidine gently shaken.

The supernatant (50 ml) was treated with a 10 mM solution of $NaCNBH_3$ (50 ml) in 50 mM NaOAc buffer (pH 3.8) and shacked at room temperature (2 h).

Intermediate 9

(S)-4-(4-(1-methoxy-4-methyl-1-oxopentan-2-ylcarbamoyl)phenoxy)benzoic acid

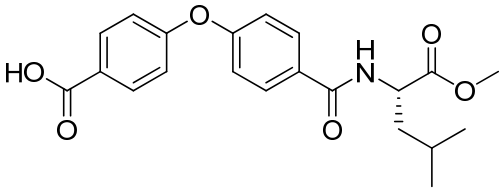

The intermediate **9** has been obtained following general procedure **D** and using the subsequent reagents:

- 1.40 g Leucine methylester HCl, 7.74 mmol (1eq)
- 2,00 g Oxybisbenzoic acid, 7.74 mmol (1eq)
- 11 ml DMF
- 1.98 g TBTU, 6.19 mmol (0.8 eq)
- 3.41 ml NMM, 30.96 mmol (4 eq)

The reaction have been controlled using TLC, CH_2Cl_2/CH_3OH (90:10) and extracted with CH_2Cl_2. The crude product was purified by silica gel flash chromatography (CH_2Cl_2/MeOH+10%NH3, from 99:1 to 95:5). The intermediate was a yellow oil. The reaction yield was 28.2%

^{1}H NMR (300 MHz, DMSO) δ 8.73 (d, *J* = 7.4 Hz, 1H), 7.97 (d, *J* = 8.3 Hz, 4H), 7.15 (dd, *J* = 22.2, 8.5 Hz, 4H), 4.60 – 4.41 (m, 1H), 3.64 (s, 3H), 1.86 – 1.50 (m, 3H), 0.90 (dd, *J* = 13.5, 6.2 Hz, 6H).

Intermediate 10

benzyl 2-aminoethylcarbamate

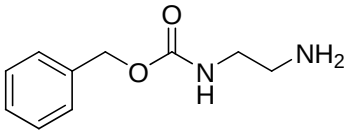

The intermediate **10** has been obtained following general procedure **E** and using the subsequent reagents:

- 2 g Ethylendiammine, 33.27 mmol 1 (eq)
- 2.45 g Benzychlorophormiate, 14.41 mmol (3eq)
- 19.74 ml DCM

The reaction have been controlled using TLC, CH_2Cl_2/CH_3OH (90:10) and extracted with H_2O. The crude product was purified by silica gel flash chromatography (CH_2Cl_2/MeOH+10%NH3, from 99:1 to 85:15). The intermediate was a white solid. The reaction yield was 22%

^{1}H NMR (300 MHz, $CDCl_3$) δ 7.46 – 7.28 (m, 5H), 5.10 (s, 4H), 3.26 (dd, *J* = 11.5, 5.7 Hz, 2H), 2.83 (t, *J* = 5.9 Hz, 2H).

Intermediate 11

(S)- ter-butyl N-(1-(2-((benzyloxy)carbonil)amino)ethyl)carbamoyl)-3-methylbutyl)carbamate

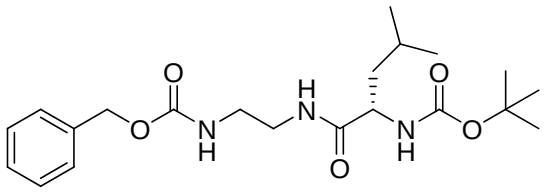

The intermediate **11** has been obtained coupling intermediate **10** and BocLeuOH following general procedure **A** and using the subsequent reagents:

- 0.852 g BocLeuOH, 3.41 mmol (1.1 eq)
- 0.640 g intermediate **10**; 3.109 mmol (1 eq)
- 0.713 g HOBT, 4.663 mmol (1.5 eq)
- 1.415 g HBTU, 3.730 mmol (1.2 eq)
- 7 ml DMF
- 1.36 ml NMM, 12.43 mmol (4 eq)

The reaction have been controlled using TLC, CH_2Cl_2/CH_3OH (90:10) and extracted with CH_2Cl_2. The crude product was purified by silica gel flash chromatography (CH_2Cl_2/MeOH+10%NH3, from 99:1 to 85:15). The intermediate was a yellow oil. The reaction yield was 58.%

^{1}H NMR (300 MHz, $CDCl_3$) δ 7.40 – 7.28 (m, 5H), 6.64 (s, 1H), 5.32 (d, *J* = 26.5 Hz, 1H), 5.09 (s, 2H), 4.89 (s, 1H), 4.03 (d, *J* = 4.2 Hz, 1H), 3.52 – 3.21 (m, 4H), 1.65 (dd, *J* = 12.0, 6.5 Hz, 2H), 1.51 – 1.34 (m, 10H), 0.99 – 0.82 (m, 6H).

Intermediate 12

(S)-methyl 2-(4-(4-((S)-1-(2-(benzyloxycarbonylamino)ethylamino)-4-methyl-1-oxopentan-2-ylcarbamoyl)phenoxy)benzamido)-4-methylpentanoate

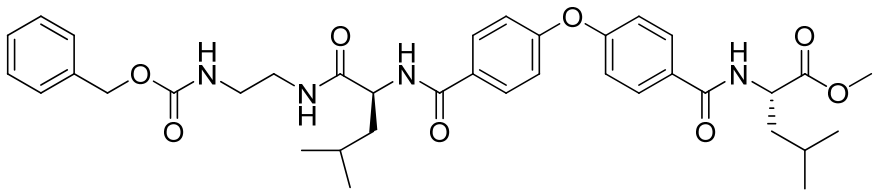

The intermediate **12** has been obtained coupling (general procedure **A**) intermediate **9** and intermediate **11**, previously deprotected using procedure **C**.

For the deprotection reaction have been used the following reagents:

- 8.07 ml HCl in dioxane anidre
- 0.807 g intermediate **11**, 1.98 mmol (1 eq)

For the coupling reaction have been used the following reagents:

- 0.843 g intermediate **9**, 2.18 mmol (1.1 eq)
- 0.901 g HBTU, 2.376 mmol (1.2 eq)
- 5 ml DMF
- 0.654 ml NMM, 5.94 mmol (3 eq)

The reaction have been controlled using TLC, CH_2Cl_2/CH_3OH (90:10) and extracted with CH_2Cl_2. The crude product was purified by silica gel flash chromatography (CH_2Cl_2/MeOH+10%NH3, from 99:1 to 95:5). The intermediate was a white solid. The reaction yield was 43.7%

^{1}H NMR (300 MHz, $CDCl_3$) δ 7.85 – 7.70 (m, 4H), 7.37 – 7.27 (m, 4H), 7.08 (s, 1H), 6.91 (d, *J* = 8.6 Hz, 5H), 5.40 (s, 1H), 5.30 (s, 1H), 5.12 – 4.99 (m, 2H), 4.83 (dd, *J* = 14.8, 7.0 Hz, 1H), 4.66 (d, *J* = 5.7 Hz, 1H), 3.77 (s, 3H), 3.32 (s, 4H), 1.88 – 1.58 (m, 6H), 0.98 (dd, *J* = 12.3, 4.9 Hz, 12H).

Compound 1

(S)-methyl 2-(4-(4-((S)-1-(2-(3,6-dihydroxy-3'-oxo-3'H,10H-spiro[anthracene-9,1'-isobenzofuran]-4'-ylcarboxamido)ethylamino)-4-methyl-1-oxopentan-2-ylcarbamoyl)phenoxy)benzamido)-4-methylpentanoate

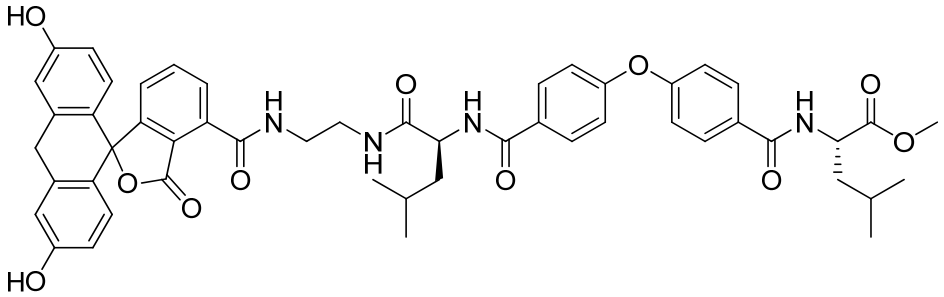

Compound **1** has been obtained coupling (general procedure **A**) carboxy-fluoresceine and intermediate **12**, previously deprotected using procedure **B**.

For the deprotection reaction have been used the following reagents:

- 2.41 ml MeOH
- 0.019 g Pd/C
- 0.162 g intermediate **12**, 0.241 mmol (1.1 eq)

For the coupling reaction have been used the following reagents:

- 0.100 g carboxy-fluoresceine, 0.265 mmol (1 eq)
- 0.110 g HATU, 0.289 mmol (1.2 eq)
- 1 ml DMF
- 96.5 ml NMM, 1.205 mmol (5 eq)

The reaction have been controlled using TLC, CH_2Cl_2/CH_3OH (90:10) and digested with CH_2Cl_2. The product have been than crystallized from CH_2Cl_2. No further purifications have been done.

^{1}H NMR (300 MHz, DMSO) δ 10.16 (s, 2H), 8.88 – 8.56 (m, 1H), 8.56 – 8.30 (m, 1H), 7.95 (d, *J* = 6.7 Hz, 4H), 7.69 – 7.28 (m, 1H), 7.19 – 6.99 (m, 4H), 6.66 (dd, *J* = 39.7, 23.2 Hz, 4H), 5.76 (s, 2H), 4.49 (s, 2H), 3.64 (s, 4H), 3.33 (s, 9H), 1.90 – 1.41 (m, 6H), 1.18 – 0.66 (m, 12H).

Compound 2

(S)-methyl 2-(4-(4-((S)-1-(2-(7-(diethylamino)-2-oxo-2H-chromene-3-carboxamido)ethylamino)-4-methyl-1-oxopentan-2-ylcarbamoyl)phenoxy)benzamido)-4-methylpentanoate

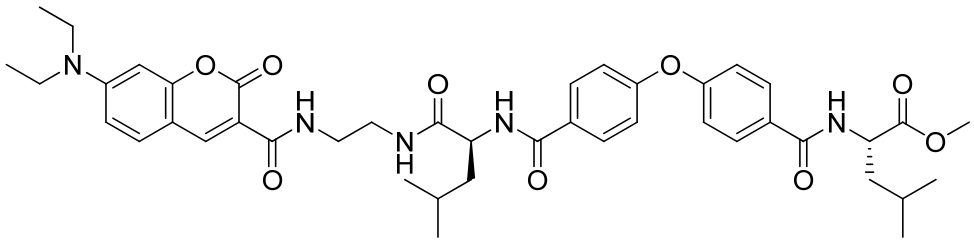

Compound **2** has been obtained coupling (general procedure **A**) carboxy-coumarine and intermediate **12**, previously deprotected using procedure **B**.

For the deprotection reaction have been used the following reagents:

- 2.0 ml MeOH
- 0.016 g Pd/C
- 0.116 g intermediate **12**, 0.173 mmol (1 eq)

For the coupling reaction have been used the following reagents:

- 0.050g carboxy-coumarine, 0.191 mmol (1.1 eq)
- 0.079 g HATU, 0.208 mmol (1.2 eq)
- 0.8 ml DMF
- 0.076 ml NMM, 0.692 mmol (4 eq)

The reaction have been controlled using TLC, CH_2Cl_2/CH_3OH (90:10) and extracted with CH_2Cl_2. The crude product was purified by silica gel flash chromatography (CH_2Cl_2/MeOH, from 100 to 97:3). The intermediate was a yellow solid. The reaction yield was 56.6.%

^{1}H NMR (300 MHz, $CDCl_3$) δ 9.04 (d, *J* = 5.6 Hz, 1H), 8.57 (s, 1H), 7.82 (dd, *J* = 11.2, 8.7 Hz, 4H), 7.41 (d, *J* = 8.9 Hz, 1H), 7.01 (d, *J* = 7.2 Hz, 4H), 6.80 (d, *J* = 8.1 Hz, 1H), 6.69 (d, *J* = 8.9 Hz, 1H), 6.61 – 6.47 (m, 1H), 4.90 – 4.80 (m, 1H), 4.77 – 4.64 (m, 1H), 3.77 (s, 3H), 3.67 – 3.36 (m, 8H), 1.91 – 1.60 (m, 6H), 1.29 – 1.17 (m, 6H), 1.03 – 0.90 (m, 12H).

Compound 3

(S)-methyl 2-(4-(4-((S)-1-(2-(5-(dimethylamino)naphthalene-1-sulfonamido)ethylamino)-4-methyl-1-oxopentan-2-ylcarbamoyl)phenoxy)benzamido)-4-methylpentanoate

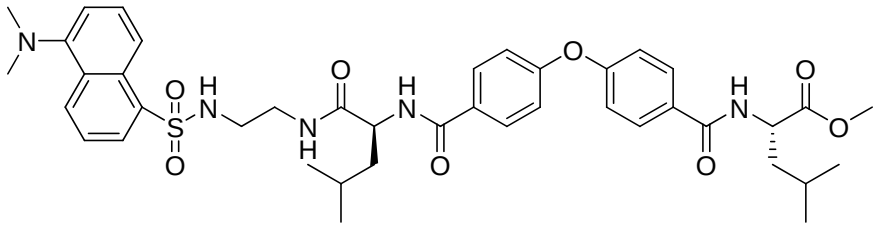

Compound **3** has been obtained coupling (general procedure **A**) dansyl and intermediate **12**, previously deprotected using procedure **B**.

For the deprotection reaction have been used the following reagents:

- 5.0 ml MeOH
- 0.040 g Pd/C
- 0.192 g intermediate **12**, 0.285 mmol (1 eq)

For the coupling reaction have been used the following reagents:

- 0.100 g dansyl, 0.370 mmol (1.3 eq)
- 10 ml DCM
- 0.06 ml NMM, 0.57 mmol (2 eq)

The reaction have been controlled using TLC, CH_2Cl_2/CH_3OH (90:10). The crude product was purified by silica gel flash chromatography (CH_2Cl_2/MeOH, from 100 to 97:3). The intermediate was a yellow solid. The reaction yield was 58.5%

^{1}H NMR (300 MHz, $CDCl_3$) δ 8.58 (s, 2H), 8.43 – 8.29 (m, 1H), 8.18 (d, *J* = 7.1 Hz, 1H), 7.92 – 7.71 (m, 5H), 7.61 – 7.43 (m, 2H), 7.20 (s, 1H), 7.08 – 6.78 (m, 5H), 6.13 (s, 1H), 4.84 (d, *J* = 11.0 Hz, 1H), 4.57 (d, *J* = 6.7 Hz, 1H), 3.78 (s, 3H), 3.31 (dd, *J* = 24.9, 16.5 Hz, 2H), 3.23 – 2.99 (m, 2H), 2.98 – 2.80 (m, 6H), 1.75 (dd, *J* = 22.9, 18.2 Hz, 6H), 0.95 (dd, *J* = 15.3, 3.6 Hz, 12H).

Intermediate 13
benzyl 3-aminopropylcarbamate

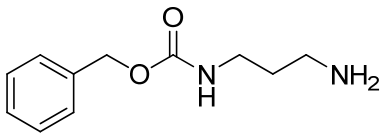

The intermediate **13** has been obtained following general procedure **E** and using the subsequent reagents:

- 3.0 g diaminopropane, 36,00 mmol (3 eq)
- 2.21 g benzylchlorophormiate, 12,00 (1 eq)
- 26.6 ml DCM

The reaction have been controlled using TLC, CH_2Cl_2/CH_3OH (90:10) and extracted with H_2O. No further purifications have been done. The reaction yield was 78.5% .

^{1}H NMR (300 MHz, $CDCl_3$) δ 7.34 (s, 5H), 5.13 (d, *J* = 22.9 Hz, 4H), 3.35 – 3.15 (m, 2H), 2.79 (dd, *J* = 12.8, 6.4 Hz, 2H), 1.73 – 1.58 (m, 2H).

Intermediate 14

(S)-ter-butyl N-(1-(3-((benzyloxy)carbonil)amino)propyl)carbamoyl)-3-methylbutyl)carbamate

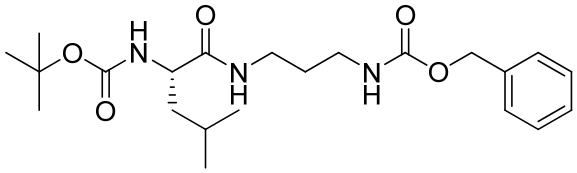

The intermediate **14** has been obtained coupling intermediate **13** and Boc-Leucine following general procedure **A** and using the subsequent reagents:

- 0.466 g intermediate **13**, 2.240 mmol (1 eq)
- 0.569 g BocLeuOH, 2.462 mmol (1.1 eq)
- 1.024 g HBTU, 2.69 mmol (1.2 eq)
- 0.466 g HOBT, 3.40 mmol (1.5 eq)
- 10 ml DCM
- 0.490 ml NMM, 4.480 mmol (4 eq)

The reaction have been controlled using TLC, CH_2Cl_2/CH_3OH (90:10) and extracted with CH_2Cl_2. The crude product have been digested with Et_2O. No further purification have been done. The reaction yield was 90.0%.

^{1}H NMR (300 MHz, $CDCl_3$) δ 7.38 – 7.28 (m, 5H), 5.09 (s, 2H), 4.04 (s, 1H), 3.38 – 3.13 (m, 4H), 1.65 (dd, *J* = 14.3, 8.3 Hz, 4H), 1.45 (d, *J* = 14.3 Hz, 10H), 0.93 (d, *J* = 3.9 Hz, 6H).

Intermediate 15

tert-butyl (2S,3R)-3-methyl-1-oxo-1-(2-(pyrrolidin-1-yl)ethylamino)pentan-2-ylcarbamate

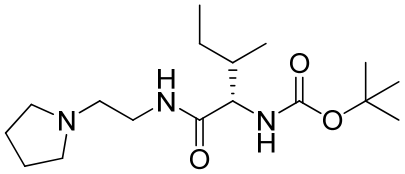

The intermediate **15** has been obtained coupling 1-(2-aminoethyl)pyrrolidine and Boc-Isoleucine following general procedure **A** and using the subsequent reagents:

- 3.00 g BocIleOH, 12.97 mmol (1.1 eq)
- 2.69 g 1-(2-aminoethyl)pyrrolidine, 23.58 mmol (2 eq)
- 2.38 g HOBT, 17.68 mmol (1.5 eq)
- 4.54 g TBTU, 14.14 mmol (1.2 eq)
- 10 ml DCM
- 3 ml NMM, 27.11 mmol (2.5eq)

The reaction have been controlled using TLC, CH_2Cl_2/CH_3OH (90:10) and extracted with CH_2Cl_2. The crude product have been digested with Et_2O/AcOEt. No further purification have been done. The reaction yield was 79.0%

^{1}H NMR (300 MHz, $CDCl_3$) δ 6.48 (s, 2H), 4.02 – 3.83 (m, 1H), 3.45 – 3.28 (m, 2H), 2.70 – 2.44 (m, 6H), 1.78 (s, 5H), 1.46 (d, *J* = 20.4 Hz, 11H), 0.90 (t, *J* = 7.0 Hz, 6H).

Intermediate 16

4-(4-((2S,3R)-3-methyl-1-oxo-1-(2-(pyrrolidin-1-yl)ethylamino)pentan-2-ylcarbamoyl)phenoxy)benzoic acid

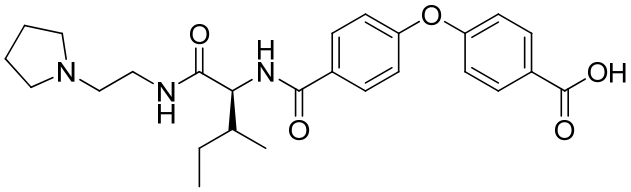

Intermediate **16** has been obtained coupling (general procedure **D**) 4,4'-oxybisbenzoic acid and intermediate **15**, previously deprotected using procedure **C**.

For the deprotection reaction have been used the following reagents:

- 10 ml HCl in dioxane anidre
- 1.016 g intermediate **15**, 3.10 mmol (1 eq)

For the coupling reaction have been used the following reagents:

- 0.800 g 4,4'oxybisbenzoic acid, 3.10 mmol (1 eq)
- 1.175 g HBTU, 3.10 mmol (1 eq)
- 7 ml DMF
- 2 ml NMM, 18.6 mmol (6 eq)

The reaction have been controlled using TLC, CH_2Cl_2/CH_3OH (90:10). The crude product was purified by silica gel flash chromatography (CH_2Cl_2/MeOH, from 99:1 to 97:3). The intermediate was a white solid. The reaction yield was 59%.

^{1}H NMR (300 MHz, $CDCl_3$) δ 7.85 – 7.70 (m, 4H), 7.37 – 7.27 (m, 4H) δ 6.48 (s, 2H), 4.02 – 3.83 (m, 1H), 3.45 – 3.28 (m, 2H), 2.70 – 2.44 (m, 6H), 1.78 (s, 5H), 1.46 (m, 2H), 0.90 (t, *J* = 7.0 Hz, 6H).

Intermediate 17

benzyl 3-((S)-4-methyl-2-(4-(4-((2S,3R)-3-methyl-1-oxo-1-(2-(pyrrolidin-1-yl)ethylamino)pentan-2-ylcarbamoyl)phenoxy)benzamido)pentanamido)propylcarbamate

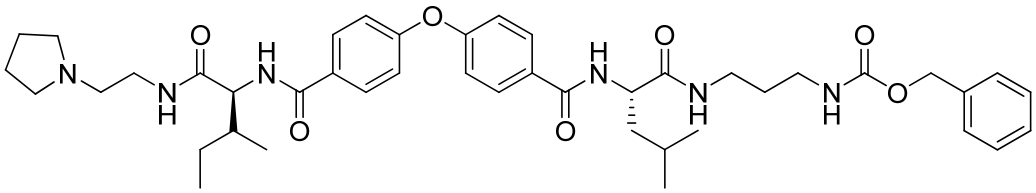

Intermediate **17** has been obtained coupling (general procedure **A**) intermediate **16** and intermediate **14**, previously deprotected using procedure **(C)**.

For the deprotection reaction have been used the following reagents:

- 8 ml HCl in dioxane anidre
- 0.704 g intermediate **14**, 1.67 mmol (1 eq)

For the coupling reaction have been used the following reagents:

- 0.859 g intermediate **16**, 1.83 mmol (1.1 eq)
- 0.695 g HATU, 1.83 mmol (1.1 eq)
- 5 ml DMF
- 1.104 ml NMM, 10.02 mmol (6 eq)

The reaction have been controlled using TLC, CH_2Cl_2/CH_3OH (90:10) and extracted with CH_2Cl_2. The crude product was purified by silica gel flash chromatography (CH_2Cl_2/MeOH, from 100 to 97:3). The intermediate was a yellow solid. The reaction yield was 28%

^{1}H NMR (300 MHz, $CDCl_3$) δ 8.05 – 7.70 (m, 4H), 7.29 (d, *J* = 10.6 Hz, 5H), 6.85 (dd, *J* = 16.2, 8.2 Hz, 4H), 5.57 (s, 1H), 5.08 (d, *J* = 17.5 Hz, 2H), 4.74 – 4.61 (m, 1H), 4.58 (t, *J* = 7.3 Hz, 1H), 3.64 (s, 1H), 3.49 (s, 1H), 3.35 – 2.97 (m, 6H), 2.21 – 1.94 (m, 7H), 1.89 – 1.52 (m, 8H), 1.44 – 1.18 (m, 1H), 1.09 – 0.83 (m, 12H).

Compound 4

7-(diethylamino)-N-(3-((S)-4-methyl-2-(4-(4-((2S,3R)-3-methyl-1-oxo-1-(2-(pyrrolidin-1-yl)ethylamino)pentan-2-ylcarbamoyl)phenoxy)benzamido)pentanamido)propyl)-2-oxo-3,8a-dihydro-2H-chromene-3-carboxamide

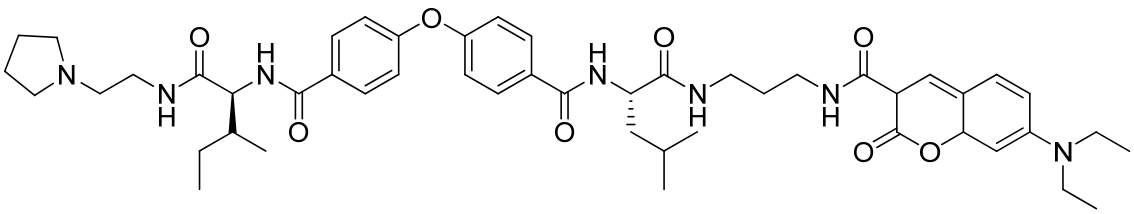

Compound **4** has been obtained coupling (general procedure **A**) carboxy-coumarinee and intermediate **17**, previously deprotected using procedure **B**.

For the deprotection reaction have been used the following reagents:

- 10.0 ml MeOH
- 0.080 g Pd/C
- 0.100 g intermediate **17**, 0.129 mmol (1 eq)

For the coupling reaction have been used the following reagents:

- 0.037 g carboxy-coumarinee, 0.142 mmol (1.1 eq)
- 0.053g HATU, 0.142 mmol (1.1 eq)
- 1 ml DMF
- 0.5 ml DCM
- 0.028 ml NMM, 0.258 mmol, (2 eq)

The reaction have been controlled using TLC, CH_2Cl_2/CH_3OH (90:10) and extracted with CH_2Cl_2. The crude product have been digested with Et_2O. No further purification have been done. The reaction yield was 83.0%.

^{1}H NMR (300 MHz, $CDCl_3$) δ 8.93 (s, 1H), 8.06 – 7.66 (m, 4H), 7.64 – 7.31 (m, 2H), 6.97 (dd, *J* = 12.8, 8.7 Hz, 4H), 6.65 (d, *J* = 8.9 Hz, 1H), 6.49 (s, 1H), 4.82 – 4.57 (m, 2H), 3.75 (s, 1H), 3.61 – 3.21 (m, 10H), 3.00 (d, *J* = 29.6 Hz, 7H), 2.24 – 1.49 (m, 11H), 1.38 – 1.10 (m, 6H), 0.95 (dd, *J* = 17.6, 10.1 Hz, 12H).

Intermediate 18

(S)-tert-butyl 4-methyl-1-oxo-1-(prop-2-ynylamino)pentan-2-ylcarbamate

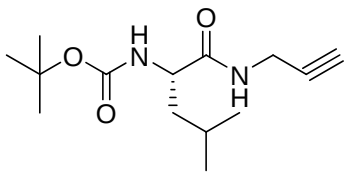

Intermediate **18** has been obtained coupling (general procedure **A**) Boc-Leucine and propargylamine using the subsequent reagents:

- 1.00 g BocLeuOH, 4.01 mmol (1.1 eq)
- 0.401 g propargylamine, 7.29 mmol (2 eq)
- 0.837 g HOBT, 5.47 mmol (1.5 eq)
- 1.70g HBTU, 4.37 mmol (1.2 eq)
- 10 ml DCM
- 0.080 ml NMM, 7.3 mmol (2 eq)

The reaction have been controlled using TLC, CH_2Cl_2/CH_3OH (90:10) and extracted with CH_2Cl_2. The crude product was purified by silica gel flash chromatography (CH_2Cl_2/MeOH, from 100 to 98:2). The intermediate was a white solid. The reaction yield was 58.3%.

^{1}H NMR (300 MHz, $CDCl_3$) δ 6.58 (s, 1H), 4.90 (s, 1H), 4.19 – 3.98 (m, 3H), 2.21 (t, *J* = 2.5 Hz, 1H), 1.75 – 1.58 (m, 1H), 1.57 – 1.36 (m, 11H), 0.93 (dd, *J* = 6.0, 4.1 Hz, 6H).

Intermediate 19

4-(4-(benzyloxycarbonyl)phenoxy)benzoic acid

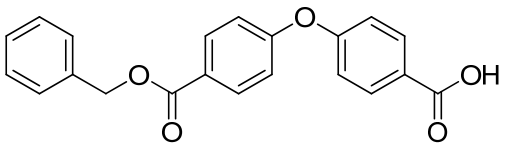

Acid 4.4 '-ossibisbenzoico (5.00 g, 19:36 mmol) is dissolved into a flask with DMF (10 ml for each gram of acid), then is added TEA (3.23 ml, 23.2 mmol). Benzyl bromide (2.77 ml, 23,23 mmol) and is added dropwise to the reaction mixture. It is than reacted for 3 hours at 60° C and controlled with a TLC, CH_2Cl_2/CH_3OH (90:10). DMF is evaporated the in vacuo and the crude product is extracted with AcOEt, following these washes: three times with 2N HCl, 1 time with distilled water and 1 time with a saturated solution of NaCl. The organic phase is evaporated in vacuo and the obtained solid is washed with $CHCl_3$ (about 30 ml), and filtered. Subsequently, after that the organic phase is evaporated and the crude product is digested with CH_2Cl_2. The final product is a white solid. The reaction yield is 53%.

^{1}H NMR (300 MHz, DMSO) 12.96 (bs, 1H); 8.02 (m, 4H); 7.4 (m, 5H); 7.2 (m, 4H); 5.35 (s, 2H).

Intermediate 20

benzyl 4-(4-((2S,3R)-3-methyl-1-oxo-1-(2-(pyrrolidin-1-yl)ethylamino)pentan-2-ylcarbamoyl)phenoxy)benzoate

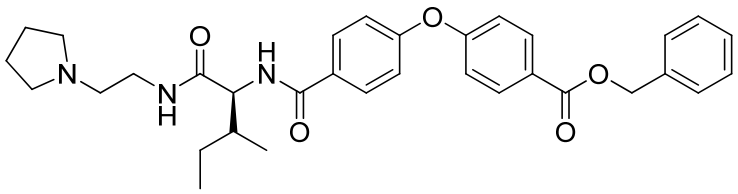

Intermediate **20** has been obtained coupling (general procedure **A**) intermediate **19** and intermediate **15**, previously deprotected using procedure **C**.

For the deprotection reaction have been used the following reagents:

- 13.97 ml HCl in dioxane anidre
- 1.397 g intermediate **15**, 4.27 mmol (1 eq)

For the coupling reaction have been used the following reagents:

- 1.640 g intermediate **19**, 4.69 mmol (1.1 eq)
- 1.944 g HBTU, 5.12 mmol (1.2eq)
- 5.0 ml DMF
- 2.36 ml NMM, 21.41 mmol (5 eq)

The reaction have been controlled using TLC, CH_2Cl_2/CH_3OH (90:10) and extracted with CH_2Cl_2. The crude product have been digested with Et_2O. No further purifications have been done. The reaction yield was 88.0%.

^{1}H NMR (300 MHz, $CDCl_3$) δ 8.06 (dt, *J* = 12.8, 6.6 Hz, 4H), 7.74 (s, 1H), 7.39 (tt, *J* = 13.5, 7.1 Hz, 5H), 7.03 (dt, *J* = 19.7, 9.8 Hz, 4H), 5.36 (s, 2H), 4.70 (dd, *J* = 8.7, 6.1 Hz, 1H), 3.89 – 3.69 (m, 1H), 3.50 – 3.33 (m, 1H), 3.05 (d, *J* = 25.8 Hz, 6H), 2.19 – 1.96 (m, 5H), 1.64 – 1.48 (m, 1H), 1.37 – 1.18 (m, 1H), 0.98 (dq, *J* = 14.7, 7.4 Hz, 6H).

Compound 5

N-((2S,3R)-3-methyl-1-oxo-1-(2-(pyrrolidin-1-yl)ethylamino)pentan-2-yl)-4-(4-((S)-4-methyl-1-oxo-1-(prop-2-ynylamino)pentan-2-ylcarbamoyl)phenoxy)benzamide

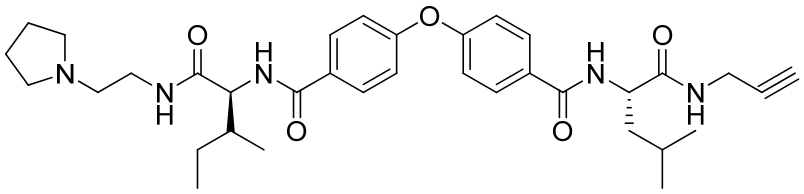

Compound **5** has been obtained coupling (general procedure **A**) intermediate **20**, previously deprotected using procedure **B** and intermediate **18**, previously deprotected using procedure **C**.

For the intermediate **20** deprotection reaction have been used the following reagents:

- 51.5 ml MeOH
- 0.412 g Pd/C
- 0.588 g intermediate **20**, 1.05 mmol (1.1 eq)

For the intermediate **18** deprotection have been used the following reagents:

- 2.56 ml HCl in dioxane anidre
- 0.257 g intermediate **18**, 0.96 mmol (1 eq)

For the coupling reaction have been used the following reagents:

- 0.437 g HBTU, 1.056 mmol (1.2 eq)
- 5.5 ml DMF
- 0.212 ml NMM, 1.92 mmol (2eq)
-

The reaction have been controlled using TLC, CH_2Cl_2/CH_3OH (90:10) and extracted with CH_2Cl_2. The crude product was purified by silica gel flash chromatography (CH_2Cl_2/MeOH+10%NH3 from 100 to 90:10). The intermediate was a white solid. The reaction yield was 63.3%.

^{1}H NMR (300 MHz, $CDCl_3$) δ 8.24 – 7.91 (m, 3H), 7.68 (dd, *J* = 40.8, 8.3 Hz, 4H), 6.64 (dd, *J* = 30.8, 8.1 Hz, 4H), 4.88 (d, *J* = 6.7 Hz, 1H), 4.53 (t, *J* = 8.0 Hz, 1H), 4.17 – 3.85 (m, 2H), 3.80 – 3.47 (m, 2H), 3.07 (s, 6H), 2.30 – 2.16 (m, 1H), 2.01 (s, 4H), 1.91 – 1.59 (m, 5H), 1.44 – 1.19 (m, 2H), 1.11 – 0.83 (m, 12H).

Intermediate 21

2-(2-(2-(2-hydroxyethoxy)ethoxy)ethoxy)ethyl 4-methylbenzenesulfonate

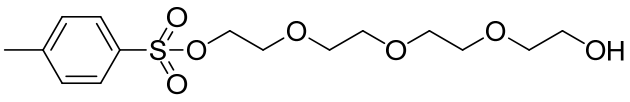

An NaOH aqueous solution (0.69g / 4 mL) was added to a THF solution (4 mL) of tetraethylene glycol (21.95 g, 113 mmol) at 0 °C and then a THF solution (13 mL) of *p*-toluenesulfonyl chloride (2.08 g, 10.93 mmol) was added while stirring (1 h). After stirring at 0 °C (2 h), the reaction mixture was poured into ice H2O (65 mL). The organic layer was separated, and the aqueous layer was extracted with CH_2Cl_2 (3 × 50 mL). The combined organic layers were washed twice with H_2O (50 mL). The organic layer was dried (Na_2SO_4) and evaporated in vacuo to yield 3.64 g (96%) of crude product as a yellow oil. No further purifications have been done.

^{1}H NMR (300 MHz, $CDCl_3$) δ 7.79 (d, *J* = 8.3 Hz, 2H), 7.33 (d, *J* = 8.1 Hz, 2H), 4.20 – 4.10 (m, 3H), 3.76 – 3.50 (m, 14H), 2.43 (s, 3H).

Intermediate 22

2-(2-(2-(2-azidoethoxy)ethoxy)ethoxy)ethanol

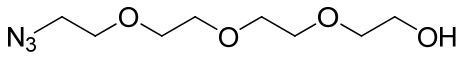

NaN3 (1.40 g, 21.55 mmol) was added to an EtOH solution (60 mL) of intermediate **21** (3.00 g, 8.62 mmol). After stirring at 70 °C (18 h), H_2O (50 mL) was added and the solvent was concentrated to ~1/3 volume in vacuo. The remaining solution was extracted with EtOAc (3 × 50 mL). The combined organic phases were dried (Na_2SO_4) and evaporated in vacuo, and the crude product purified by column chromatography (CH_2Cl_2/MeOH from 100 to 98:2) to yield (86%) of compound as a yellow oil.

^{1}H NMR (300 MHz, $CDCl_3$) δ 3.80 – 3.56 (m, 14H), 3.40 (t, *J* = 4.4 Hz, 2H), 2.24 (s, 1H).

Intermediate 23

2-(2-(2-(2-azidoethoxy)ethoxy)ethoxy)acetaldehyde

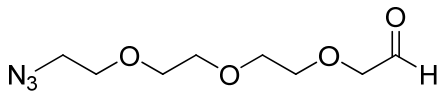

To an anhydrous CH_2Cl_2 solution (2 ml) of oxalyl chloride (0.10 ml, 1.10 mmol) maintained at -78°C under Argon was slowly added freshly distilled DMSO (0.19 ml, 3.29 mmol). The mixture was sti-rred (30 min), and then intermediate **22** (0.20 g, 0.91 mmol) was added via syringe. The mixture was stirred for an additional 30 min at -78°C, and then Et_3N (0.78 ml, 6.57 mmol) was added (10 min) and the mixture was stirred (15 min) at this temperature and warmed to ambient temperature. The reaction solution was diluted with CH_2Cl_2 (10 ml) and washed with H_2O (2 x 10 ml). The organic layer was dried (Na_2SO_4), and evaporated under vacuo obtaining intermediate **23**. The yield of reaction is 62%.

^{1}H NMR (300 MHz, $CDCl_3$) δ 9.73 (s, 1H), 4.17 (s, 2H), 3.79 – 3.55 (m, 8H), 3.39 (t, *J* = 4.7 Hz, 2H), 1.45 (dt, *J* = 18.9, 7.3 Hz, 2H).

Intermediate 24

methyl 5-((3aS,4R,6aR)-2-oxohexahydro-1H-thieno[3,4-d]imidazol-4-yl)pentanoate

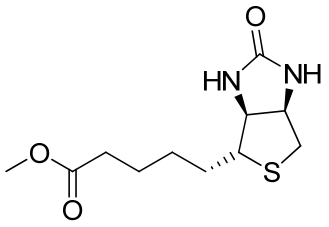

$SOCl_2$ is added dropwise to a biotin suspension in MeOH. The solution is stirred overnight at room temperature. The solvent is than evaporated under vacuo. No further purification have been done. The yield of reaction is 80%

For the reaction have been used the following reagents:

- 0.100 g biotin, 0.410 mmol
- 1.0 ml MeOH
- 0.967 ml $SOCl_2$

^{1}H NMR (300 MHz, DMSO) δ 9.05 (s, 2H), 6.51 (d, *J* = 50.3 Hz, 2H), 5.86 (s, 3H), 5.38 (s, 1H), 5.11 (dd, *J* = 12.0, 4.2 Hz, 1H), 5.00 – 4.71 (m, 1H), 4.59 (t, *J* = 6.8 Hz, 2H), 4.11 – 3.40 (m, 6H).

Intermediate 25

5-((3aS,4R,6aR)-2-oxohexahydro-1H-thieno[3,4-d]imidazol-4-yl)pentanehydrazide

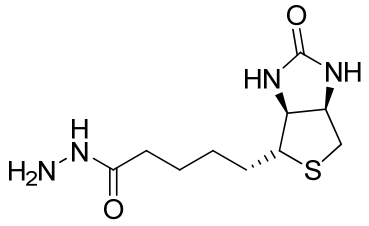

Hydrazine is added to a MeOH solution of intermediate **24**. The reaction mixture is stirred at room temperature for 16h. The solution is concentrated and then diluted with H_2O. (14.2 ml) The aqueous phase is washed with $CHCl_3$ (9 ml x 3). The aqueous solution is evaporated under vacuum obtaining intermediate **25**. The reaction yield is 71.3%

For the reaction have been used the following reagents:

- 0.084 g intermediate **(24)**, 0.328 mmol
- 0.720 ml MeOH
- 0.140 ml hydrazine, 2.88 mmol

^{1}H NMR (300 MHz, DMSO) δ 8.95 (s, 1H), 6.41 (d, *J* = 18.9 Hz, 2H), 4.36 – 4.22 (m, 1H), 4.12 (s, 1H), 3.49 – 3.23 (m, 1H), 3.09 (s, 1H), 2.80 (dt, *J* = 21.7, 10.9 Hz, 1H), 2.60 – 2.52 (m, 2H), 2.08 – 1.88 (m, 2H), 1.69 – 1.14 (m, 6H).

Compound 6

(E)-N'-(2-(2-(2-(2-azidoethoxy)ethoxy)ethoxy)ethylidene)-5-((3aS,4R,6aR)-2-oxohexahydro-1H-thieno[3,4-d]imidazol-4-yl)pentanehydrazide

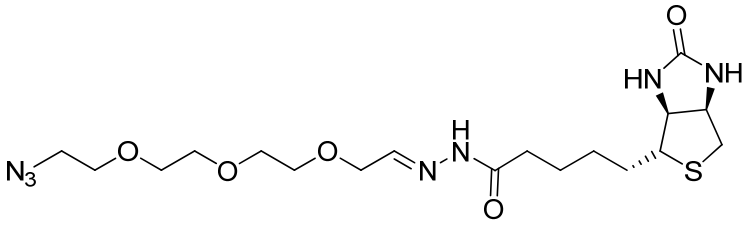

Compound **6** has been obtained stirring overnight a solution of intermediate **23** in CH_2Cl_2 and a solution of intermediate **25** in THF/H_2O (1:1) using the following reagents:

- 0.270 g intermediate **23**, 1.24 mmol (1.5 eq)
- 1.41 ml CH_2Cl_2
- 0.211 g intermediate **25**, 0.82 mmol (1 eq)
- 7.07 ml THF/H_2O (1:1)

The reaction have been controlled using TLC, CH_2Cl_2/CH_3OH (90:10). The crude product was purified by silica gel flash chromatography (CH_2Cl_2/MeOH from 100 to 90:10). The intermediate was a white solid. The reaction yield was 50%.

^{1}H NMR (300 MHz, D_2O) δ 7.52 (s, 1H), 7.42 – 7.34 (m, 1H), 4.61 – 4.48 (m, 1H), 4.39 (d, *J* = 4.3 Hz, 1H), 4.21 (d, *J* = 4.5 Hz, 2H), 3.67 (s, 12H), 3.45 (d, *J* = 4.8 Hz, 2H), 3.35 – 3.22 (m, 1H), 2.95 (dd, *J* = 13.1, 4.7 Hz, 1H), 2.73 (d, *J* = 12.9 Hz, 1H), 2.28 (t, *J* = 7.2 Hz, 2H), 1.50 (dd, *J* = 62.4, 19.4 Hz, 6H).

Compound 7

N-((S)-4-methyl-1-oxo-1-(1-((E)-14-oxo-18-((3aR,4S,6aS)-2-oxohexahydro-1H-thieno[3,4-d]imidazol-4-yl)-3,6,9-trioxa-12,13-diazaoctadec-11-enyl)-1H-1,2,3-triazol-4-ylamino)pentan-2-yl)-4-(4-((2S,3R)-3-methyl-1-oxo-1-(2-(pyrrolidin-1-yl)ethylamino)pentan-2-ylcarbamoyl)phenoxy)benzamide

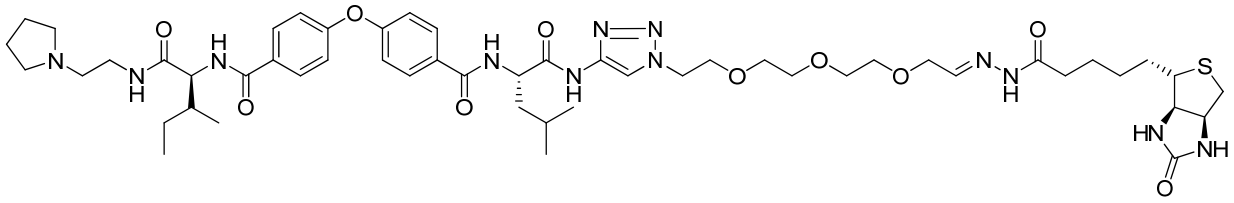

A solution (5 mM) of compound **6** in 5%CH_3CN / HEPES is added to a solution (25μM) of compound **5**. Then CuBr is added and the reaction mixture is stirred at room temperature for 1h.

The final compound has been analyzed through a direct infusion analysis using an ESI- triple-quadrupole.

Compound 8

N-((S)-4-methyl-1-oxo-1-(1-(2-oxo-7,10,13-trioxa-3,4-diazapentadecan-15-yl)-1H-1,2,3-triazol-4-ylamino)pentan-2-yl)-4-(4-((2S,3R)-3-methyl-1-oxo-1-(2-(pyrrolidin-1-yl)ethylamino)pentan-2-ylcarbamoyl)phenoxy)benzamide

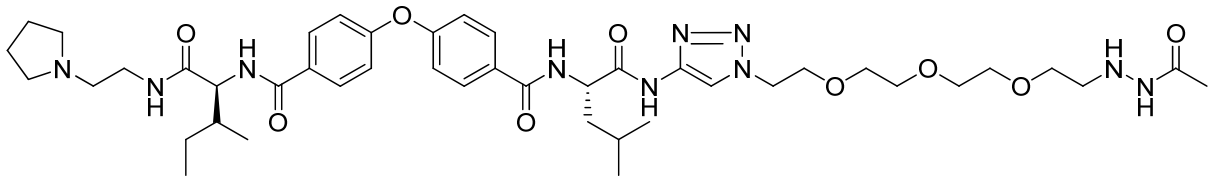

Compound **(8)** has been synthesized following general procedure **F**, **G**, **H**, described in "general procedure for proteomic reactions", using the following reagents:

- 0.025 mM solution of compound **5** in HEPES 50 mM
- 5.0 mM solution of compound **6** in 5%CH_3CN/HEPES 50 mM
- 0.2 mg CuBr, 0.0014 mmol
- 0.78 mg acetyldrazide, 0.010 mmol
- 0.123 mg p-anisidine, 0.001 mmol

The final compound has been analyzed through a direct infusion analysis using an ESI- triple-quadrupole.

7. Bibliography

1. Sutton, C. W. *British Journal of Pharmacology* **2012,** *166*, 457.
2. Han, S.-Y.; Kim, S. H. *Archiv der Pharmazie (Weinheim, Germany)* **2007,** *340*, 169.
3. WHO. 2011, www.who.int.
4. WHO. 2010, www.who.int.
5. Enayati, A.; Hemingway, J. *Annual review of entomology* **2010,** *55*, 569.
6. www.iss.it.
7. www.segretariatosociale.rai.it/codici/malaria/malaria.html.
8. Porter-Kelley, J. M.; Cofie, J.; Jean, S.; Brooks, M. E.; Lassiter, M.; Mayer, D. C. G. *Infection and Drug Resistance* **2010,** *3*, 87.
9. Rug, M.; Prescott, S. W.; Fernandez, K. M.; Cooke, B. M.; Cowman, A. F. *Blood* **2006,** *108*, 370.
10. Haldar, K.; Murphy Sean, C.; Milner Dan, A.; Taylor Terrie, E. *Annual review of pathology* **2007,** *2*, 217.
11. Uyoga, S.; Skorokhod, O. A.; Opiyo, M.; Orori, E. N.; Williams, T. N.; Arese, P.; Schwarzer, E. *British Journal of Haematology* **2012,** *157*, 116.
12. Chang, K.-H.; Tam, M.; Stevenson, M. M. *Blood* **2004,** *103*, 3727.
13. Wickramasinghe, S. N.; Abdalla, S. H. *Bailliere's best practice & research. Clinical haematology* **2000,** *13*, 277.
14. Chasis, J. A.; Mohandas, N. *Blood* **2008,** *112*, 470.
15. Skorokhod, O. A.; Caione, L.; Marrocco, T.; Migliardi, G.; Barrera, V.; Arese, P.; Piacibello, W.; Schwarzer, E. *Blood* **2010,** *116*, 4328.
16. Mosca, A.; Basilico, N.; Grande, R.; Taramelli, D. *Biochimica clinica* **2011,** *35*, 442.
17. Liu, J.; Gluzman, I. Y.; Drew, M. E.; Goldberg, D. E. *Journal of Biological Chemistry* **2005,** *280*, 1432.
18. Omara-Opyene, A. L.; Moura, P. A.; Sulsona, C. R.; Bonilla, J. A.; Yowell, C. A.; Fujioka, H.; Fidock, D. A.; Dame, J. B. *Journal of Biological Chemistry* **2004,** *279*, 54088.
19. Boss, C.; Richard-Bildstein, S.; Weller, T.; Fischli, W.; Meyer, S.; Binkert, C. *Current Medicinal Chemistry* **2003,** *10*, 883.

20. Francis, S. E.; Sullivan, D. J., Jr.; Goldberg, D. E. *Annual Review of Microbiology* **1997,** *51*, 97.
21. Francis, S. E.; Banerjee, R.; Goldberg, D. E. *Journal of Biological Chemistry* **1997,** *272*, 14961.
22. Arav-Boger, R.; Shapiro, T. A. *Annual Review of Pharmacology and Toxicology* **2005,** *45*, 565.
23. Banerjee, R.; Liu, J.; Beatty, W.; Pelosof, L.; Klemba, M.; Goldberg, D. E. *Proceedings of the National Academy of Sciences of the United States of America* **2002,** *99*, 990.
24. Hof, F.; Schutz, A.; Fah, C.; Meyer, S.; Bur, D.; Liu, J.; Goldberg, D. E.; Diederich, F. *Angewandte Chemie, International Edition* **2006,** *45*, 2138.
25. Bailly, E.; Jambou, R.; Savel, J.; Jaureguiberry, G. *Journal of Protozoology* **1992,** *39*, 593.
26. Rosenthal, P. J.; McKerrow, J. H.; Aikawa, M.; Nagasawa, H.; Leech, J. H. *Journal of Clinical Investigation* **1988,** *82*, 1560.
27. Rosenthal, P. J. *International Journal for Parasitology* **2004,** *34*, 1489.
28. Sunil, S.; Chauhan, V. S.; Malhotra, P. *BMC Molecular Biology* **2008,** *9*, No pp given.
29. O'Neill, P. M.; Posner, G. H. *Journal of medicinal chemistry* **2004,** *47*, 2945.
30. Janse, C. J.; Waters, A. P.; Kos, J.; Lugt, C. B. *International Journal for Parasitology* **1994,** *24*, 589.
31. Sowunmi, A.; Oduola, A. M. J. *Acta Tropica* **1996,** *61*, 57.
32. Brossi, A.; Venugopalan, B.; Dominguez Gerpe, L.; Yeh, H. J.; Flippen-Anderson, J. L.; Buchs, P.; Luo, X. D.; Milhous, W.; Peters, W. *Journal of medicinal chemistry* **1988,** *31*, 645.
33. Mandal, P. K.; Sarkar, N.; Pal, A. *Indian Journal of Medical Research* **2004,** *119*, 28.
34. Price, R.; Van Vugt, M.; Nosten, F.; Luxemburger, C.; Brockman, A.; Phaipun, L.; Chongsuphajaisiddhi, T.; White, N. *American Journal of Tropical Medicine and Hygiene* **1998,** *59*, 883.
35. Barradell, L. B.; Fitton, A. *Drugs* **1995,** *50*, 714.
36. WHO. *WHO Report* **2001**.
37. Selmeczi, K.; Robert, A.; Claparols, C.; Meunier, B. *FEBS Letters* **2003,** *556*, 245.
38. Robert, A.; Dechy-Cabaret, O.; Cazelles, J.; Benoit-Vical, F.; Meunier, B. *Journal of the Chinese Chemical Society (Taipei, Taiwan)* **2002,** *49*, 301.

39. Srivastava, I. K.; Vaidya, A. B. *Antimicrobial Agents and Chemotherapy* **1999,** *43*, 1334.
40. Vaidya, A. B.; Mather, M. W. *Drug Resistance Updates* **2000,** *3*, 283.
41. Suswam, E.; Kyle, D.; Lang-Unnasch, N. *Experimental Parasitology* **2001,** *98*, 180.
42. Baggish, A. L.; Hill, D. R. *Antimicrobial Agents and Chemotherapy* **2002,** *46*, 1163.
43. Srivastava, I. K.; Rottenberg, H.; Vaidya, A. B. *Journal of Biological Chemistry* **1997,** *272*, 3961.
44. Danis, M.; Bricaire, F. *Fundamental & Clinical Pharmacology* **2003,** *17*, 155.
45. Greenwood, B. *American Journal of Tropical Medicine and Hygiene* **2004,** *70*, 1.
46. Karen, I. B. *Milestones in drug ther.* **2012**.
47. Trape, J. F. *The American journal of tropical medicine and hygiene* **2001,** *64*, 12.
48. Sanchez, C. P.; McLean, J. E.; Stein, W.; Lanzer, M. *Biochemistry* **2004,** *43*, 16365.
49. Sidhu, A. B. S.; Verdier-Pinard, D.; Fidock, D. A. *Science (Washington, DC, United States)* **2002,** *298*, 210.
50. Reed, M. B.; Saliba, K. J.; Caruana, S. R.; Kirk, K.; Cowman, A. F. *Nature (London)* **2000,** *403*, 906.
51. Vaidya, A. B.; Lashgari, M. S.; Pologe, L. G.; Morrisey, J. *Molecular and Biochemical Parasitology* **1993,** *58*, 33.
52. Srivastava, I. K.; Morrisey, J. M.; Darrouzet, E.; Daldal, F.; Vaidya, A. B. *Molecular Microbiology* **1999,** *33*, 704.
53. Mok, S.; Imwong, M.; MacKinnon, M. J.; Sim, J.; Ramadoss, R.; Yi, P.; Mayxay, M.; Chotivanich, K.; Liong, K.-Y.; Russel, B.; Socheat, D.; Newton, P. N.; Day, N. P. J.; White, N. J.; Preiser, P. R.; Nosten, F.; Dondorp, A. M.; Bozdech, Z. *BMC Genomics* **2011,** *12*, 391.
54. Noedl, H.; Se, Y.; Schaecher, K.; Smith, B. L.; Socheat, D.; Fukuda, M. M. *New England Journal of Medicine* **2008,** *359*, 2619.
55. Dell'Agli, M.; Parapini, S.; Galli, G.; Vaiana, N.; Taramelli, D.; Sparatore, A.; Liu, P.; Dunn, B. M.; Bosisio, E.; Romeo, S. *Journal of medicinal chemistry* **2006,** *49*, 7440.
56. Philip, A.; Kepler, J. A.; Johnson, B. H.; Carroll, F. I. *Journal of medicinal chemistry* **1988,** *31*, 870.
57. Comley, J. C. W.; Yeates, C. L.; Frend, T. J. *Antimicrobial Agents and Chemotherapy* **1995,** *39*, 2217.
58. Saari, W. S.; Schwering, J. E.; Lyle, P. A.; Smith, S. J.; Engelhardt, E. L. *Journal of medicinal chemistry* **1990,** *33*, 97.

59. Romeo, S.; Dell'Agli, M.; Parapini, S.; Rizzi, L.; Galli, G.; Mondani, M.; Sparatore, A.; Taramelli, D.; Bosisio, E. *Bioorganic & Medicinal Chemistry Letters* **2004,** *14*, 2931.

60. Park, K. D.; Liu, R.; Kohn, H. *Chemistry & Biology (Cambridge, MA, United States)* **2009,** *16*, 763.

61. Barton, V.; Ward, S. A.; Chadwick, J.; Hill, A.; O'Neill, P. M. *Journal of Medicinal Chemistry* **2010,** *53*, 4555.

Part II

Proteomic approaches in Biomarker discovery

8 Introduction

8.1 Biomarker discovery

A biomarker is a measurable indicator of a specific biological state, particularly one relevant to the risk of contraction, the presence or the stage of disease.

Better biomarkers are urgently needed to improve diagnosis, guide molecularly targeted therapy and monitor activity and therapeutic response across a wide spectrum of disease.

Proteomics methods based on mass spectrometry hold special promise for the discovery of new biomarkers that might form the foundation for new clinical blood tests, but to date their contribution to the diagnostic armamentarium has been disappointing.

Biomarkers can be used clinically to screen for diagnose or monitor the activity of diseases, guide molecularly targeted therapy or assess therapeutic response.

The utility and importance of biomarkers has been recognized by substantial public and private funding, and biomarker discovery efforts are now commonplace in both academic and industrial settings.

The principal enabling technology of proteomic discovery is MS. All mass spectrometers, regardless of type, ionization mode or performance characteristics, produce mass spectra, which plot the mass-to-charge ratio of the ions observed (*x*-axis) versus detected ion abundance (*y* axis)[62].

The typical proteomics experiment consists of five stages. In stage 1, the proteins to be analysed are isolated from cell lysate or tissues by biochemical fractionation or affinity selection.

This often includes a final step of one-dimensional gel electrophoresis, and defines the 'sub-proteome' to be analysed. MS of whole proteins is less sensitive than peptide MS and the mass of the intact protein by itself is insufficient for identification. Therefore, proteins are degraded enzymatically to peptides in stage 2, usually by trypsin, leading to peptides with C-terminally protonated amino acids, providing an advantage in subsequent peptide sequencing.

In stage 3, the peptides are separated by one or more steps of high-pressure liquid chromatography in very fine capillaries and eluted into an electrospray ion source where they are nebulized in small highly charged droplets. After evaporation, multiple protonated peptides enter the mass spectrometer and, in stage 4, a mass spectrum of the peptides eluting at this point is taken (MS1 spectrum, or 'normal mass spectrum'). The computer generates a

prioritized list of these peptides for fragmentation and a series of tandem mass spectrometric or 'MS/MS' experiments ensues (stage 5). These consist of isolation of a given peptide ion, fragmentation by energetic collision with gas, and recording of the tandem or
MS/MS spectrum. The MS and MS/MS spectra are typically acquired for about one second each and stored for matching against protein sequence databases. The outcome of the experiment is the identification of the peptides and therefore the proteins making up the purified protein population[63] **(Figure 11)**.

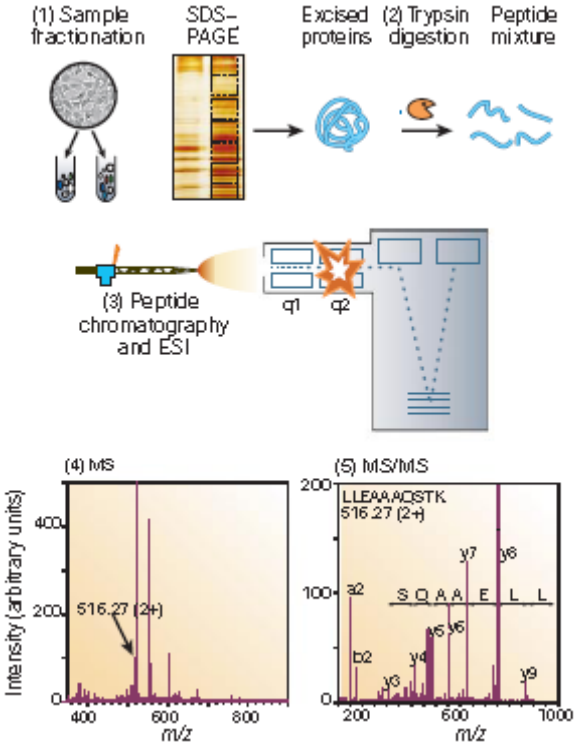

Figure 11

8.2 Oxidative stress

The term oxidative stress defines an alteration of the basal red ox balance in favour of the oxidation reactions. This impairment could be triggered by endogenous and/or exogenous factors, and is the result of an increase of the concentration of pro-oxidant species or the depletion of the endogenous antioxidants[64].

The direct consequence of the oxidative stress is a widespread oxidation of biological substrates (DNA, proteins, lipids and sugars), through nonphysiological reaction mechanisms. The extent and the reversibility of the molecular damages, the adaptation capability of the biological system involved and the rate of the defensive response are the main factors which lead up to a restore of the physiological condition or the development of a dysfunction[64]. The main molecular mediators of oxidative stress are the reactive oxygen species (ROS), which are generated in cells by both enzymatic and nonenzymatic sources[65, 66]. The ROS are essentially radicals and are characterized by unpaired electrons, which are responsible of the high reactivity of these compounds towards any type of substrate. ROS are produced physiologically at small concentration and are implicated in a multitude of physiological processes including ageing and cell mediated immune response.

A massive increase of the basal levels of oxidative stress has been associated in the genesis and/or progression of many chronic and degenerative cardiovascular diseases and in many metabolic disorders like diabetes, atherosclerosis, hypertension, ischemia/reperfusion damages but also in many neurodegenerative diseases such as Alzheimer's disease (AD), amyotrophic lateral sclerosis (ALS), and Parkinson's disease (PD)[64, 67-70].

However, it is still unclear whether the oxidative stress is the primary cause and directly contributes to the development of these pathologies, or it is only the result of the tissues degeneration, which characterize the progression of these diseases. Anyway, it represents a valid pharmacological target when the corresponding redox imbalance is still reversible. This, however, requires detailed knowledge on the biochemical mechanisms involved.

8.3 Carbonyl stress

Oxidative decomposition of polyunsaturated fatty acids (PUFAs) and sugars initiates chain reactions lead to the formation of a variety of molecules of three to nine carbon atoms, characterized by one or more carbonyl functions.

These products, named as reactive carbonyl species (RCS), are characterized by a strong electrophilicity and can react with nucleophilic endogenous substrates such as DNA or proteins, forming irreversible covalent adducts called advanced lipoxidation end-products (ALEs) and advanced glycation end-products (AGEs). The overall reaction is named carbonylation. Miyata was the first to define as ‘‘carbonyl stress’’ the accumulation in serum of RCS derived from lipids and carbohydrates and the subsequent massive proteins carbonylation[71]. Compared to free radicals and ROS, lipid and sugar-derived RCS have a longer half-life. Furthermore, while ROS are mainly radical and/or ionic species, these compounds are neutral molecules, with LogP values ideal to permeate cellular membranes and diffuse within or even escape from the cell to react with targets far from the site of formation. Therefore, these soluble reactive intermediates, precursors of ALEs, are not only cytotoxic, but they also behave as mediators and propagators of oxidative stress and tissue damage, acting as second messengers.

RCS could be classified by considering the chemical structure and their reactivity. The most reactive and cytotoxic RCS are α,β-unsaturated aldehydes [4-hydroxy-trans-2-nonenal (HNE) and acrolein (ACR)], dialdehydes [malondialdehyde (MDA) and glyoxal (GO)], keto-aldehydes [4-oxo-trans-2-nonenal (ONE) and isoketals (IsoK)].

Other less reactive compounds are 2-Hydroxyheptanal, product to lipid peroxidation of ω-6 PUFAs (linoleic acid, arachidonic acid) and 2-Hydroxyalkanales with 8, 9, 10, and 11 C-atoms, generated from hydroperoxides of oleic acid[72].

8.4 Reactive Carbonyl Species (RCS)

One mechanism of free radical-mediated damage occurs through initiation events such as lipid peroxidation and is particularly interesting for researchers in applied toxicology, as protein

carbonylation via toxic reactive aldehydes is known to result in altered protein function. The generation of free radicals in close proximity to lipid rich cellular membranes containing

PUFAs initiates lipid peroxidation occurs when HO• and ONOO_ abstract an allylic hydrogen from PUFAs. The initial step of this process demonstrates the basic principle that

reaction of a radical (HO• and ONOO_) with a nonradical species typically results in the generation of a new, less reactive radical, which, in this case, is a carbon-centered lipid radical (L•) (**Figure 12**).

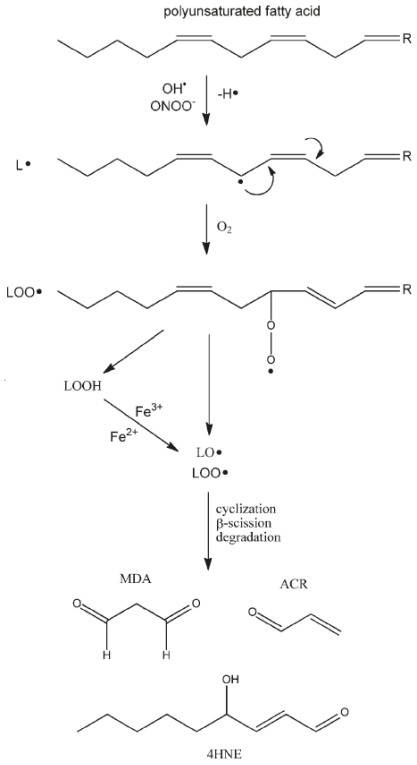

Figure 12: Lipid peroxidation

This L•, in turn, reacts with molecular oxygen to yield a lipid peroxyl radical (LOO•), resulting in the formation of lipid hydroperoxide (LOOH). These LOOHs react with trace metals to form lipid alkoxyl radicals (LO•). Both LO• and LOO• radicals generate reactive R,β-unsaturated aldehydes through cyclization and/or β-scission and degradation, most commonly generating highly electrophilic products such as 4-hydroxynonenal (4-HNE),

malondialdehyde (MDA), and acrolein (ACR). As defined, these reactive aldehyde species result from free radical-initiated lipid peroxidation and are fairly
long-lived within the cell, persisting for up to 2 min, allowing for intracellular diffusion and covalent modification of DNA, lipid, and protein throughout the cell. The mobility and reactivity of these products of lipid peroxidation are central to their involvement in altered cellular signaling and diseases of oxidative stress.

8.4.1 α,β-Unsaturated Aldehydes

(HNE) 4-Hydroxy-trans-2-Nonenal

HNE (**Figure 13**) is the most abundant and toxic α,β-unsaturated aldehyde, generated through the β-cleavage of hydroperoxides from ω-6 PUFAs which also plays a role in a variety of physiopathological processes[73-76]. HNE is known to exert a wide range of biological activities, among these, inhibition of protein and DNA synthesis, inactivation of enzymes, stimulation of phospholipase C, induction of cyclooxygenase 2, reduction of gap-junction communication, stimulation of neutrophil chemotaxis and modulation of platelet aggregation[73, 75, 77-80].

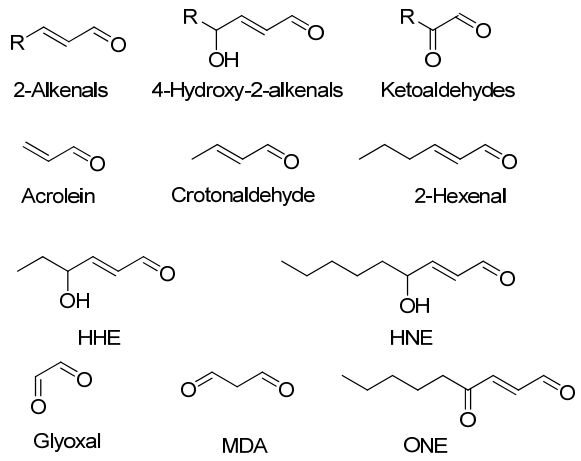

Figure 13: Molecular formulas of the main RCS produced during oxidation of lipids and sugars

Furthermore, HNE modulates the expression of various genes and the cell signal transduction, is involved in the oxidative stress-induced apoptosis activating the caspase cascade[80-83], furthermore is also a potent mutagen agent[84, 85] and has been reported to inactivate several enzymes[73, 86-109]. HNE reacts with cellular nucleophiles, in particular sulfhydryl groups of

proteins or peptides such as glutathione (GSH), via 1,2- and 1,4-Michael addition and the thioether adducts further undergo cyclization (fig 2) to form cyclic hemiacetals[73, 75, 77].

The high rate constant for the reaction of GSH with HNE indicates a half-life of approximately 2 min in the presence of physiological concentrations of GSH (5 mM). HNE reacts also with the imidazole moiety of His residues[110] and with the ε-amino group of Lys residues to form Michael adducts, which further undergo cyclization between the aldehyde moiety and the C-4 position of HNE to form a hemiacetal structure[111, 112]. Alternatively, HNE reacts with the ε-amino group of Lys (1,2-addition) forming a carbinolamine intermediate that rearranges and loses water to produce a Schiff base, which can eventually lead to the formation of a 2-pentylpirrole derivative **(Figure 14)** through an enammine intermediate[113].

The di-functional nature of HNE (electrophilic C-3 and carbonyl group) makes it able to form intra- and inter-molecular protein cross-links through Michael addition at C-3 followed by Schiff base formation[114].

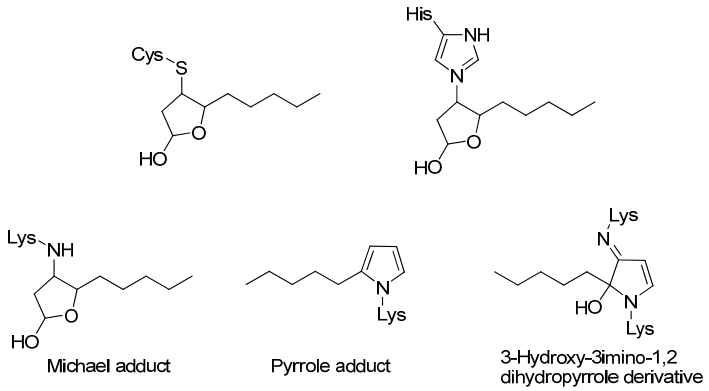

Figure 14: Chemical structures of HNE-cysteine, HNE-histidine and HNE-lysine

(ACR) Acrolein

ACR **(Figure 13)** is not only a lipoxidation product, but it is also produced during the myeloperoxidase-catalyzed metabolism of hydroxy-amino acids. For this reason, some data suggest that phagocyte-mediated formation of ACR may be of central importance in promoting tissue injury at sites of inflammation[115].

ACR can be generated from the oxidative deamination of spermine and spermidine catalyzed by polyamine oxidase, that is an ubiquitous pollutant in the environment (a by-product of overheating organic matter) and is a main component of the gas phase of cigarette smoke (25–140 mg/cigarette)[116, 117].

ACR is the strongest electrophilic α,β-unsaturated aldehyde, showing the highest reactivity with thiols and amines (ACR reacts more than 100 times faster with GSH than HNE). The mechanism of reaction with GSH and protein thiol groups is the same of HNE, without the cyclization rearrangement. The thiol adducts of ACR are considerably more stable than those formed by all other α,β- unsaturated aldehydes dissociation constants for ACR adducts being 10–10,000 times lower[75].

Like HNE, ACR reacts preferentially with Cys, Lys, and His residues. The Lys can reacts with more than one acrolein molecules to form a Nε-(3-formyl-3,4- dehydropiperidino)-lysine (FDP-Lys) and Nε-(3-methylpyridinium)-lysine (MPLys)[117, 118].

FDP-Lys is not a stable end-product, but a reactive intermediate that covalently binds to thiols, suggesting a new mechanism of protein thiolation in which the FDP-Lys, generated in the ACR-modified protein, reacts with sulfhydryl groups to form thioether adducts[119].

Like HNE, ACR inhibits many enzyme systems and cell proliferation[86-89, 119-123]. The mechanism of such effects may be related to the ability of ACR to deplete cellular thiols and/or to induce gene activation, either directly or following interaction with transcription factors, particularly the red ox-regulated[124].

The acute effects of ACR have been extensively investigated in several experimental models, such as rat aortic rings[125]. ACR is a powerful respiratory tract irritant and instigates asthma-like symptoms during inhalation, causing consequent pulmonary edema and respiratory distress[126].

8.4.2 Keto-Aldehydes

4-oxo-trans-2-Nonenal (ONE)

4-oxo-trans-2-nonenal (ONE), the two electron oxidation product of HNE **(Figure 13)**, is an end product of lipoxidation of ω-6 PUFAs[127, 128]. ONE contains a keto group at C4 position that makes the compound more reactive towards nucleophils than HNE (e.g., at 3–10 mM, ONE is more neurotoxic than HNE)[129]. Unfortunately, because 4-ONE has only recently been recognized as a potentially pathogenic compound, estimates regarding its intracellular concentrations are lacking, even if it has been detected in human plasma as ascorbyl conjugate[80]. The predominant initial reaction of ONE with nucleophilic sites in proteins appears to involve Michael addition to the central ONE double bond, more at C3 than at C2, to give substituted 4-oxononanals [130, 131].

This adducts may then condensate with the Nε-amino group of Lys to form substituted pyrrole cross-links. Unlike HNE, ONE was found to modify also peptides containing Arg residues (in addition to His, Lys, Cys) to give stable, covalent adducts. While the order of potency for amino acid adduction is similar for HNE and ONE (Cys, His, Lys, Arg), the difference in absolute potency (i.e., rate constants) between the two aldehydes is remarkable, because ONE is much more reactive than HNE towards thiols and amines.

8.4.3 Di-Aldehydes

(MDA) Malondialdehyde

MDA **(Figure 13)** precursors are mainly arachidonic acid (20:4) and docosahexaenoic acid (22:6), it cannot be considered a highly reactive compound under physiological conditions, because the main species existing in aqueous solution at pH 7.4 is the enolate anion, stabilized by a conjugated π-bond system.

Resonance stabilization reduces the electrophilicity of MDA, decreasing its reactivity with protein amine groups such as Lys and Arg. At lower pH, when the β-hydroxyacrolein becomes the predominant species, its reactivity is significantly increased. This makes the molecule able to react with nucleophiles in a Michael type 1,4-addition reaction, similarly to other α,β-unsaturated aldehydes, such as HNE or ACR. Resonance stabilization of the intermediate anion favours this reaction, which results in the formation of a β-substituted acrolein as end-products.

At least 80% MDA in tissues is bound reversibly to proteins *in vivo*. Lys and Arg are the only amino acids whose side-chains react with MDA to form the semi-stable Nε-β-lysyl-amino-acrolein (β-LAA) and the stable Nδ-(2-pyrimidyl)-L-ornithine (NPO)[132, 133].

(GO) Glyoxal

GO **(Figure 13)** is an α-ketoaldehyde intermediate formed by oxidative degradation of glucose and degradation of glycated proteins, by ascorbate autoxidation, and by peroxidation of lipids[134, 135] and is indeed formed during UV irradiation of PUFAs and autoxidation of arachidonic acid.

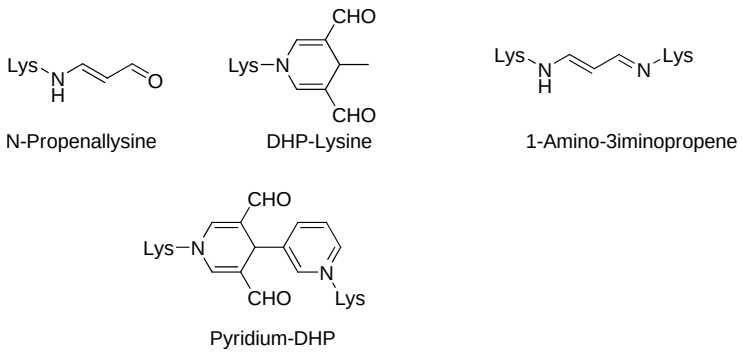

Figure 15: Chemical structures of MDA-Lys adducts and cross-links

GO reacts with the free amino groups of proteins to give Schiff's bases (by the non-enzymatic reaction of glycation), which undergo rearrangement to form relatively stable ketoamines (Amadori products). The glycated proteins undergo further dehydration, cyclization, oxidation and rearrangement to generate advanced glycation end-products (AGEs). GO reacts with Cys and Lys to form the EAGLE oxidative adduct, Nε-(carboxymethyl)-lysine (CML) and (carboxymethyl)-cysteine (CMC).

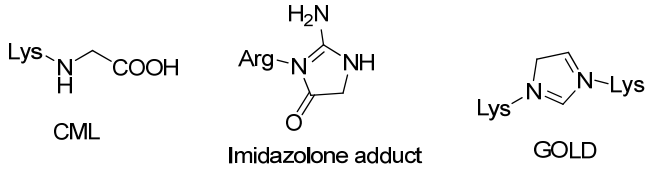

Figure 16: Chemical structures of GO adducts and cross-link

The ability of GO to cross-link proteins has widely been reported and elevated levels of this products have been measured in serum of uremic and haemodialysis patients[111, 136].
However, many of the GO cross-links likely occurring in vivo remains uncharacterized, because the molecular mechanisms of the cross linking reaction needs to be fully elucidated. GO has been demonstrated to induce mutagenesis in several cellular models, an effect that is inhibited by thiol compounds[137, 138].

1.4 Protein oxidation and carbonylation

Emerging evidence indicates that ROS can cause specific protein modifications that may lead to a change in the activity or function of the oxidized protein.
Several major forms of oxidative modifications occur on amino acid residue side chains, including new chemical moieties such as hydroxy or carbonyl group.

Oxidation of proteins is irreversible and irreparable and may alter the conformation of the polypeptide chain, determining the partial or total inactivation of proteins[64, 70, 139-141].

The consequent loss of function or structural integrity of modified proteins can have a wide range of downstream functional consequences and may be the cause of subsequent cellular dysfunctions and tissue damages. The introduction of carbonyl moieties into proteins may arise from a direct oxidation of amino acid side-chains, resulting in the formation of 2-pyrrolidone (Pro oxidation), glutamic semialdehyde (Arg and Pro oxidation), α-aminoadipic semialdehyde (Lys oxidation), and 2-amino-3-ketobutyric acid from (Thr oxidation).

Protein carbonyl derivatives can also be generated through oxidative cleavage of proteins, through the α-amidation pathway or through oxidation of glutamine side chains, leading to the formation of a peptide in which the N-terminal amino acid is blocked by an α-ketoacyl derivative **(Figure 17)**.

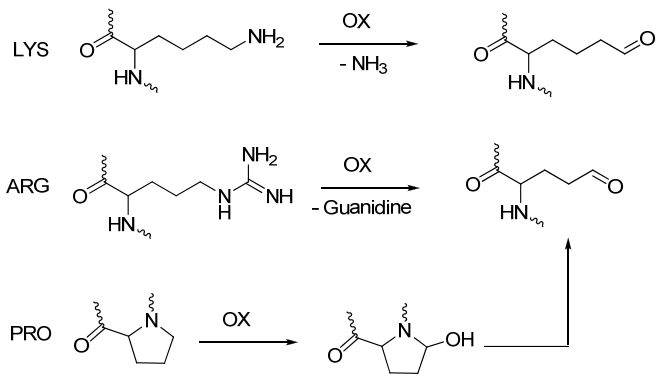

Figure 17: Generation of protein carbonyls through direct oxidation of Lys, Arg and Pro residues

The second mechanism to include carbonyl moieties in protein is the reaction of the nucleophilic side chains of Cys, His, and Lys residues with glucid and lipid-derived reactive carbonyl species (RCS) to generate AGEs and ALEs[77, 142, 143].

Furthermore, carbonyls are produced during oxidation of glycated proteins. Glycation is a spontaneous reaction recognized as the initial step of a very complex process, the Maillard cascade, which involves the formation of several end-stage products responsible for protein modification and is catalyzed by oxidative stress and ROS. Complex interactions between oxidation and glycation (the glycoxidation process) are considered to play a key role in protein modification[144-146].

8.5 Protein carbonyls in cardiovascular diseases and neurodegeneration.

Protein modification by lipoxidation-derived RCS is little known, although numerous evidences indicate their involvement in physiological ageing and in the onset and/or progression of several diseases such as cardiovascular (e.g., atherosclerosis, long-term complications of diabetes) and neurodegenerative diseases (e.g., AD, PD), cerebral ischemia, rheumatoid arthritis, and post-ischemic reperfusion injury[73, 78, 147, 148]. The increased protein carbonylation by lipids and carbohydrates in chronic diseases is the result of carbonyl overload on metabolic pathways involved in detoxification of RCS[145, 149]. This leads to a general increase in steady-state levels of RCS formed by both oxidative and non-oxidative reactions. In fact, in both diabetes and uraemia, not only glycoxidation and lipoxidation products are increased, but also the products of reaction of proteins with dicarbonyl compounds formed by non-oxidative mechanisms[150].

By reacting with nucleophilic sites in proteins, RCS generate typical ALEs such as MDA-Lys (Schiff base adduct), HNE-Lys (Michael adduct), HNE-Lys (pyrrole derivative) and FDP-Lys [Nε-(3-formyl-3,4 dehydropiperidino)-lysine].

These adducts have been detected in oxidized lipoproteins and/or atherosclerotic lesions of varying severity from human aorta by immunohistochemical or chemical assays[146, 148, 151-153]. The clinical relevance of the reaction between MDA and proteins is highlighted in atherosclerosis.

MDA-LDL, in addition to oxidized LDL, mediates several pro-inflammatory and pro-atherogenic processes, which ultimately lead to foam cell generation[154]. MDA plasma concentration is increased in diabetes mellitus and MDA is found in the atherosclerotic plaques promoted by diabetes[155].

Adducts of apolipoprotein B-100 Lys residues with MDA and HNE and of apolipoprotein A-1 with ACR, have been extensively characterized in human atherosclerotic lesions[156, 157]. Protein-ACR adducts have been found to be significantly elevated in serum of end-stage renal disease patients receiving haemodialysis and in AD[158, 159].

Carbonyl stress has been implicated in cardiac reperfusion injury, since the reperfusion-induced mitochondrial dysfunction is mediated in part by specific mitochondrial proteins modified by RCS[160, 161]. Unsaturated aldehyde levels were found to be consistently elevated in plasma of patients with congestive heart failure, associated with impairment of left ventricular

contractility[162]. Lipid-derived RCS are massively involved in hyperglycaemia and in development of complications in diabetes[150].

Increased plasma levels of free RCS or RCS adducts have been measured in patients with chronic kidney failure and in long-term complications associated to haemodialysis, such as dialysis-related amiloydosis, and in uremic subjects[97, 163-165]. Protein-ACR adducts, in addition to MDA-Lys and HNE-protein adducts, have been also detected in glomerular lesions from patients with diabetic nephropathy and in kidney (especially in the glomerular epithelial cells) from patients with congenital nephritic syndrome, a human model disease of proteinuria[166, 167].

The inter- and intra-molecular cross-linking of collagen by MDA (formation of pyridyl crosslinks), and the resultant modification of collagen properties and cell-matrix interactions, are particularly relevant in the late complications of diabetes mellitus, contributing to the stiffening of the cardiovascular tissue[155].

In addition, significant higher levels of HNE-modified albumin were detected in serum of type 2 diabetes mellitus outpatients than in the matched nondiabetics[168].

Therefore, lipid peroxidation and the consequent lipoxidative modification of proteins play a key role in the development of cardiovascular and kidney diseases in diabetes.

The involvement of toxic RCS as products and propagators of oxidative damage in neurodegenerative diseases, mainly in AD, was elucidated in several experiments[169-171]. Elevated levels of carbonyl species have been determined in plasma and in different brain regions of AD patients, HNE is elevated in plasma and in cerebrospinal fluid, whereas ACR in the amygdala and hippocampus/ parahippocampal gyrus[172-175]. MDA accumulation has been detected immunohistochemically in the cytoplasm of astrocytes and neurons in both normal ageing and AD and the extent of deposition is similar in both conditions[176]. Increased concentrations of MDA (in plasma and serum) and HNE (in plasma and cerebrospinal fluid) have been reported in PD patients[177].

HNE levels are significantly elevated also in the sera and spinal fluid of ALS patients and positively correlate with the extent of the disease but not with the rate of progression, suggesting HNE as a possible biomarker of the disease[178].

The residual aldehyde group in some ALEs (Schiff's base and Michael's adducts) can further react to give protein cross-links and fluorescent products that are very similar to AGEs.

Lipofuscin, the non degradable intralysosomal fluorescent pigment that accumulates with age in post-mitotic cells, is a recognized hallmark of ageing occurring with a rate inversely related to longevity. Since its formation proceeds through iron-catalyzed oxidation/polymerization of

protein and lipid residues, lipofuscin is now also considered the residual debris from lipoxidation reactions[179].

Other important toxic products formed during non-enzymatic modification and cross-linking or proteins in ageing and diseases are referred to as ‘‘either advanced glycation or lipoxidation end-products’’ (EAGLEs), Nε-(carboxymethyl)-lysine (CML) and Nε-(carboxyethyl)-lysine (CEL) are, the major EAGLE modifications that have been measured in tissue proteins[146, 151, 152].

8.6 Determination of RCS in biological matrixes

Based on growing evidence of RCS role as causative/effective factors in CVD, an accurate and sensitive method to measure RCS in biological matrices is strictly required.

The aim is not only to better understand the pathogenetic role of RCS and to characterize a biomarker of the onset and progression of the disease, but also to identify a tool for evaluating the efficacy of the RCS sequestering agents, a new class of compounds designed to prevent/retard the carbonyl related diseases.

From an analytical point of view, RCS analysis in biological matrices can be carried out through two different approaches: a direct way, by measuring free aldehydes, and an indirect approach, based on identifying the corresponding adducts with reactive and nucleophilic macromolecules and peptides. Since the pioneering work of Esterbauer and his colleagues on HNE measurement in biological matrices by HPLC analysis[180] several progress have been made, although the golden method is far to be reached. Measurement of the free form of HNE in plasma samples has been reported by using various analytical methods, developed by applying different techniques such as HPLC[181], GCMS[182] and immunoassays[183]. However, HNE is highly unstable in plasma, and only a minor fraction is detected as free form. Accordingly, Salomon[184] found that the highest levels reported of free HNE (about 0.7 nmol/mL for normal healthy individuals) accounted only about 10% of the levels of HNE-protein adducts, determined as HNE-pyrrole epitopes in the blood of healthy individuals.

The short half-life of RCS in the biological matrix is due to the high reactivity of these electrophilic species towards nucleophilic macromolecules and due to phase I and II detoxification processes[76].

Hence, it is quite clear that the direct analytical approach only allows quantitating a minor fraction of the free aldehyde, which is greatly affected by several variables such as metabolism and reaction with nucleophilic substrates. One of the main fate of carbonyls in biological matrices is represented by the adduction to the reactive sites of proteins, forming the corresponding carbonylated adducts which, being relatively stable, can undergo accumulation and hence can represent a suitable biomarker of carbonyls formation as well as protein carbonylation damage[185].

8.7 Carbonylated proteins as biomarkers of carbonyl stress

The amount of protein carbonylation is still determined by two main techniques, immunological and spectroscopic. When the analytical essay is applied directly to the sample it is possible to obtain a global index of carbonylation[186]. Although this approach permitted to evaluate a significant increase of carbonylation protein in patients with oxidative damage (as in hemodialysis patients with chronic kidney disease[187, 188]), it is nevertheless limited because it provides only a general index and non-specific damage by carbonylation. In particular, the approach does not allow a distinction between direct carbonylation, for oxidative reaction, and carbonylation induced by a mechanism mediated by electrophilic carbonyl adduction, and in this case between aldehydes arising from damage induced by lipid peroxidation or other oxidative pathways as the autoxidation of sugars. Finally, this technique is not suitable for accurate quantitative analysis, a fundamental characteristic for the identification and validation of biomarkers. Recently, the analytical techniques described above were applied after protein separation, using 1D or 2D electrophoretic techniques, in order to identify the target protein involved in the carbonyl process. This approach has greatly improved the knowledge about the carbonylation protein targets, allowing a greater understanding of the biochemical mechanisms involved in the carbonylation damage. The technique does not allow however to identify the carbonylation mechanisms and in particular the main carbonyl species responsible for the carbonylation process.

Therefore, it is evident that it is a priority to develop an analytical method able not only to identify the target protein of the carbonylation process, but also the structure of the modification in order to better understand the carbonylation mechanism. The analytical approach should also include the quantitative aspect.

Multiple proteomic approaches indicate HSA as the main target of carbonylation in the serum[188, 189]. HSA could be carbonilated through different mechanisms, such as oxidative reactions due to reactive oxygen species (ROS) or covalent adduction induced by electrophilic compounds such as HNE and ACR[64]. The proteomic analysis and mass spectrometry (MS)[185, 190, 191] have demonstrated that HSA represents a highly reactive target for RCS in plasma. For this reason, it is a primary endogenous target to the RCS. The high reactivity of HSA against RCS is due to the different nucleophilic accessible sites, in particular the Cys34, followed by His146 and Lys199[185, 191].

8.8 Oxidative stress in hepatic resection (hepatectomy)

In many liver surgery is required the maintenance of the liver in a condition of ischemia that can be prolonged from 15 to 50 minutes. Although the development of surgical techniques has allowed a significant reduction of the ischemic period, the liver modifications resulting from partial hepatectomy interventions are still frequent[192]. Similarly, during the various stages of liver transplantation, the liver is exposed to prolonged periods of ischemia which can cause failure or temporary liver malfunction[193-195]. It is generally known that the liver damage resulting from partial hepatectomy or transplantation is caused by alterations that are produced during the ischemic period and the subsequent reperfusion[195]. The lack of oxygen during the ischemic phase determines the de-energization of mitochondria and the reduction in the content of intracellular ATP. This cause the alterations Na^+, H^+ and Ca^{2+} [196-199]. The reintroduction of oxygen, during reperfusion, is instead responsible for an incremented production by the mitochondria of reactive oxygen species (ROS) that induce oxidative stress and mitochondrial permeability transition[200].

During the phase of reperfusion occurs also the activation of Kupffer cells with the consequent release of ROS, nitric oxide (NO) and pro-inflammatory cytokines, such as TNF, IL-6, IL-1beta, MCP-1, IL- 12, IL-18 and CXC[201] and inhibition of the synthesis of anti-inflammatory cytokines (IL-10)[202].

The liver resection, and in particular the condition of ischemia and reperfusion associated with, therefore represents a condition of oxidative stress by now consolidated. Furthermore, the possibility to perform blood samples before, during and after the condition of ischemia and reperfusion, allows to monitor the onset of oxidative process compared to the baseline condition, the pre-ischemic.

9. Purpose of research

One of the most exciting areas of proteomic research is the identification and validation of disease biomarkers which can be used as measurements within clinical studies and for the purpose of predictive diagnosis. The study of proteomics is considered to be a key for the characterization of human diseases and disease states, and mass spectrometry technology plays a crucial role in this disease research.

We focused in particular on detection and quantization of post-translational modifications of proteins caused by oxidative and carbonyl stress. While the development of specific antibodies against modified proteins has made it possible to confirm the occurrence of oxidative stress in vivo and its involvement in several physio-pathological conditions, the resultant chemical modifications of proteins has not yet been explored. Proteomic tools, can sensitively detect oxidative damage on peptides and proteins: these tools would be helpful to understand exactly when, how, and where the damage occurs, and to gain deeper insights into the mechanism of onset, progression, and/or complication of the diseases.

Proteomics approaches have led to the identification of the protein/s showing high sensitivity to oxidation/carbonylation, and among them human serum albumin (HSA) was found to be the main target in the circulation.

The purpose of research of this second part of my PhD thesis was the investigation and validation of disease biomarkers in order to predict and monitor carbonyl stress under different pathological condition such as cardiovascular disease, neurodegenerative disease, cerebral ischemia, ischemia reperfusion.

In particular, the overall work can be divided into two main parts:

1. Tuning up of a mass spectrometric approach based on a triple quadrupole mass spectrometer in precursor and product ion scan mode in order to identify unknown modifications of HSA Cys 34.
2. Tuning up of a mass spectrometric approach based on a triple quadrupole mass spectrometer in precursor and product ion scan mode in order to identify unknown modifications of HSA His 146.

10. Experimental section

10.1 Materials and methods

The diethylacetal derivative of 4-hydroxy-trans-2-nonenal (HNE-DEA) was prepared as reported by Rees (Rees et al., 1995). The 4-hydroxy-trans-2-nonenal (HNE) was prepared by hydrolysis of HNE-DEA in 1 mM HCl for one hour, at room temperature and protected from light. The titration HNE was determined by UV spectrophotometric analysis (λmax 224 nm; ε 13,750 M^{-1} cm^{-1}).

Acrolein (ACR), crotonaldehyde (CRO), glyoxal (GO), methylglyoxal (MGO), 4-hydroxy-2-hexenal (HHE) and nonenal (NONE) were purchased from Fluka Company (Buchs, Switzerland). The MDA was prepared by hydrolysis of MDA bis (diethyl acetal) (Sigma-Aldrich, Milan, Italy).

The peptide LQQCPF was obtained by synthesis, with purity greater than 95% (Sigma-Aldrich, Milan, Italy). The isotope deuterated peptide (LQQCPF-D8) was prepared by solid phase synthesis with L-phenyl-alanine-2,3,3-D5-D3-N-FMOC (CDN isotopes; Chemical Research 2000 Srl, Rome, Italy), with purity greater than 95%.

The peptide HPYFYAPELLFFAK was obtained by solid phase synthesis, with purity greater than 99% in Professor Romeo's laboratory (Università degli Studi di Milano, Milan, Italy)

The human serum albumin (HSA), the iodoacetamide and the (±)-threo-1 ,4-dimercapto-2 ,3-butanediol (DTT) were purchased from Sigma-Aldrich (Milan, Italy). The modified trypsin for peptide mapping has been provided by Promega (Milan, Italy) and chymotrypsin by Roche Diagnostics SpA (Monza, Italy).

The organic solvents of analytical purity and for HPLC were purchased from Sigma-Aldrich (Milan, Italy). The water for HPLC was prepared with a purification system Milli-Q (Millipore, Bedford, MA, USA). The compound 2,2 '-azobis (2-amidinopropano) dihydrochloride (AAPH) was purchased from Wako (Italian Society of Chemistry, Rome, Italy).

10.2 Samples preparation and analytical methods

- **HPYFYAPELLFFAK solid phase synthesis**

The peptide HPYFYAPELLFFAK was synthesized using the following procedure:

1. ***Resin swelling:***

   Suspend the resin in a solution of NMP (1 ml per 150 mol of resin) and DCM (7.5 mL) and sonicate for 5 minutes. Transfer to a reactor the swollen resin and filter under vacuum to obtain the dry resin.

2. ***Introduction the first amino acid***

   Dissolve Fmoc-aa (150 mmol, 1equivalente) in DCM/NMP (2:1) and basify with DIEA (2eq). Suspend the resin in the solution and leave the reactor under stirring for 50 minutes, at the end add 400 μl of MeOH for the capping of the functional groups still free on the resin and stir for another 5 minutes. Once the reaction is finished, filter and wash 6 times with DMF.

3. ***Fmoc cleavage***

   Add to the resin a solution of Pip (20% in DMF) and stir for 5 minutes. Filter the resin and repeat the operation by increasing the stirring time to 15 minutes. Once the reaction is finished, filter and wash 6 times with DMF.

4. ***Coupling***

   Dissolve the Fmoc-aa (3 equivalents) in a solution of TBTU/HOBt (0.45 M in DMF, 4 equivalents) and subsequently basify with DIEA (8 equivalents). Add the solution into the reactor containing the resin and leave the suspension under stirring for 50 minutes.
   At the end of the coupling, if necessary proceed with the insertion of a new amino acid, repeat the procedure for the removal of the Fmoc group, followed by the new coupling, and proceed in this way until the end of the sequence. Once the deprotected N-terminal amino acid, the resin washed 3 times with DCM and let it dry completely, then the cleavage.

5. ***Resin cleavage***

   After the removal of the Fmoc group from the last amino acid, wash 4 times with DCM and dry the resin under vacuum. Prepare the cocktails suitable for the cleavage and add it to the resin under magnetic stirring for 2 hours. After the cleavage, filter the suspension in a suitable solvent to precipitate the compound. Centrifuge the resulting suspension and remove the supernatant and repeated these steps twice to remove all

the scavenger used in the cleavage cocktail. The precipitate is, finally, solubilized and purified by preparative HPLC.

6. ***Peptide purification***

   The compounds are purified by preparative reverse phase HPLC, using an appropriate gradient of eluents A (H_20/CH_3CN/TFA, 97:3:0,1) and B (CH_3CN/H_2O/TFA, 70:30:0,1) with a flow of 14 ml / min.

   The fractions containing the compound were concentrated in vacuo and acidified with a few drops of HCl (1M) to obtain the compound as the hydrochloride salt, instead of trifluoroacetate, and the mixture is finally lyophilized.

- **LQQCPF-RCS adducts preparation**

The peptide LQQCPF (final concentration 200 μM) was incubated with different aldehydes (HNE, HHE, or ACR; final concentration 2 mM) in 1 mM phosphate buffer (pH 7.4) for 24 h at 37 ° C.

An aliquot of the synthesized adducts was reduced using $NaBH_4$ (final concentration 5 mM) by a 60 min incubation at 37 °C and was subsequently desalted using a purification column (DSC-18 Supelco Discovery, 1 mL/100 mg Sigma-Aldrich Milan , Italy).

- **HPYFYAPELLFFAK-RCS adducts preparation**

The peptide HPYFYAPELLFFAK (final concentration 200 μM) was incubated with different aldehydes (HNE, CRO, NONE, or ACR; final concentration 2 mM) in 1 mM phosphate buffer (pH 7.4) for 24 h at 37 ° C. An alioquot of the synthesized adducts was reduced using $NaBH_4$ (final concentration 5 mM) by a 60 min incubation at 37 °C and was subsequently desalted using a purification column (DSC-18 Supelco Discovery; 1 mL/100 mg Sigma-Aldrich Milan , Italy).

- **ESI-MS direct infusion analysis of the peptide-RCS adducts**

The LQQCPF and HPYFYAPELLFFAK-RCS adducts, reduced or not, were diluted (1:10, v/v) with a solution of MeOH: H_2O: HCOOH (50:50:0.1, v/v/v) and analyzed by ESI-MS direct infusion approach.

The analysis were performed using the mass spectrometer TSQ Quantum Ultra (Thermo Finnigan, Milan, Italy) using the following experimental conditions:

- injection flow rate: 5μL/min
- capillary temperature: 270 °C
- ionization voltage: 5 kV
- capillary voltage: 12.5 V
- gas sheet (nitrogen) 0.5 L/min

The MS/MS analysis were performed by applying an energy of collision of 20, 30, 40, and 50 eV.

- **LC-ESI-MS precursor ion scan analysis of LQQCPF-RCS adducts**

The mixture containing LQQCPF native peptide and the reduced form of LQQCPF adducts with HNE, HHE, or ACR (25 μM each) was prepared in phosphate buffer 1 mM and diluted 1:1 with MeOH:H_2O:HCOOH (50:50:0.1 v/v/v). Aliquots of 50 μL was analyzed using HPLC system Surveyor LC system (ThermoQuest, Milan, Italy) equipped with a quaternary pump, detector UV/VIS photodiodes (PDA detector), autosampler, online degasser and thermostat; instrument control and data analysis were performed using the Xcalibur software (version 2.0, Thermo Electron Corporation).

The elution of the peptides was obtained with a reversed phase column Agilent Zorbax SB-C18 (150 mm x 4 mm id, particle Size 3.5 μM) (CPS analytical, Milan, Italy) protected by a guard column Agilent Zorbax RP; the mobile phase flow was maintained at 0.2 ml min^{-1}, using a gradient eluition from 100% of phase A (H_2O + 0.1% HCOOH) to 60% of phase B (CH_3OH/H_2O/HCOOH;90/10/0.1, v/v/v) in 80 minutes, followed by a period of 20 minutes of rebalancing; the pre-column and column temperature was maintained at 25°C.

Samples were on line desalted and concentrated using a cartridge Opti-Lynx C18 (40 μM) (El-Chimie srl, Bresso, Milan, Italy) inserted into an injection valve Rheodyne 7010 (Rheodyne, USA). ESI-MS analyses were performed using a mass spectrometer TSQ Quantum triple quadrupole Ultra (ThermoQuest, Milan, Italy), in positive ions scan, using the following experimental conditions:

- capillary temperature 270 °C;
- voltage of the spray 4,5 kV
- capillary voltage of 12.5 V
- nebulizer gas flow (nitrogen) 5 L/min

Each sample was analyzed twice. First a full scan analysis in data-dependent scan mode was performed obtaining an isolation of the most abundant ions and their subsequent MS/MS fragmentation.

Here below summarized the experimental conditions used are as follows:

- repeat count 1
- repetition duration 0.5 min
- duration of the exclusion phase 2 min.

The second analysis was performed in precursor ions scan mode, selecting the following product ions: m/z 242.1, 263.1 and 370.2 (collision energy 40 V).

Both quadrupoles, Q1 and Q3, were set as follow:

- resolution of mass of 1
- scan time of 1 sec
- Q1 the scan range m/z 300-1500.

After the adducts were characterized by product ion scan analysis using the following experimental conditions:

- Q1 resolution 0.7 m/z
- scan time 1 s
- collision energy 30 V
- scan range 50-1500 m/z.

- **LC-ESI-MS precursor ion scan analysis of HPYFYAPELLFFAK-RCS adducts**

The same approach was used for the mixture containing the reduced form HPYFYAPELLFFAK native peptide and the HPYFYAPELLFFAK adducts with HNE, CRO, NONE, or ACR (25 μM each).

The only difference was obviously in the product ions selected for the precursor ion scan analysis: m/z 512.13 and 964.60 (collision energy 40 V).

- **Albumin-RCS adducts preparation**

Blood samples of six healthy volunteers, aged between 25 and 30 years, were collected in tubes containing sodium citrate as an anticonvulsivant. The plasma was separated by centrifugation at 2000 g for 20 min (4°C) and aliquots of 500 µl have been stored in liquid nitrogen until the analysis. The human serum albumin (HSA) was isolated using the Montage Albumin depleted Kit (Millipore, Milan, Italy) with 1 M NaCl as eluent phase (mean plasma HSA content 570 ± 34 µM).

The HSA concentration was determined by spectrophotometry, setting the length wave at 279 nm (E 1% 1 cm = 5.31). Subsequently the samples were desalted using Microcon YM30 centrifuge filter (Millipore, Milan, Italy), after a washing phase with distilled water.

Then the samples were diluted in 20 mM phosphate buffer (PBS, pH 7.4) to obtain a final concentration of 20 µM. The aldehydes HNE, HHE or ACR were added to a final molar ratio of 1:10 HSA:RCS.

After 120 min of incubation at 37°C, the samples were reduced with $NaBH_4$ (final concentration 5 mM) at 37°C for 60 min, and were desalted with Microcon YM30 centrifuge filter, as described above. They have been stored in liquid nitrogen until the digestion step.

- **Samples proteolytic digestion**

The samples proteolytic digestion was performed according to the following scheme:

1. Dissolution in NH_4HCO_3 (50 mM) to a final concentration of 1mg/mL
2. Addition to a 40 µL aliquot of 4 µL of $NaBH_4$ (500 mM) and incubation at 37°C for 45 min
3. Desalification phase using Microcon YM30 filter centrifuge (Millipore, Milan, Italy), after a washing phase with NH_4HCO_3 (50 mM).
4. Addition of 4 µL of DTT (20 mM) as a reducing agent of the disulfide bridges and denaturation by one hour incubation at 60°C
5. Alkylation of the cysteine thiol residues, by the addition of 16 µL of iodoacetamide (20 mM) and incubation for 1 h, at 37°C and protected from light
6. Elimination of the exceeding iodoacetamide excess by further incubation for 1 h in the dark at 37°C after addition of 20 µL of DTT.
7. Addition 20 µL of $CaCl_2$

8. Trypsin or chimotripsin digestion at 37°C for 24 hours, using a enzyme/protein ratio equal to 1:20 (w/w). When both enzymes were necessary the samples were digested at 37°C for 3 hours with trypsin and then overnight with chimotrypsin.
9. Addition of TCA (40% w/v, 50 µL), stored on ice for 10 minutes, to a 200 µL samples aliquot and centrifugation at 18000 rpm for 10 minutes.

Finally aliquots of 50 µL were injected into the LC-ESI-MS system (Surveyor LC system, ThermoFinnigan, Milan, Italy). The analysis by LC-ESI-MS were carried out in data-dependent scan mode with precursor ion scan, as described above.

- **Tripsin-chimotripsin digested HSA-RCS adducts precursor ion scan analysis**

HSA isolated from serum plasma by affinity chromatography was incubated with different RCS (as describe in the paragraph "*Albumin-RCS adducts preparation*") and digested with tripsin and chimotripsin (as described in paragraph "*Samples proteolytic digestion*").

The mixture containing HSA and HSA adducts with HNE, HHE, or ACR in reduced form (25 µM each) was prepared in phosphate buffer 1 mM and diluted 1:1 with MeOH:H_2O:HCOOH (50:50:0.1 v/v/v). Aliquots of 50 µL were analyzed using LC-ESI-MS precursor ion scan analysis as described in the paragraph "*LC-ESI-MS precursor ion scan analysis of LQQCPF-RCS adducts*".

10.3 Cys 34 covalent modifications determination in patients undergoing hepatectomy surgery.

In the present study plasma samples taken from three patients undergoing liver resection were analyzed.

During the surgery, it was possible to withdraw two different blood samples:

1) Before anesthesia

2) 10 min after de-clamping.

Each sample was subjected to isolation of HSA and enzymatic digestion (as described in the paragraph "Albumin-RCS adducts preparation" and "Samples proteolytic digestion) and was analyzed according to the following scheme:

1. precursor ion scan analysis of LQQCPF-RCS adducts
2. characterization of the selected species by a product ion scan analysis
3. quantitative analysis of the identified adduct(s) by Multiple Reaction Monitoring (MRM)
4. MRM quantitative analysis of the LQQC(HNE)PF adduct
5. direct infusion of isolated HSA

- **Development of a method for quantitative analysis of the LQQC(HNE)PF adduct in Multiple Reaction Monitoring (MRM)**

The chromatographic separation was obtained with a reversed phase column Agilent Zorbax SB-C18 (150 mm x 4 mm id, particle Size 3.5 uM) (CPS analytical, Milan, Italy) protected by a guard column Agilent Zorbax RP; the phase flow of the mobile was maintained at 0.2 mL/min with a linear gradient from 100% of phase A (0.1% HCOOH in H20) to 80% of phase B (CH3OH/H2O/HCOOH; 90/10/0.1, v/v/v) in 30 minutes, followed by a 5 minute period of rebalancing; the temperature of the system pre-column-column was maintained at 25°C.

The ESI-MS analysis was performed using a mass spectrometer TSQ Quantum triple quadrupole Ultra (ThermoQuest, Milan, Italy), using a positive ions scan mode, in the following experimental conditions: capillary temperature 270°C; voltage of the spray 3.2 kV; capillary voltage of 12.5 V; nebulizer gas flow (nitrogen) 5l/min. The optimization of the ESI instrumental parameters was performed by infusion of an analyte solution in mobile phase A (flow 10μL/min) through a T-connection, and maintaining the flow of the mobile phase at 0.2 mL/min . The intensity of the ion $[M + H]^+$ was optimized using the software Quantum Tune Master®. The quantitative analysis was performed in MRM mode (voltage multiplier 2:00

kV), by using the most stable and abundant product ions at optimized collision energy. The following $[M + H]^+$ precursor ion → product ions transitions were used for the quantitative analysis:

LQQC(HNE)PF m/z 893.4→ 262.0 + 372.0 (collision energy: 40 eV)
LQQC(HNE)PF (D8) (IS) m/z 901.4 → 242.0 + 271.0 (collision energy: 40 eV)

The instrumental parameters relating to these transitions were optimized as described below: collision (argon) gas pressure in cell Q2: 1.5 mbar; peak width at half height (FWMH): 0.70 m/z for Q1 and Q3; scan range: 1 m/z, scan rate (dwell time): 0.2 s/scan.
A calibration curve of the LQQC(HNE)PF adduct was then obtained using the following calibration solutions, analyzed in duplicate in three replicates: 0.01 μM, 0.05 μM, 0.1 μM, 0.5 μM, 1 μM, 5 μM, 10 μM; The calibration samples were diluted in a solution of internal standard (LQQC(HNE)PF (D8)) to a final concentration of 0.5 μM in 10 mM phosphate buffer, pH 7.4.
The calibration line was obtained using the linear regression analysis of least squares (1/x2), using the peak area ratio of the analyte and of the IS versus the nominal concentration of the analyte.
The limit of quantitation (LOQ) was determined as the concentration of the analyte which provides a peak whose height is equal to 9 times that of the background noise, while the limit of detection (LOD) as the concentration of the analyte which provides a peak whose height is equal to 3 times that of the background noise.

- **Direct infusion of isolated HSA**

The lyophilized albumin was solubilized in 200 μL of a denaturant mixture CH_3CN/H_2O/HCOOH (70/30/0.4, v/v/v) and the solution obtained was analyzed by direct infusion MS approach (injection speed 5 μL/min).
Each sample was analyzed in two different mass range: m/z 900-1500 (Q = m/z 1) and m/z 1400-1500 (Q = m/z 0.5) using the following instrumental conditions: positive ion mode; capillary temperature 270°C; spray voltage 3kV; capillary voltage 46 V; gas flow (nitrogen): 0.5 L/min; acquisition time: 10 min.

11. Results

11.1 Development of the method: ESI-MS characteristics of LQQCPF-RCS adducts

The development of ESI-MS approach for the identification of Cys34 oxidative stress modifications involves several stages which may be summarized as follows:

1. selection of proteolytic enzymes for the HSA digestion, aiming to generate a 4-6 amino acids peptide (optimal for LC-MS/MS analysis) containing the Cys34 residue;
2. identification of at least three product ions of the LQQCPF target peptide not containing the Cys 34 target residue. The precursor ions analysis of these fragments first leads to the selective identification of the molecular ions containing the three selected product ions linked to the LQQCPF peptide sequence. This approach allows to identify all the peptides containing the residue Cys 34, variously modified because the selected product ions do not contain the residual target. It is important also to highlight that this approach allows also the identification of the peptide having a differently modified Cys34 residue. Indeed, the identification is based on three selected product ions not including this target residue.
3. characterization of the Cys34 modifications by MS/MS analysis in product ion scan mode.

Considering the procedure described above, a particular digestion procedure was developed based on the use of both trypsin and chymotrypsin. This procedure allows us to obtain the LQQCPF peptide containing the residue Cys 34 and characterized by a number of amino acid suitable for the MS analysis.

The development of the precursor ion scanning approach started with the selection of the most stable and abundant product ions not involving the target residue. These particular product ions belongs to the b and y series, before and after the Cys34 respectively. The selection involved a two steps approach. First, on the basis of the of theoretical fragmentation pattern a list of potential product ions was prepared namely: y1 (m/z 166.1), y2 (m/z 263.1), b2 (m/z 242.1), b2-NH_3 (m/z 225.1), b3 (m/z 370.2), b3-NH_3 (m/z 353.2), RM (*m/z* 735.3) and finally, the ions immonio of Leu (m/z 86.0), Gln (m/z 101.1), Cys (m/z 76.0), Pro (m/z 70.1) and Phe (m/z 120.1).

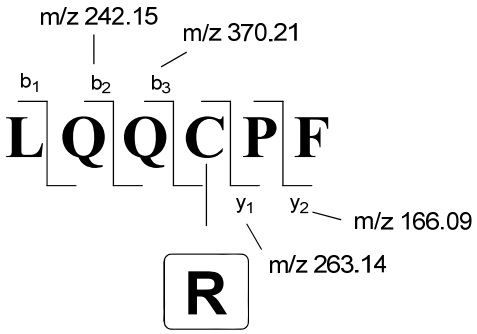

Considering the theoretical fragmentation pattern above reported, in the second step, the most abundant and stable ions not containing the target residue Cys 34 were selected. A list of LQQCPF adducts was prepared, using α, β unsaturated aldehydes, with different side chains (HNE, HHE, ACR, CRO, NONE), dialdehydes (GO, MDA) and ketoaldehyde (MGO).

The covalent products were identified and characterized by ESI-MS analysis and ESI-MS/MS analysis (direct infusion, in positive ion mode). As example, **figure 18** shows the ESI-MS spectrum recorded in positive ion mode of LQQCPF incubated in the presence (panel A) or absence (panel B) of HHE;

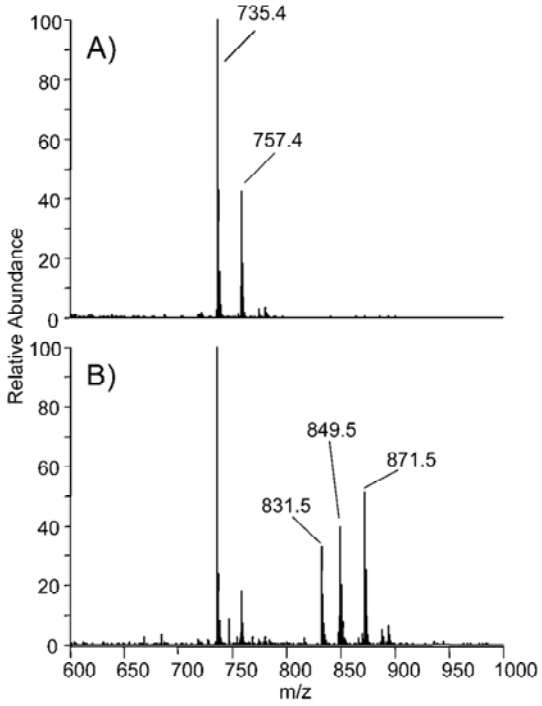

Figure 18 ESI-MS spectrum recorded in positive ion mode of LQQCPF incubated in the presence (panel A) or absence (panel B) of HHE

The spectrum relative to the peptide incubated in the absence of HHE is characterized by the peptide molecular ion (m/z 735.4 $[M+H]^+$), and by the corresponding sodium adduct m/z 757.4 $[M+Na]^+$) **(Figure 18 A)**. The spectrum for the reaction mixture containing LQQCPF

incubated for 24h with HHE is characterized beside the $[M+H]^+$ of the unmodified LQQCPF, also by the ion at m/z 849.5, attributed to the $[M+H]^+$ of the Michael adduct with HHE (confirmed by analysis in MS/MS) **(Figure 18 B)**.

Table 11.1 summarizes the reaction products, obtained by the incubation of the LQQCPF peptide with the different selected aldehydes.

Aldehyde	LQQCPF adducts			
	Structure	abbreviations	$[M+H]^+$	$[M+H]^+$ ($NaBH_4$)
ACR	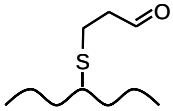	LQQC(ACR)PF	791.5	793.5
CRO	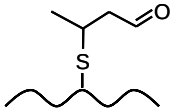	LQQC(CRO)PF	805.5	807.5
HNE	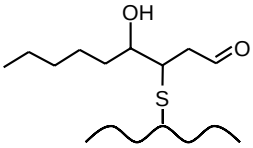	LQQC(HNE)PF	891.6	893.6
HHE	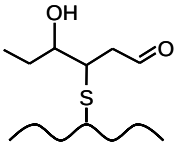	LQQC(HHE)PF	849.6	851.6
NONE	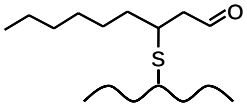	LQQC(NONE)PF	875.6	877.6
MDA	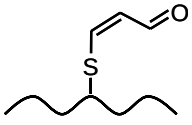	LQQC(MDA)PF	789.5	791.5
GO	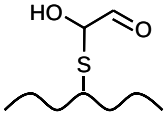	LQQC(GO)PF	793.9	795.9
MGO	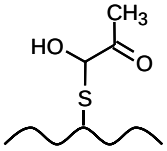	LQQC(MGO)PF	807.5	809.5

Table 11.1

It can be observed that all the α,β-unsaturated aldehydes formed the corresponding Michael adducts, and ACR and CRO gave an additional cross-link with an amino propene structure, involving the terminal amino group of the peptide (data not shown). The reaction product between MDA and LQQCPF was attributed to a thio-propenal adduct through Michael adduction, followed by a dehydration step. GO and MGO formed the corresponding hemi-thioacetal derivatives. We selected the diagnostic product ions for LC-ESI MS/MS analysis on the basis of the relative abundances at different collision energies (20, 30, 40, and 50 V) for native and modified LQQCPF.

Figure 19 shows the isoplots of the relative intensities of these target product. At 20 V, the only detectable product ions were the retro-Michael fragments for LQQC(HNE)PF, LQQC(HHE)PF and LQQC(MGO)PF.

At 30 V, the b2 and b3 ions were clearly detectable for all the covalent adducts, but the intensity of the y ions was negligible. At 40 V, b2, b3 and y2 were prominent for all the adducts, together with the immonium ion of the Leu residue (*m*/*z* 86.1). At 50 V, the b-ion series was conserved, while the y ions had almost completely disappeared.

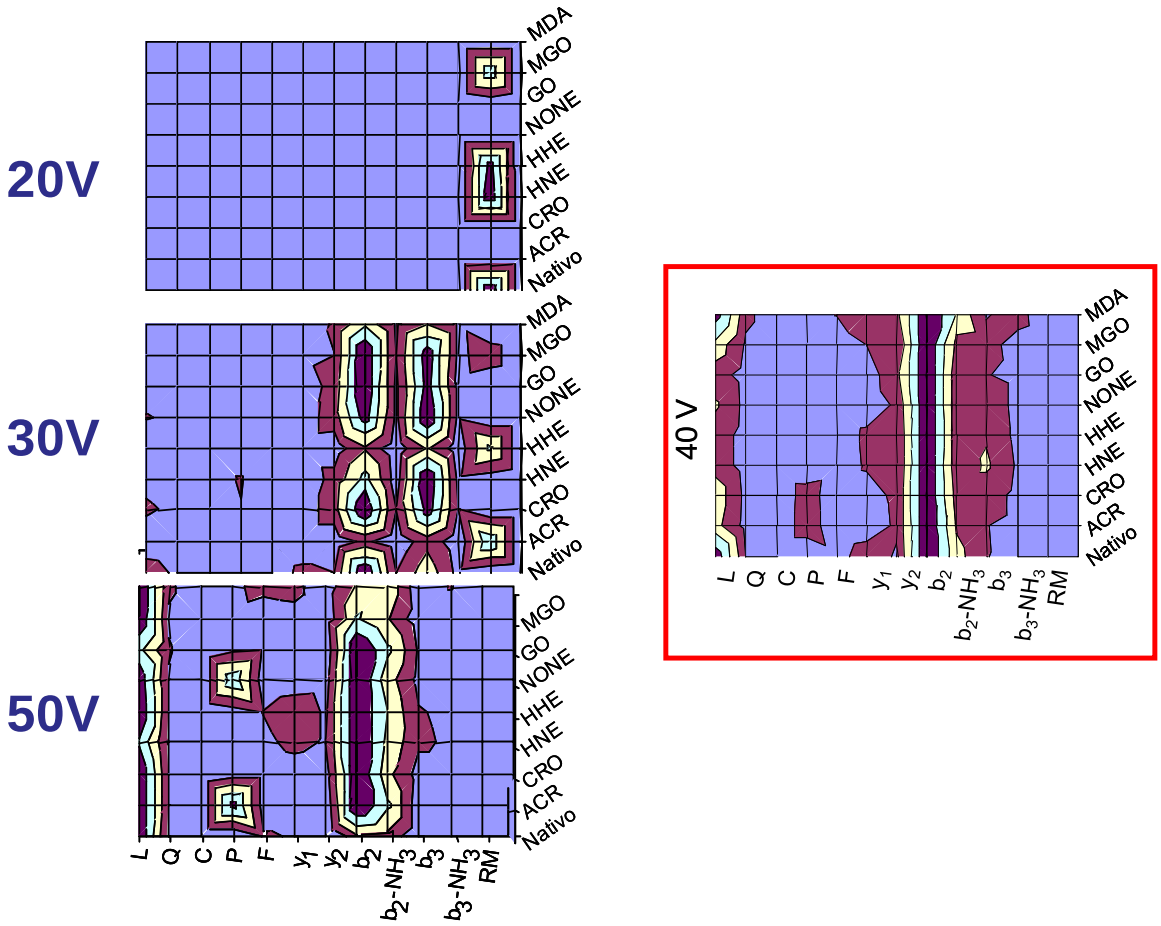

Figure 19 shows the isoplots of the relative intensities of these target product.

We then did a similar study for the LQQCPF adducts reduced with NaBH4. This procedure is required to stabilize the carbonylated peptide adducts and prevent them being lost during protein digestion (DDT for 60 min at 70 °C).

ESI-MS and MS/MS direct infusion experiments confirmed, for each adduct, the quantitative reduction of the aldehyde to the alcohol group, as evidenced by the $[M + H]^+$ values listed in **Table 11.1**. The fragmentation patterns at different collision energies were superimposable on those with non reduced LQQCPF adducts, except for the retro-Michael fragments which were not detectable at any collision energy. From these results we identified the collision energy that gives the most abundant, stable, and diagnostic fragment ions for LQQCPF covalently modified at the Cys34 residue, regardless of the adducted moiety. From the isoplots, we selected the following product ions at a collision energy of 40 V: y2 (*m*/*z* 263.1), b2 (*m*/*z* 242.1) and b3 (*m*/*z* 370.2).

11.2 LC-ESI-MS analysis of the LQQCPF-RCS adducts

The ESI-MS/MS was then coupled to LC to analyze a mixture of native and covalently modified LQQCPF, using the product ions listed above. The total ion current (TIC) showed several peaks eluting between 60 and 95 min (**Figure 20 A**). The ion current traces in precursor ion scanning mode were superimposable **(Figure 20** B, C, D**)**, and permitted the identification of all eight LQQCPF adducts in the mixture, as confirmed by the $[M+H]^+$ of the precursor ions and the MS/MS spectra obtained in product-ion scan mode (data not shown).

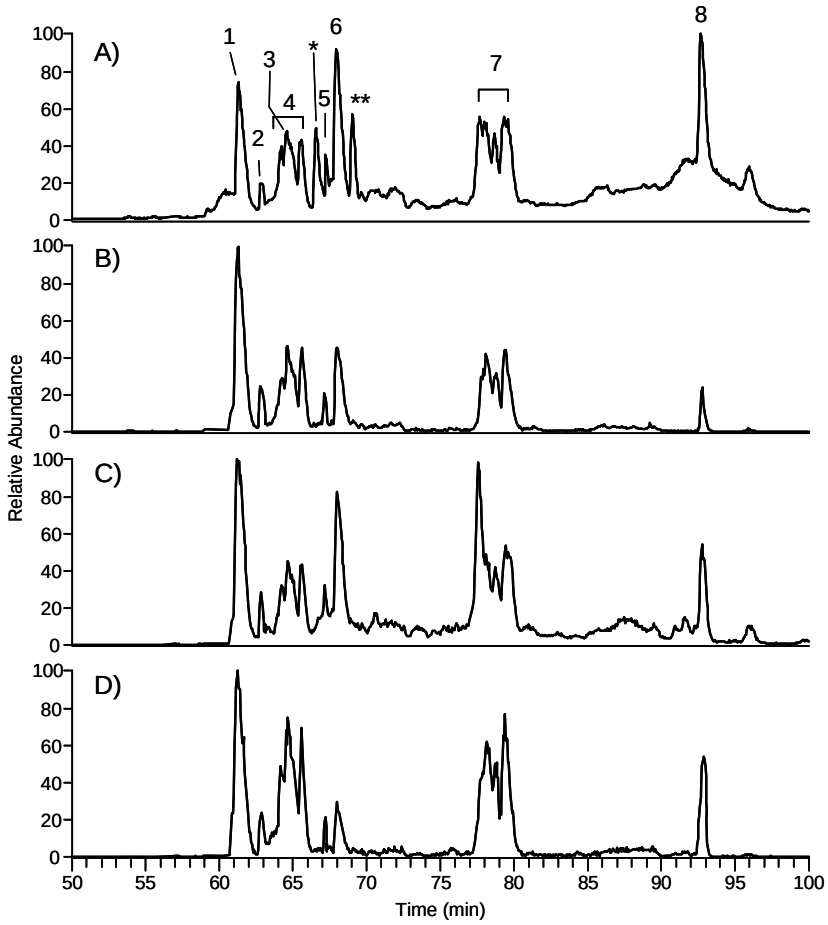

Figure 20 LC-ESI-MS/MS analysis of a mixture of native and covalently modified LQQCPF, using the product ions listed above. Panel A shows the total ion current (TIC). Panel B, C, D show the ion current traces in precursor ion scanning mode

Two additional peaks, not detectable in the precursor ion currents, were seen in the TIC trace at 66.5 min and 69.9 min, and assigned to the LQQCPF peptides cross-linked by ACR and CRO. Structure attribution was based on direct infusion experiments (data not shown), indicating that the cross-linked peptides had different fragmentation patterns from LQQCPF adducted to Cys34, not including the b2, b3 and y2 ions.

11.3 Application of the method: LC-MS/MS analysis of covalently modified HSA

The method was applied to albumin incubated with HNE, HHE and ACR. **Figure 21 A** shows the TIC for digested native HSA, with several peaks corresponding to the different peptides.

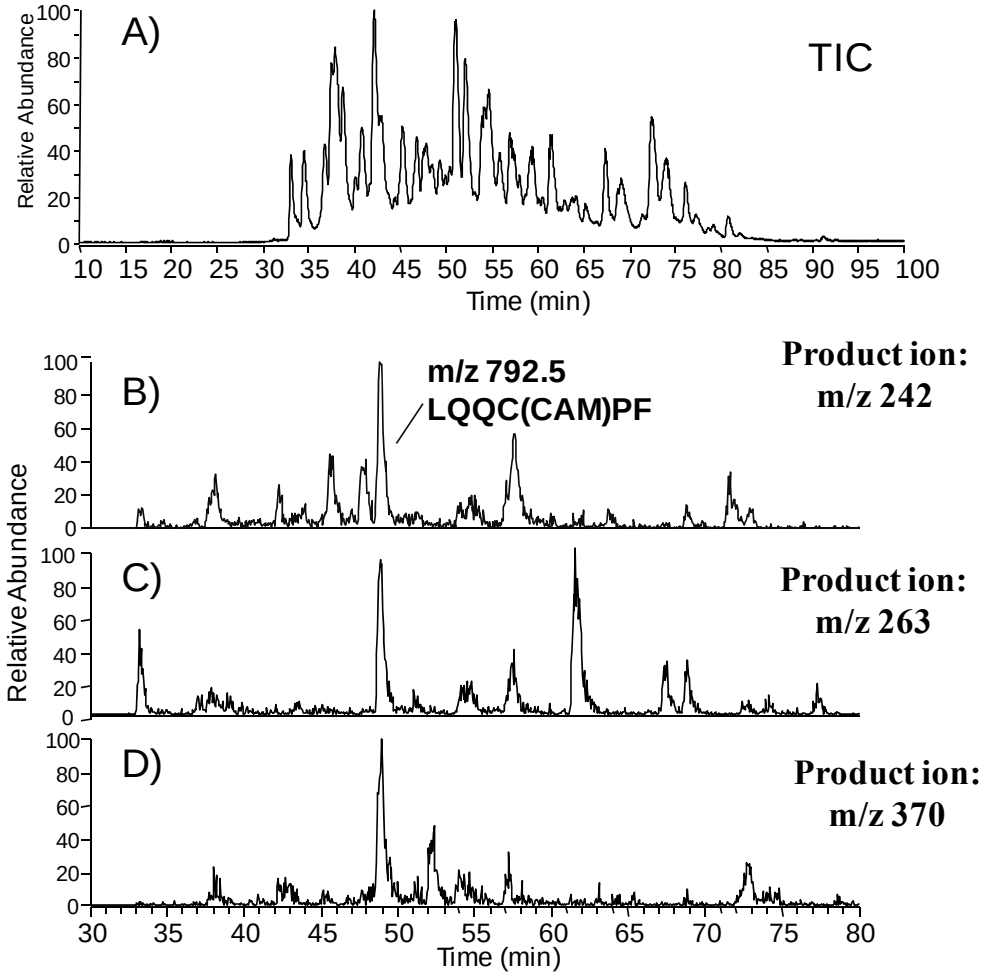

Figure 21 Panel A TIC for digested native HAS. Panel B,C,D precursor-ion scan current recorded with the product ion set at *m*/*z* 242.1, 263.1 and 370.2 respectively.

The precursor-ion scan current recorded with the product ion set at *m*/*z* 242.1 (**Figure 21 B**) contains not only a peak eluting at 49.3 min relative to the carboamidomethylated LQQCPF peptide [LQQC(CAM)PF] (precursor ion at *m*/*z* 792.5) but several other peaks too. The product ions at *m*/*z* 263.1 and 370.2 **(Figure 21** panels **C** and **D)** gave similar results.

Figure 22 (panels A, B, C) shows the precursor-ion scan traces of HSA adducted by HNE and digested with trypsin/chymotryspin. In particular we have isolated only two peaks since they were presented in all the three chromatograms and the molecular weight resulted the same in all the three recorded (*m*/*z* 792.5 and 893.6) attributed respectively to native LQQC(CAM)PF and LQQC(HNE)PF.

This approach was then employed successfully to study the Cys34-covalent modifications of HSA incubated with the other two α,β-unsaturated aldehydes, HHE and ACR. The Michael adducts between LQQCPF and HHE (parent ion *m*/*z* 851.6) and ACR (parent ion *m*/*z* 793.5) (data not shown) were easily identified.

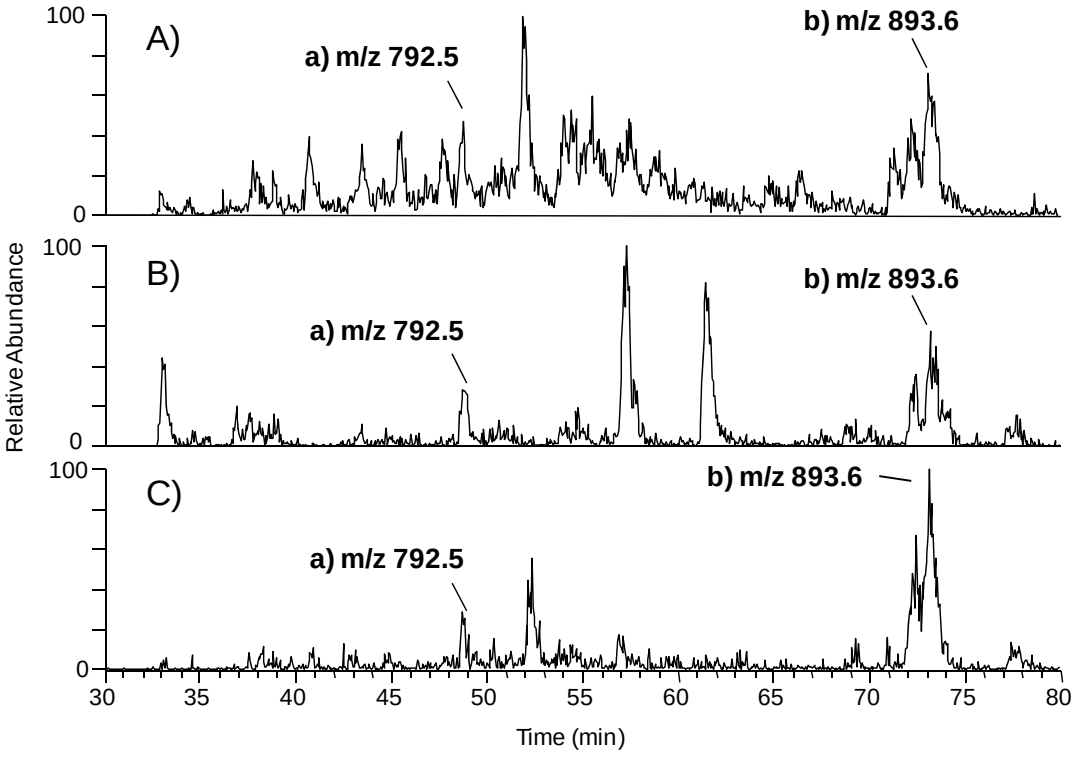

Figure 22 Panels A, B, C precursor-ion scan traces of HSA adducted by HNE and digested with trypsin/chymotryspin

As a further validation of the approach, **Figure. 23** reports the LC-MS chromatograms of a mixture containing digested HSA after incubation with HHE, HNE, ACR (5 μM final concentration for each analyte): all the peaks relative to LQQC(CAM)PF (peak a), LQQC(ACR)PF (peak b), LQQC(HHE)PF (peak c) and LQQC(HNE)PF (peak d) were easily identified and characterized.

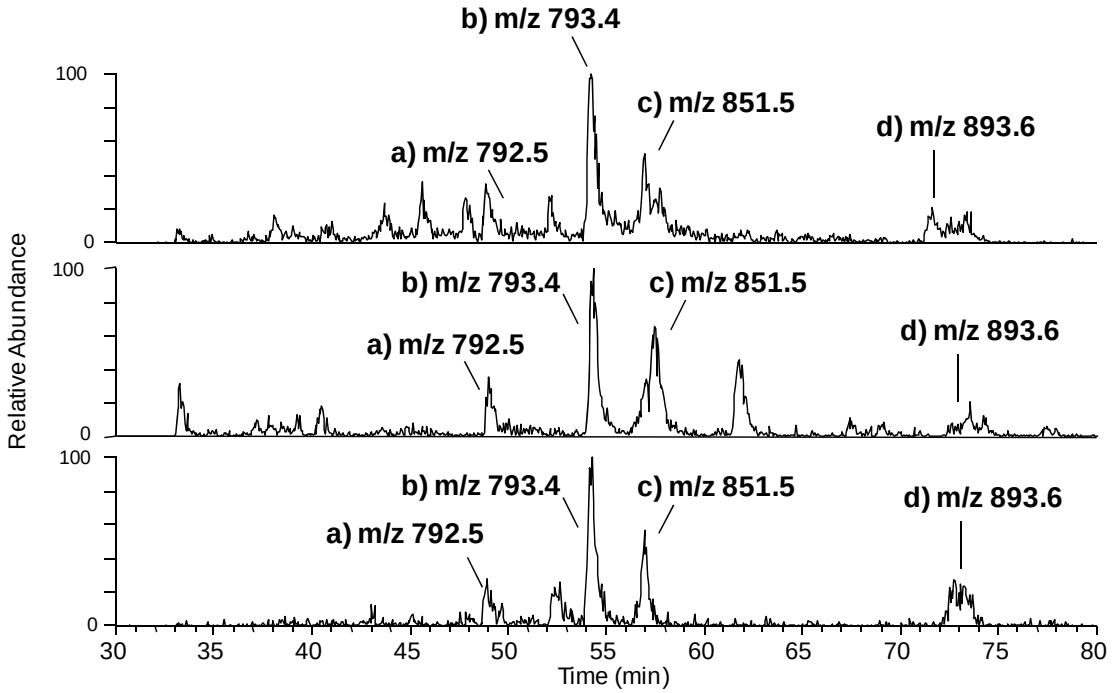

Figure 23: LC-MS chromatograms of a mixture containing digested HSA after incubation with HHE, HNE, ACR (5 µM final concentration for each analyte)

11.4 Cys 34 covalent modifications determination in patients undergoing hepatectomy surgery.

In the present study plasma samples taken from 3 patients undergoing hepatectomy surgery were analyzed at the following times:

1) before anesthesia,

2) 10 min after de-clamping.

HSA was isolated from plasma by affinity chromatography and digested with trypsin/chimotrypsin (see 10.2 Samples preparation and analytical methods). The peptide mixture was analyzed by LC-MS/MS in precursor ion scan mode (see 11.3 Application of the method: LC-MS/MS analysis of covalently modified HSA). As example, **Figure 24** shows the result of the analysis of sample 2 of subject 1 (10min after de-clamping), acquired by setting the product ions at m/z 242.1 (panel A), 263.1 (panel B), 370.2 (panel C).

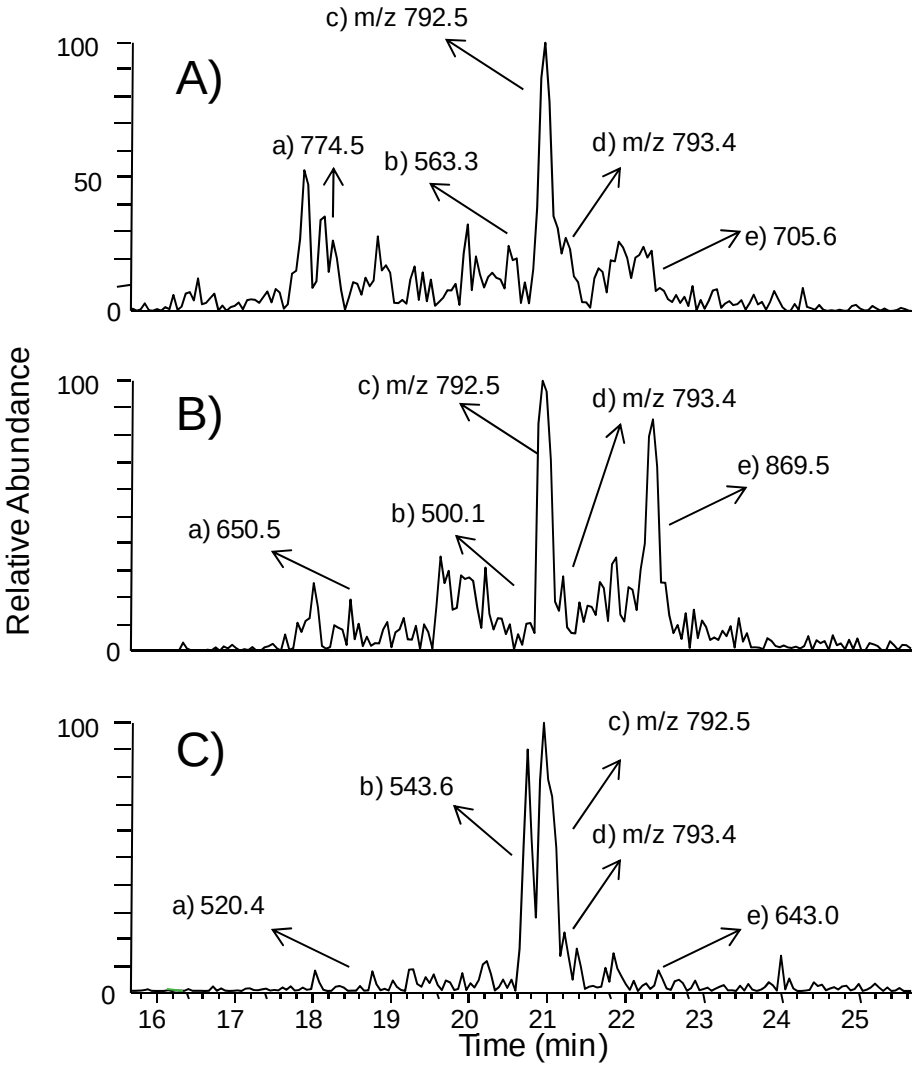

Figure 24: Result of the analysis of sample 2 of subject 1 (10min after de-clamping), acquired by setting the product ions at m/z 242.1 (panel A), 263.1 (panel B), 370.2 (panel C).

All the three chromatograms are characterized by a main peak eluting at 20.98 minutes attributed to the peptide LQQC(CAM)PF (peak c). It is well evident that at least four other peaks can be detected: m/z 774.5 (a); m/z 543.65, (b); m/z 793.4 (d); m/z 869.5 (e).

Among these, the peaks a), b) and e) were discarded since their molecular weight resulted different in the three traces.

Peak d) was instead isolated since it was presented in all the three chromatograms and the molecular weight resulted the same in all the three recorded (at m/z 793.4).

The analysis of the samples related to subjects 2 and 3 showed the same peaks listed above.

11.5 Structural characterization: analysis by product ions scan mode

An aliquot of the same sample was then analyzed using product ion scan mode, in order to confirm the peak at m/z 793.4 as a Cys 34 adduct peptide.

The chromatogram obtained are reported in **Figure 25**: the MS/MS spectrum relative to the peak at m/z 793.4 was analyzed with the software Molecular Weight calculator (ver. 6.15) for the characterization of the fragment ions and permitted to assign the structure of LQQC(ACR)PF adduct.

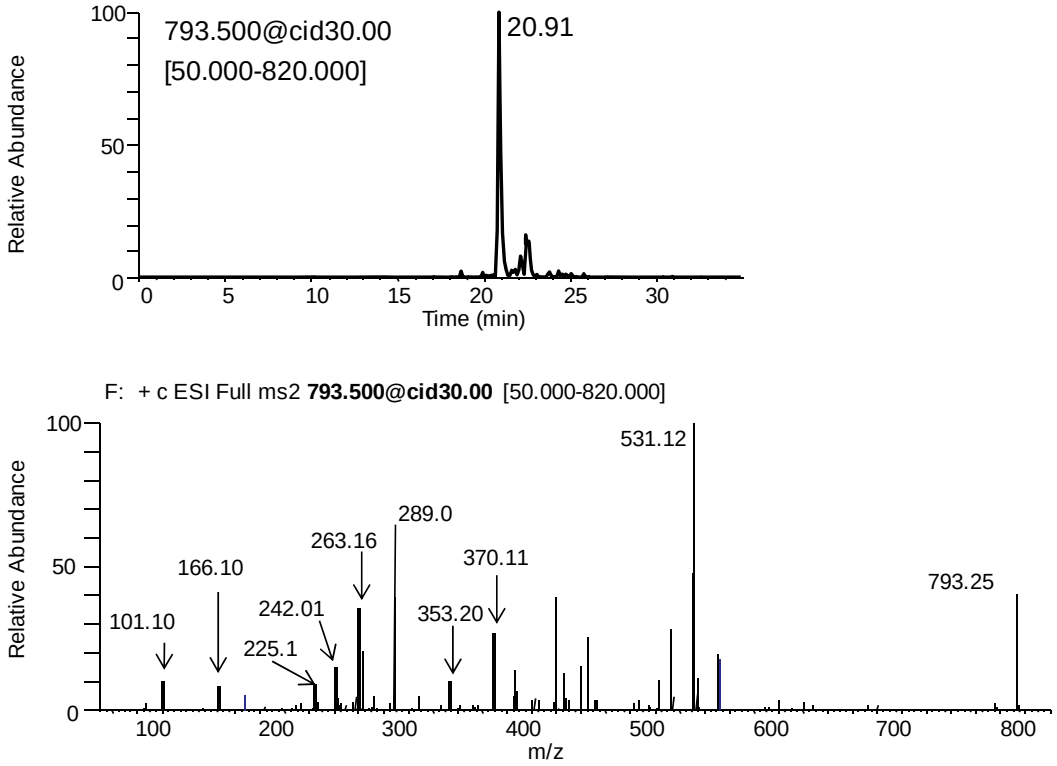

Figure 25: MS/MS spectrum relative to the peak at m/z 793.4 was analyzed with the software Molecular Weight calculator (ver. 6.15)

In particular, the following characteristic product ions were well evident in the MS/MS spectrum, as shown in **Figure 25 B**: y1 (m/z 166.1), y2 (m/z 263.1), b2 (m/z 242.1), b2-NH3 (m/z 225.1), b3-NH3 (m/z 353.2), b3 (mz 370.2), and finally, the ion immonio of Gln (m/z 101.1).

11.6 Quantitative analysis of the adduct LQQC(ACR)PF: analysis in MRM mode

The previously described results led to the identification of the modified peptide LQQC(ACR)PF as the main biomarker of HSA oxidation. Therefore an MRM method for quantitative analysis of this adduct was developed, selecting the two most stable and abundant product ions (m/z 289.0 and m/z 531.1). Therefore, the following precursor ion → product ions transition was selected for the quantitative analysis:

LQQC(ACR)PF m/z 793.4 → 289.0 + 531.1 (collision energy: 40 eV).

As internal standard, the adduct LQQC(HNE)PF (D8) (final concentration of 0.5 μM) was used (being not available the corresponding deuterated adduct). The results obtained by the MRM analysis of the samples related to subject 1 and 2 are reported in **Figure 26**. After 10 minutes of reperfusion (by de-clamping), the concentration of LQQC(ACR)PF increased by 3 times (18.7 ± 7.1 nmol/mg albumin) compared to the concentration determined in pre-anesthesia blood sample (5.9 ± 0.8 nmol/mg albumin). It is interesting to note that, in each case, the LQQC(ACR)PF adduct was well detectable also in samples taken before induction of ischemia-reperfusion injury, confirming the condition of oxidative stress of all the subjects analyzed.

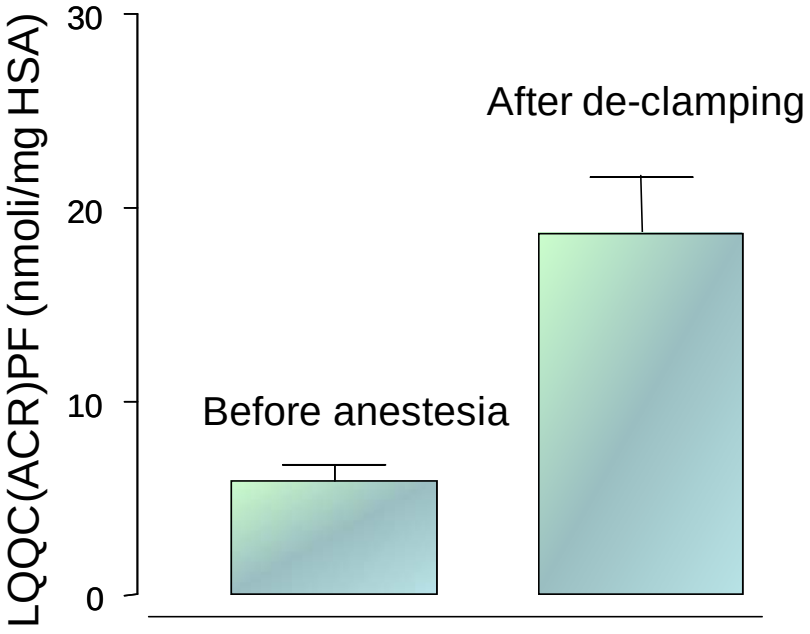

Figure 26: results obtained by the MRM analysis of the samples related to subject 1 and 2

11.7 Development and application of a MRM method for the quantitative determination of the LQQC(HNE)PF adduct

We then decided to set-up an MRM method for the quantitative determination also of the LQQC(HNE)PF taking account of the main role of HNE in oxidative stress. This choice could appear contrasting with the results obtained by precursor ion scan analysis, which couldn't be able to detect any LQQC(HNE)PF adducts. However the product ion scan analysis is not a very sensible method, so it can detect only species at a high concentration.

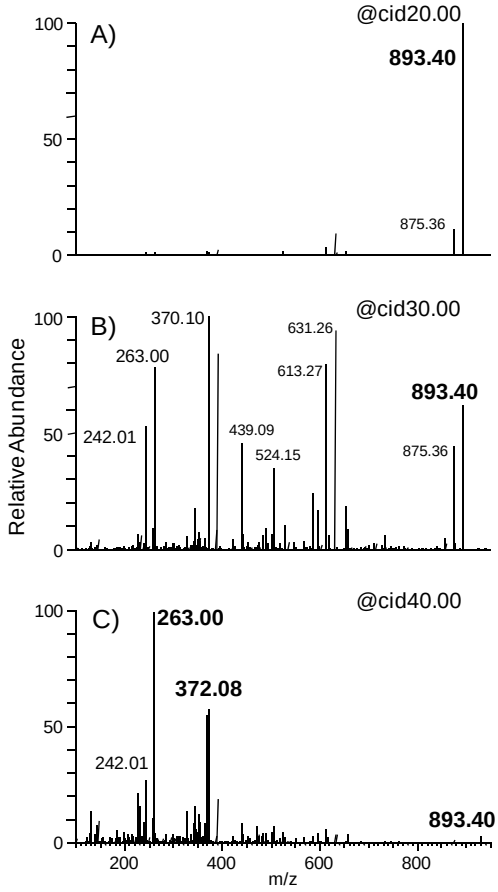

Figure 27: MSMS spectra of the adduct LQQC(HNE)PF (m/z 893.4), after reduction with $NaBH_4$, obtained by direct infusion analysis setting three different collision energies (20, 30 and 40 eV A,B,C respectively)

Figure 27 shows the MS/MS spectra of the adduct LQQC(HNE)PF (m/z 893.4), after reduction with $NaBH_4$, obtained by direct infusion analysis setting three different collision energies (20, 30 and 40 eV A,B,C respectively). It is well evident that increasing the collision

energy the most stable and abundant ions produced are characterized by a $[M+H]^+$ at m/z 262.0 (100% of relative abundance) and 372.0 (60% relative abundance).

Similarly, the direct infusion of a solution of an equal concentration of the deuterated adduct LQQC(HNE)PF (D8) (m/z 901.4) **(Figure 28)** provided the ions at m/z 242.0 (100% relative abundance) and 271.0 (88% relative abundance) as the most abundant.

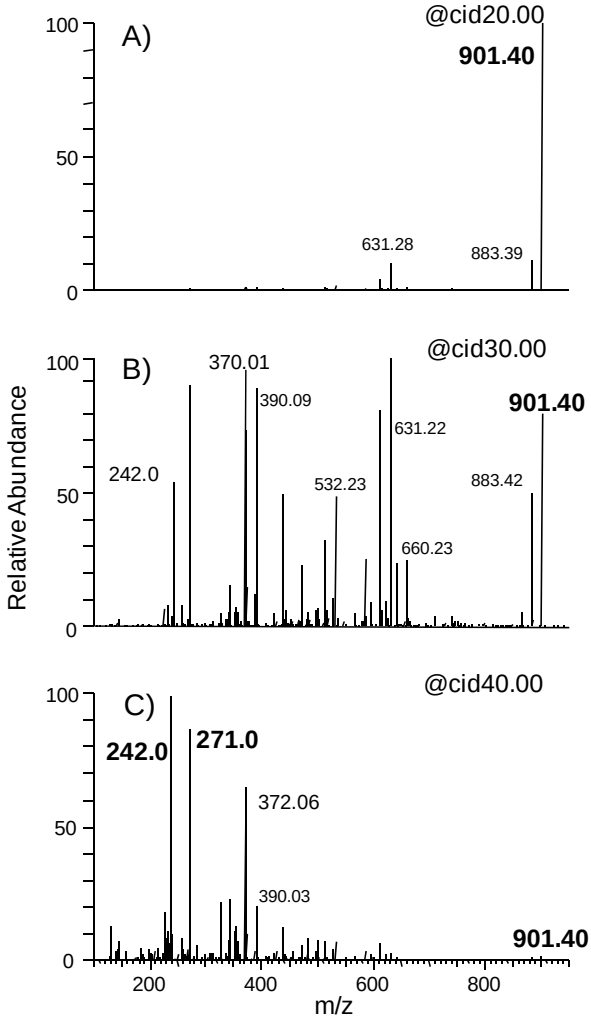

Figure 28 direct infusion of a solution of an equal concentration of the deuterated adduct LQQC(HNE)PF (D8) (m/z 901.4)

Therefore the following precursor ion → product ions transitions for the quantitative analysis of the adduct LQQC(HNE)PF were used:

LQQC (HNE) PF m / z 893.4 → 262.0 + 372.0 (collision energy: 40 eV)

LQQC (HNE) PF (D8) (IS) m / z 901.4 → 242.0 + 271.0 (collision energy: 40 eV)

Figure 29 is shown the LC-MS/MS profile of a sample of blank human plasma, added with mixture of analyte **(Figure 29 A)** and internal standard **(Figure 29 B)** to a final concentration 0.5 μM (LOQ); the analytes elute at about 24 min in a range of 0.6-0.8 min.

The calibration curve was linear over the entire range of calibration (0.01 μM - 10 μM), with a correlation coefficient r^2 greater than 0.999. The relative equation is the following: y = 1.345 (± 0067) x - 0096 (± 0.0008).

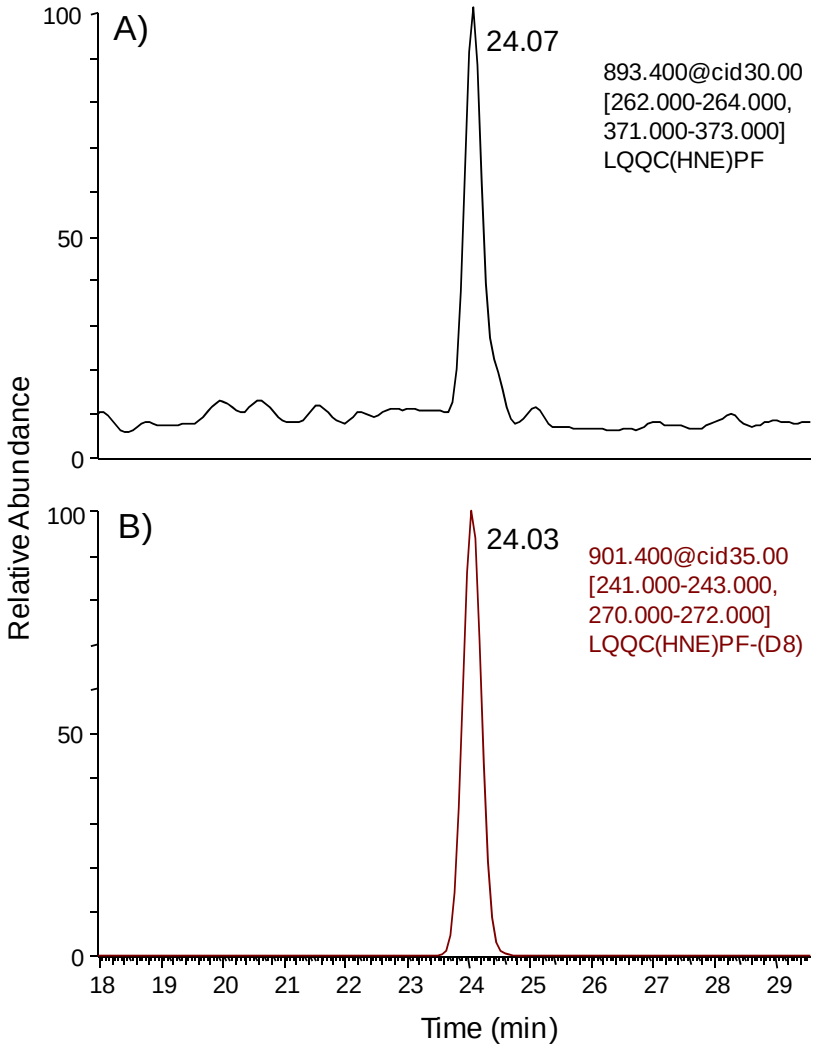

Figure 29: shown the LC-MS/MS profile of blank human plasma, added with mixture of analyte **(A)** and internal standard **(B)** to a final concentration 0.5 μM

The LOD, defined as a signal/noise ratio equal to 3, was 0.005 mM, while the LOQ defined as a signal/noise ratio equal to 9, was 0.01 μM.

The method was then applied for the quantitative analysis of the samples of the three subjects underwent hepatotectomy. In all plasma samples, the levels of LQQC(HNE)PF adduct were below the LOD (data not shown).

11.8 Analysis of native HSA by direct infusion

- **Determination of cysteinylated HSA by ESI-MS direct infusion**

The cysteinylated HSA is considered an extracellular potential biomarker of oxidative stress. This adduct is formed by reaction between the thiol group and oxidative species leading to the formation of the corresponding sulfenic acid which, in a second step, reacts with cysteine forming the mixed disulfide.

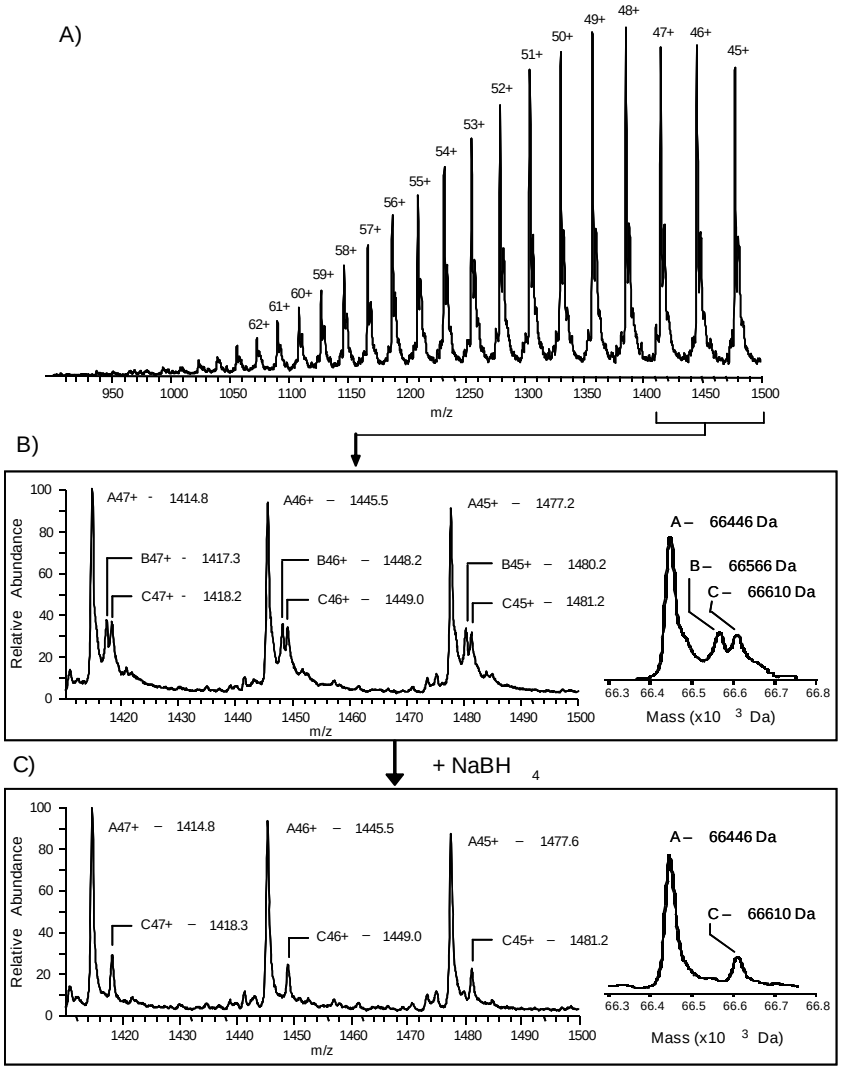

Figure 30: Panel A shows the ESI-MS spectrum relative to HSA serum acquired in positive ion. Panel B) shows the ESI-MS spectrum in positive ion mode of HSA isolated from human serum, characterized by three series of multicharged ions related to three species.

Therefore, a MS methodology was developed in direct infusion in order to determine the relative percentage of cysteinylated HSA.

Figure 30 (panel A) shows the ESI-MS spectrum relative to HSA serum (scan range m/z 900-1500), acquired in positive ion. The spectrum presents a series of multicharged ions in the range between m/z 1073 and m/z 1478 (addition of 62-45 protons). To further improve the resolution we then analyzed the sample reducing the scan range (m/z 1410-1500) and acquiring the MS spectrum for 10 min. The resolution was equal to m/z 0.5.

Figure 30 (panel B) shows the ESI-MS spectrum in positive ion mode of HSA isolated from human serum, characterized by three series of multicharged ions related to three species. The first series, resulted the most abundant, is characterized by three ions (m/z 1414.8, 1445.5 and 1477.2) attributed to multicharged ions of HSA by addition of 47, 46 and 45 protons (compound A). The second series is characterized by the three ions (m/z 1417.3, 1448.2, 1480.2 compound B) and the third at m/z 1418.2, 1449.0, 1481.2 (compound C), with a relative abundance of 30-35% compared to native HAS.

The de-convoluted compound A spectrum is characterized by the molecular weight of 66446 Da, which is similar to the HSA theoretical value 66429 (μM = +17 Da), obtained on the basis of the amino acid sequence (SwissProt: registration number P02768). The molecular weight of the compounds B and C were respectively of 66566 and 66610 Da, corresponding to a mass increase equal to 120 and 164 Da. On the basis of the mass values obtained, the compounds B and C were attributed to the cysteinylated (theoretical mass increment of 119 Da) and glycated form (162 Da) of HSA. The assignment was confirmed treating HSA with the reducing agent $NaBH_4$. In such conditions the disappearance of the signal related to compound B was observed, due to the reduction of the disulfide bond, as expected, the glycated form (compound C) resulted unmodified (Fig. 22, panel C). The percentage of the cysteinylated form can be determined by calculating the percentage ratio between the intensity of the cysteinylated form in respect to the sum of the different forms of albumin. Under physiological conditions the cysteinylated form, as well as glycated, is between 15 and 20%.

- **Determination of cysteinylated HSA in patients undergoing hepatectomy surgery**

HSA isolated from plasma samples taken from the three patients undergoing the hepatic resection was analyzed by direct infusion in order to measure the percentage of HSA cysteinylated form.

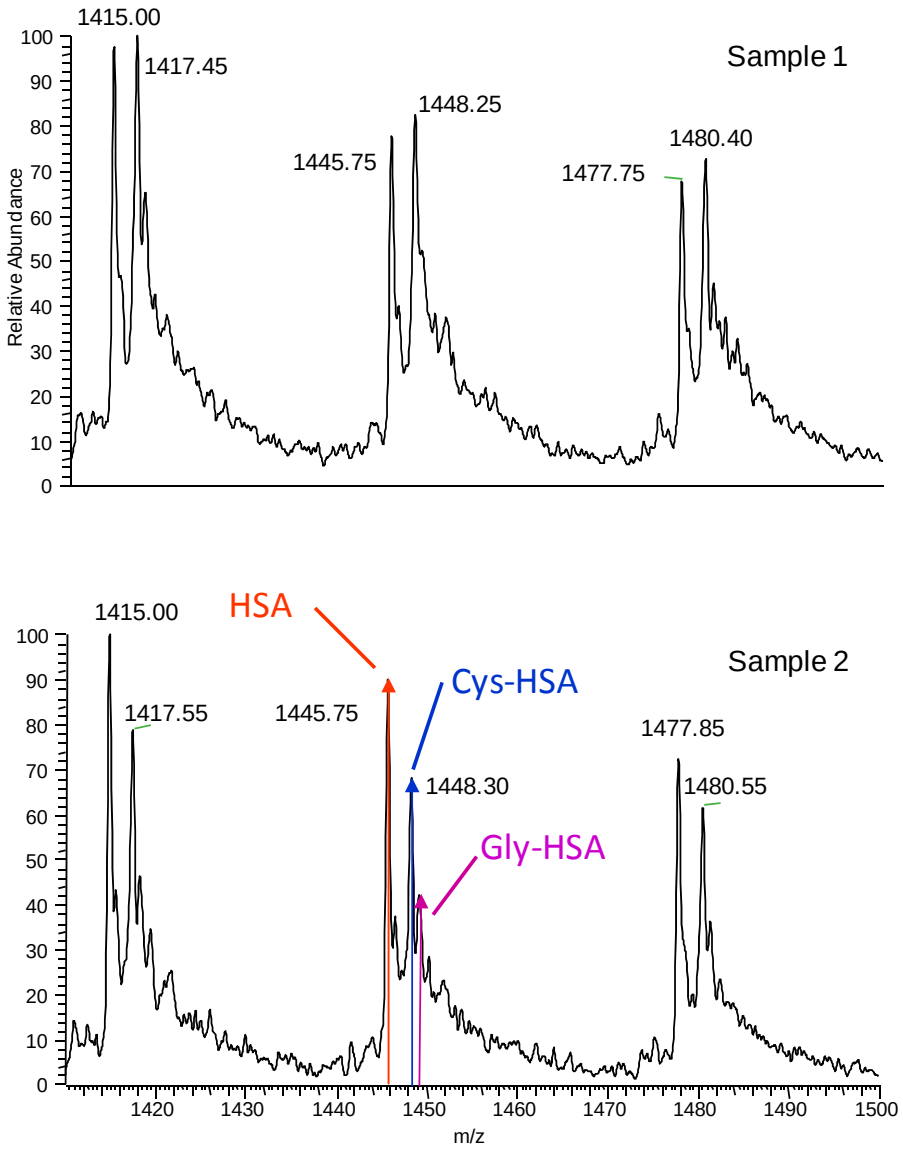

Figure 31: The spectra analysis indicates that the percentage of HSA cysteinylated form before anesthesia (sample 1)

The results related to sample 1 and 2 of subject 1 are reported in **figure 31**. The spectra analysis indicates that the percentage of HSA cysteinylated form before anesthesia (sample 1) was about 51% which is higher than the average found in the healthy subject.

The spectrum analysis relative to the sample taken 10 minutes after declamping (sample 2) shows a significant reduction of the percentage of the cysteinylated form (34%). The observed trend is completely similar for the other two patients (data not shown).

11.9 ESI-MS analyses of the HPYFYAPELLFFAK-RCS adducts: development of the method

The development of ESI-MS approach for the identification of His 146 oxidative stress induced modifications was performed following the same procedure discussed for LQQCPF adducts.

The digestion of HSA with tripsyn or with tripsyn/chimotrypsin led to two different peptides containing the target residue. In particular by tripsyn digestion a peptide characterized by 14 amino acids was obtained, with the following sequence HPYFYAPELLFFAK; on the other hand by tripsyn/chimotrypsin digestion we obtained a 3 amino acids peptide (HPY).

Starting from the first obtained peptide, we applied the same procedure above described, LQQCPF peptide, by selecting the most suitable product ions to be used for precursor ion scan analysis.

In this particular case, only the fragments belonging to the y series could be chosen as described in the sequence below reported.

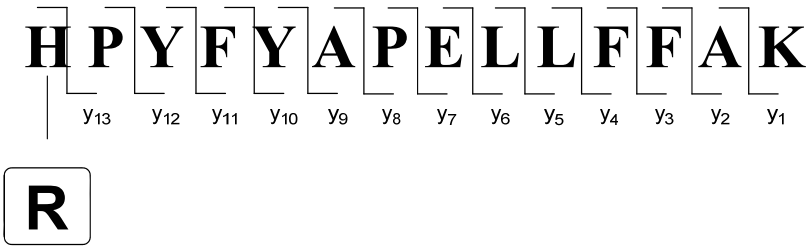

Among the y series ions, we then selected the most stable and abundant fragment ions, as performed for LQQCPF peptide. Therefore, the adducts between the HPYFYAPELLFFAK peptide and a list of α-β unsaturated aldehydes (HNE, HHE, ACR, CRO, NONE) were synthesized.

These adducts were then identified and characterized by ESI-MS and ESI-MS/MS analysis (direct infusion, in positive ion mode). As example, **Figure 32** shows the ESI-MS spectrum of HPYFYAPELLFFAK peptide, incubated in the presence (24h incubation) or absence of HNE, acquired in positive ion mode.

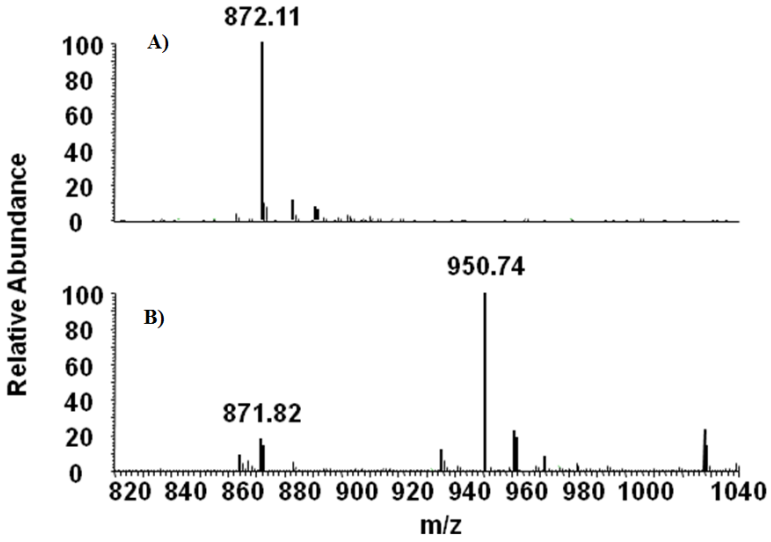

Figure 32: ESI-MS spectrum of HPYFYAPELLFFAK peptide, incubated in the presence (24h incubation) or absence of HNE, acquired in positive ion mode. Spectrum A is relative to the peptide incubated in the absence of HNE. The spectrum B corresponds to the $[M+2H]^{2+}$ adduct with HNE

The spectrum A, relative to the peptide incubated in the absence of HNE, is characterized only by the molecular ion of the peptide (m/z 872.1 $[M+2H]^{2+}$). In the spectrum B, the signal corresponding to the $[M+2H]^{2+}$ adduct with HNE (m/z 950.74) is well detectable, besides the one related to the $[M+2H]^{2+}$ of the native peptide (m/z 871.82).

Table 11.2 summarizes the products ions, obtained by the incubation of the HPYFYAPELLFFAK peptide with HNE, HHE, ACR, CRO, NONE, all identified by mass spectrometric analysis.

RCS	Structure	$[M+H]^+$
HNE	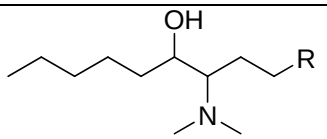	1901.94
ACR	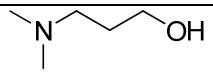	181.92
CRO	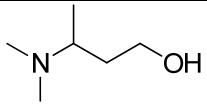	1815.94
NONE	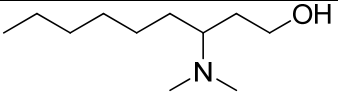	1886.12

Table 11.2

These adducts were then analyzed by MS/MS analysis using different collision energies (20, 30, 40 and 50V). Best results were obtained by choosing 40 eV as collision energy (data not shown).

In particular, y_4 and y_8 product ions resulted to be the most abundant fragment ions common to all the analyzed adducts as reported in **figure 33**, and for this reason they were choosen for the precursor ion scan method. (see paragraph 11.10)

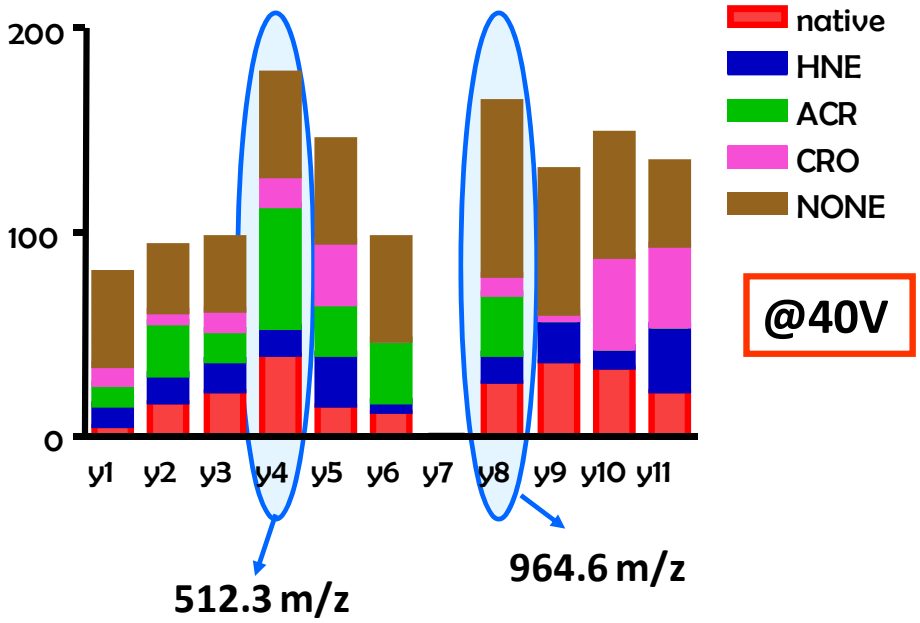

Figure 33: Best results obtained by choosing 40 eV as collision energy

11.10 LC-ESI-MS analysis of HPYFYAPELLFFAK-RCS adducts

The HPYFYAPELLFFAK native peptide and HNE adduct were then analyzed using LC-ESI-MS analysis in precursor ions scan mode. **Figure 34** shows the obtained total ion current (TIC) characterized by two peaks eluting between 19.5 and 21 min **(Figure 34 A)**. The other panels show the precursor ion traces obtained by setting the product ions to m/z 512.29.(B) and m/z 964.55 (C), as previously reported.

The two peaks are characterized by a molecular weights corresponding to the native peptide and to HNE adduct respectively.

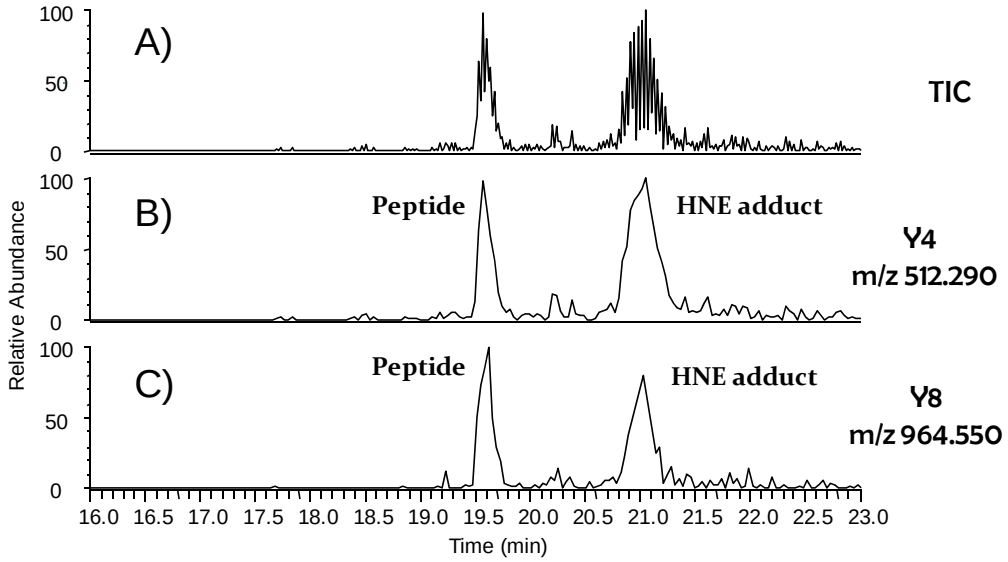

Figure 34 Panel A shows the TIC. Panels B and C show the precursor ion traces obtained setting the selected product ions

The structures of the two peaks were then confirmed by the MS/MS data obtained by a product-ion scan analysis as reported in the following chapter.

11.11 Structural characterization: analysis by product ions scan mode

An aliquot of the same sample was then analyzed by product ion scan mode, in order to confirm the nature of the peak at m/z 950.7 as an adduct peptide of His 146.

The chromatogram obtained is reported in **figure 35 (A)**.

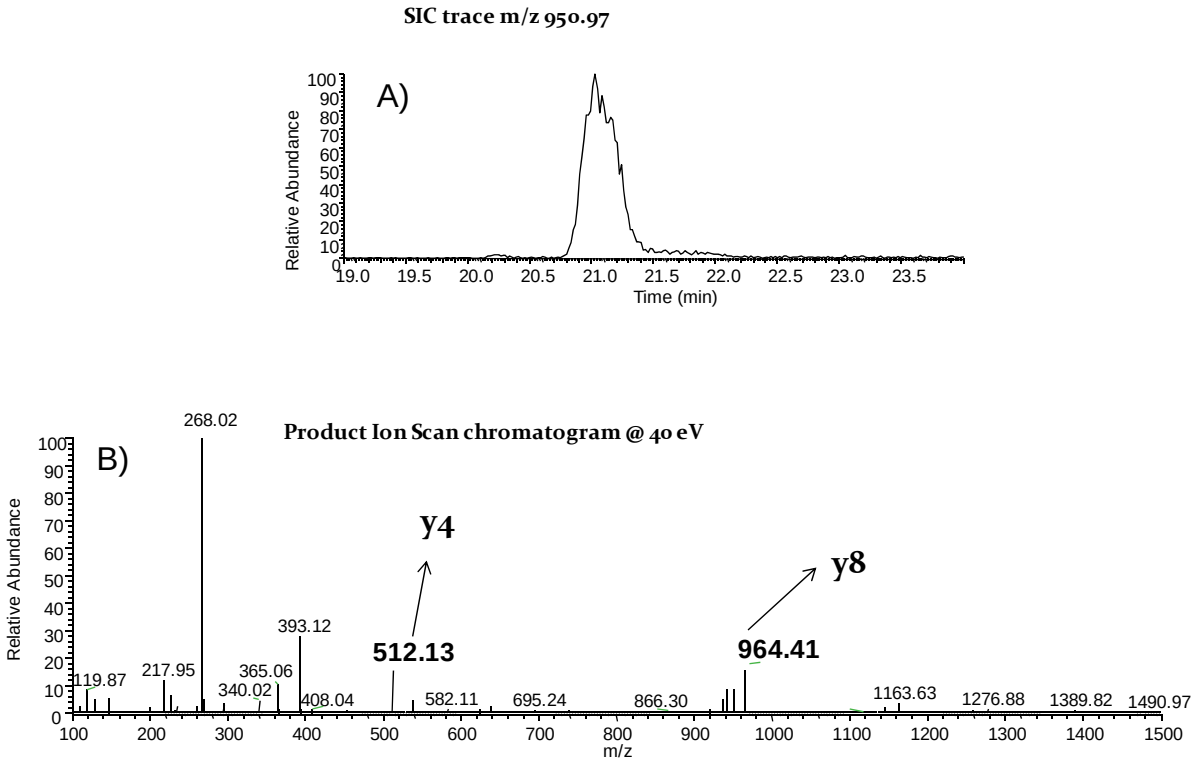

Figure 35 Panel A show the analyzed by product ion scan mode. Panel B show the MS/MS spectrum

The analysis of the MS/MS spectrum **(figure 35 B)** permitted us to assign the structure of the H(HNE)PYFYAPELLFFAK adduct because all the product ions were well evident: in particular the most abundant y4 (m/z 512.3) and y8 (m/z 964.41.1).

11.12 LC-MS/MS analysis of covalently modified HSA.

The method was then applied for the identification of the covalent HSA modifications after incubation with HNE. In particular, carbonylated HSA was subjected to enzymatic digestion with trypsin and then stabilized by reduction with $NaBH_4$.

As example, **Figure 36** reports the LC-ESI-MS/MS traces (mass range m/z 100-1500), relative to the precursor ions scan analysis of the digested native HAS. In particular, panel A reports the TIC while panels B and C the ion traces obtained selecting the ions at m/z 512.29 and m/z 964.55 as product ions.

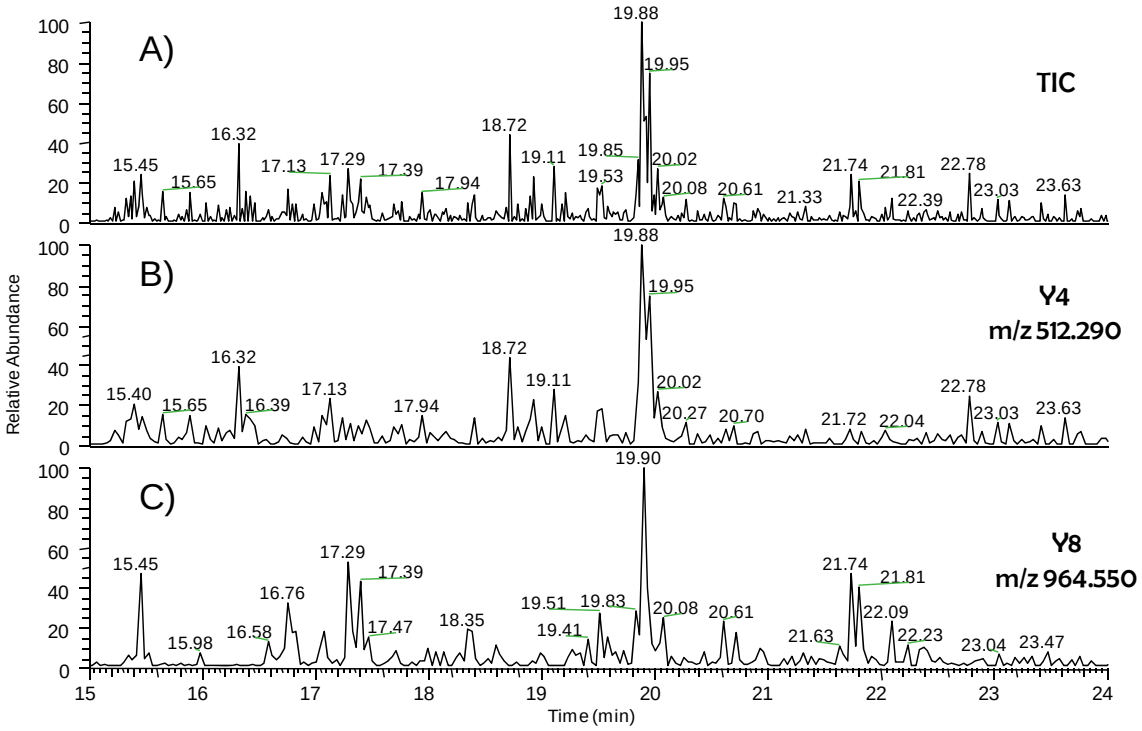

Figure 36 LC-ESI-MS/MS traces (mass range m/z 100-1500), relative to the precursor ions scan analysis of the digested native HAS

In all the three reported spectra the peak eluting at 20 min is well evident, related to the HPYFYAPELLFFAK native peptide.

The expected H(HNE)PYFYAPELLFFAK adduct at 21 minutes resulted undetectable.

For this reason the same sample was subjected to high-resolution, high mass accuracy mass spectrometry analysis using a LTQ-Orbitrap mass spectrometer.

In details a full scan analysis in data-dependent scan mode followed by data analysis with the SEQUEST algorithm was performed. The results obtained were able to explain the absence of any signals related to H(HNE)PYFYAPELLFFAK adducts with the presence of different

missed cleavages. Indeed, the SEQUEST algorithm compares the data obtained from LTQ-Orbitrap with the primary sequence of HSA and with all the possible covalent modifications induced by HNE, resulting in the identification of post-traslational modifications.
In particular the following missed cleavages were identified:

1. one missed cleavage peptides:

   RHPYFYAPELLFFAK

   HPYFYAPELLFFAK**R**

2. two missed cleavages peptide

   HPYFYAPELLFFAKR**YK**

3. three missed cleavages peptide

   RHPYFYAPELLFFAK**RYK**

To overcome the synthesis of all the possible peptides and of the corresponding RCS-adducts for a new study in precursor ion mode, we decided to carry out an alternative mass spectrometric approach, based on the direct analysis of trypsin/chymotrypsin HNE-HSA digested peptides in product ion scan mode, in order to characterize, on the basis of the predicted $[M+H]^+$ ions, all the formed adducts. In particular, considering the possible presence of different missed cleavages, we expected to obtain three different $[M+H]^+$:

- HPY (m/z = 574.23)
- **R**HPY (m/z = 730.33)
- HPY**F** (m/z = 721.30)

As example, **Figure 37** shows the LC-ESI-MS/MS chromatogram (mass range m / z 100-1500), obtained by product ions scan mode analysis of the digested native HSA.
Panel A reports the select ion chromatogram trace at 721.35 $[H(HNE)PYF+H]^+$: a single peak eluting at 88 min is well evident.
Panel B shows the MS/MS spectrum related to this peak confirming the expected molecular weight.
The SIC traces related to the other two possible peptide resulted undetectable.

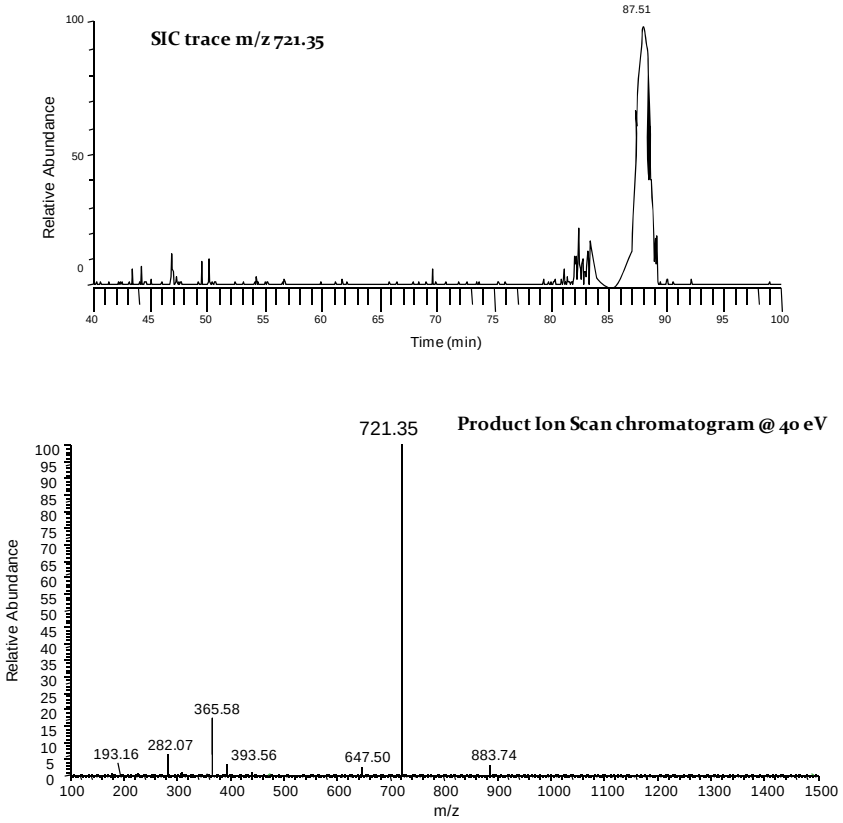

Figure 37: LC-ESI-MS/MS chromatogram (mass range m / z 100-1500), obtained by product ions scan mode analysis of the digested native HSA.

The results indicated the formation of one adduct only, H(HNE)PYF, but without a significant fragmentation of the corresponding $[M+H]^+$, even at high collision energy (40eV).

Hence considering all these results, we have finally considered as alternative approach the application of a new HSA digestion strategy, based on the use of chimotripsin only. In silico studies indicated EIARRH*PY as a new tag peptide containing the target residue His 146 in the middle of the peptide, like Cys 34 in the LQQC*PF peptide. The specific position of His 146 within the new tag peptide (that reasonably will reduce the risk of missed cleavages), and the lenght of the peptide (suitable to obtain significant MS/MS data for structure confirmation of RCS-adducts), can be considered as optimal characteristics to start a new MS strategy involving His 146 as a carbonyl adduction site on HSA.

Thus, HSA was isolated from human plasma by affinity chromatography, reduced with $NaBH_4$ and digested with chimotrypsin only, in order to obtain the expected peptide. The peptide mixture was analyzed by LTQ-Orbitrap in data-dependent scan mode and the data obtained were further analyzed by the SEQUEST algorithm.

As example, **Figure 38** shows LC-ESI-MS/MS chromatograms (mass range m / z 100-1500), obtained in data-dependent scan mode of the HSA digested native (panel A).

Panel B reports the select ion chromatogram trace at 521.28, indicating the presence of the expected tag peptide.

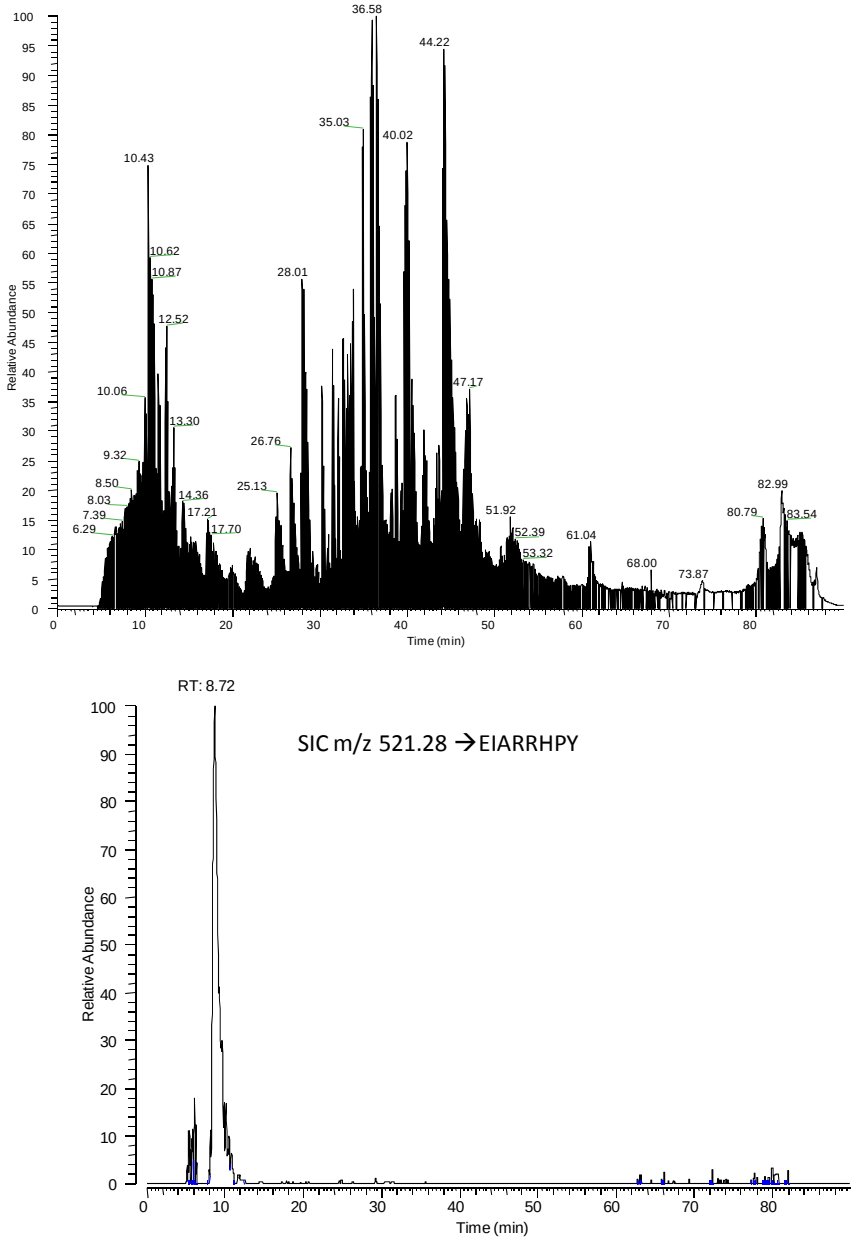

Figure 38: LC-ESI-MS/MS chromatograms (mass range m / z 100-1500), obtained in data-dependent scan mode of the HSA digested native

The SEQUEST algorithm compares the obtained data with the primary sequence of the HSA. The results **(Table 11.3)** of the analysis confirmed the formation of the expected peptide (see the last two lines of the table).

In this way we created the bases for the future studies on the EIARRH*PY peptide, in order to identify any covalent modifications of His146 induced by RCS.

Time(s)	Peptide	$[M+H]^+$
10.84	Y.AEAKDVF.L	779.39340
10.76	Y.AEAKDVF.L	779.39340
9.25 - 9.31	F.AEVSKL.V	646.37702
16.32	F.AKTC*VADESAENC*DKSLHTLF.G	2396.08569
16.21	F.AKTC*VADESAENC*DKSLHTLF.G	2396.08569
16.13 - 16.20	F.AKTC*VADESAENC*DKSLHTLF.G	2396.08569
16.87 - 16.92	Y.AKVFDEF.K	855.42470
24.27	Y.AKVFDEFKPL.V	1193.65649
23.66 - 23.73	Y.AKVFDEFKPL.V	1193.65649
24.42	Y.AKVFDEFKPL.V	1193.65649
24.34	Y.AKVFDEFKPL.V	1193.65649
24.35	Y.AKVFDEFKPL.V	1193.65649
23.74 - 23.81	Y.AKVFDEFKPL.V	1193.65649
31.28 - 31.36	Y.AKVFDEFKPLVEEPQNL.I	2003.04842
31.36 - 31.43	Y.AKVFDEFKPLVEEPQNL.I	2003.04842
12.50	Y.ARRHPDYSVVL.L	1312.71204
12.50	Y.ARRHPDYSVVL.L	1312.71204
12.60	Y.ARRHPDYSVVL.L	1312.71204
16.45 - 16.50	Y.ARRHPDYSVVLL.L	1425.79611
8.94	-.DAHKSEVAHRF.K	1296.64436
9.45	-.DAHKSEVAHRF.K	1296.64436
8.89	-.DAHKSEVAHRF.K	1296.64436
13.42	F.DEFKPL.V	748.38758
13.34	F.DEFKPL.V	748.38758
28.64	F.DEFKPLVEEPQNL.I	1557.77951
28.75	F.DEFKPLVEEPQNL.I	1557.77951
8.58 - 8.65	Y.**EIARRHPY**.F	1041.55884
8.66 - 8.71	Y.**EIARRHPY**.F	1041.55884

Table 11.3

12. Discussion

The protein carbonylation is an important mechanism of oxidative damage mediated by the formation of carbonyl species (RCS) generated by oxidation of sugars and lipids.

RCS and the related adducts with proteins (so called, carbonylated proteins) are widely used as biomarkers of lipid peroxidation and, in general, of oxidative stress[76].

Moreover, a strict correlation between carbonyl stress and certain human diseases is well established. The accumulation of carbonylated proteins is commonly recognized as a common feature of aging in tissue proteins, and the levels of these compounds resulted increased either systemically or locally in a broad range of diseases, including diabetes, atherosclerosis and kidney, hepatic, and neurodegenerative diseases[203-206]. Whether carbonylation represents a cause or an effect is still to be fully clarified, although, for some diseases, several convincing evidences support a pathogenic role, such as in the case of diabetic-related diseases[207], age-dependent tissue dysfunction, neurodegenerative diseases[208], and atherosclerosis[148]. Consequently, protein carbonylation is a predictive biomarker of oxidative damage and represents a biological target for drug discovery[209, 210].

Therefore, the need of suitable analytical methods not only for the diagnosis but also for better understanding the mechanisms involved in the carbonylation damage is well evident. Nowadays, the carbonylation damage is mainly measured by immunological techniques using mono-and poly-clonal antibodies specific for carbonylated proteins. This approach has been widely used to give an index of systemic and tissue carbonylation, but it cannot identify and characterize the sites of the reaction.

The advent of proteomics and hence separation of proteins by 2D- analysis followed by immunoblotting has given the possibility to identify the proteins most involved in the carbonylation process, providing an in-depth analysis of the mechanisms involved in protein-dependent oxidative process.

However, an analytical strategy to map a wide range of known and unknown RCS is needed to understand how they are involved in different oxidative-based disorders, and to formulate an appropriate pharmacological strategy, for example by designing carbonylation damage inhibitors.

The technique here proposed was therefore designed to establish a specific and sensitive analytical approach to identify and characterize all the oxidative modifications (even not carbonyl-derived) of an endogenous target protein (human serum albumin), without requiring external standards.

Conventional proteomic approaches indicate albumin as the main target of carbonylation in serum[188, 189]. Albumin can be carbonylated by several mechanisms, such as direct oxidative reactions sustained by reactive oxygen species (ROS) or covalent adduction induced by electrophilic compounds such as HNE and ACR[64]. Proteomics approaches have led to the identification of the protein/s showing high sensitivity to oxidation/carbonylation, and among them HSA was found to be the main target in the circulation[188-190].

The high reactivity of HSA towards electrophilic RCS[185, 211] could be explained both by the elevated HSA plasma concentration (~ 0.6mM) and to several accessible nucleophilic residues, mainly Cys 34, followed by His 146 and Lys 199[185, 191]. Among these sites, Cys 34 resulted the most reactive site, able to react with alfa, beta unsaturated aldehydes better than GSH, followed by His 146.

Thus, considering HSA Cys 34 as the main targets of carbonylation in human serum, the MS strategy proposed here seeks to identify covalent modifications induced by oxidative/carbonylation damage.

Cys 34 is a sensitive residue for various post-translational modifications besides carbonylation, including S-nitrosylation, disulfide formation and oxidation to sulfenic, sulfinic and sulfonic derivatives. These have all attracted interest because of their correlations with physiopathological conditions such as intrauterine growth restriction and kidney disease (Cys 34 cysteinylation and homocysteinylation[212, 213]), glomerulosclerosis (Cys 34 sulphonation [214]) and oxidative stress (Cys 34 oxidation[215]). A MS method to identify and characterize all the Cys 34 covalent modifications would be valuable not only for studying RCS-modified albumin, but also to check the oxidative state of Cys34 as a marker of oxidative damage.

In order to obtain a rapid identification and characterization of Cys34 covalent modifications, a MS strategy based on the precursor-ion scanning technique was used. By the application of this technique, it has been possible to selectively identify the molecular ion of all the tryptic peptides containing the Cys34 residue in native or modified form. This type of MS approach gives rapid confirmation of targeted compounds, or non-targeted detection of compounds with a common moiety, and it has been widely used in drug discovery and development[216] and in vitro/in vivo drug-metabolism studies[131].

The technique was initially validated in several in vitro models and provided very good results in terms of selectivity. In particular, the Cys-34 adducts were easily identified by incubation of HSA with different reactive carbonyl species. Once setup, the method was then

applied for the identification of the main HSA-Cys 34 oxidative modifications isolated from patients undergoing liver resection.

This type of surgery involves a blood clamping step followed by a reperfusion phase. This procedure is known to be strictly correlated with a significant oxidative stress because of the activation of xanthine oxidase and of the accumulation of hypoxanthine during the ischemic phase, followed by an oxygen intake during the reperfusion step. The co-presence of these substrates/enzymes causes the superoxide anion formation, which represents a well-known precursor of hydroxyl radicals, species mainly responsible for the oxidative process. We can therefore assist that the liver resection and the condition of induced ischemia/reperfusion represent an in vivo model of oxidative stress.

The results obtained by precursor ion scan analysis led to the identification, as the only oxidative modification, of the Michael adduct between Acrolein and Cys 34 in all three subjects who underwent the liver resection. Acrolein is an α,β-unsaturated aldehydes generated by lipid peroxidation and characterized by a very high electrophilicity.

On the basis of this qualitative evidence, a MRM (multiple reaction monitoring) method was developed, in order to perform a quantitative analysis of the LQQC(ACR)PF adduct.

The MRM analysis was able to determine the presence of this adduct also before the surgery, an evidence congruent with the medical case and the hepatic dysfunction affecting these patients, and so with the correlated oxidative stress.

The LQQC(ACR)PF adduct was also found to be significantly increased after the reperfusion step, confirming that this adduct can be considered as a sensible biomarker of the oxidative process.

In addition, the ESI/MS analysis of native albumin by direct infusion approach (see paragraph 11.8) showed the disulfide formation of Cys 34 by cysteinylation, with a 50% increased level in all three subjects before the anesthesia, a significantly higher value compared to the one found in healthy subjects. This results confirm that the oxidative stress condition is already established before the surgery, as indicated by the determination of the LQQC(ACR)PF adduct.

Unexpectedly, the level found at the end of the reperfusion injury resulted slightly decreased. Several hypotheses could be postulated to explain these data, including the reduced availability of extracellular Cys most likely involved in the oxidative detoxification processes.

In parallel, MS studies performed in our laboratory using the same approach, we confirm that Cys 34 undergoes cysteinylation also in another in vivo model of oxidative stress, such as uremic subjects (data not shown). This result confirmed that in some pathological conditions

the target site Cys 34 could be blocked by the disulfide bond, thus limiting its ability to react with RCS.

Hence, Cys 34-adducts couldn't always be useful as carbonylation biomarkers. Therefore, during my PhD study, I focused my attention on another HSA nucleophilic site (His-146), previously recognized as a potential oxidation/carbonylation target[185].

Digesting HSA with tripsin or tripsin+chimotripsin, two different peptides containing His-146 have been obtained: H*PYFYAPELLFFAK and H*PY, respectively.

Anyway, analysis of tripsin or tripsin+chimotripsin digested HNE-HSA adduct did not lead to identification of any covalent modifications on His 146.

Using an high-resolution, high mass accuracy mass spectrometer (LTQ-Orbitrap), performing a full scan analysis in data-dependent mode followed by data analysis with the SEQUEST algorithm, it was possible to explain that the absence of any signals relative to RCS-H*PYFYAPELLFFAK adducts was due to different missed cleavages.

The analyses relative to the H*PY peptide indicated the formation of one adduct only, H(HNE)PYF, but no significant fragmentation of the corresponding [M+H]+ was observed in MS/MS experiments, even working at high collision energy (40eV). Maybe the reason could be that the peptide is too short for an optimal fragmentation.

Taking account of these observations, we have considered as alternative approach the application of a new HSA digestion strategy, based on the use of chimotripsin only. In silico studies indicated the EIARRH*PY peptide as a new tag containing the target residue His 146 in the middle, exactly like Cys-34 in the LQQC*PF peptide, previously analyzed with satisfactory results. This new peptide has also the appropriate length to be analyzed by HPLC-MS/MS. Hence, the EIARRH*PY peptide seemed to possess the optimal characteristics to start a new MS strategy involving His-146 as a carbonyl adduction site on HSA.

Thus, HSA was isolated from human plasma by affinity chromatography, reduced with NaBH4 and digested with chimotripsin only in order to obtain the expected peptide. The peptide mixture was analyzed by LTQ-Orbitrap in data dependent scan mode and afterwards by the SEQUEST algorithm, comparing the obtained data with the primary sequence of the protein. The results of the analysis confirmed the formation of the expected peptide.

In this way we created the bases for the future studies on the EIARRH*PY peptide, in order to identify any covalent modifications of His146 induced by RCS.

13 Conclusions

In this second part of my PhD thesis, it has been developed a mass spectrometry method for the rapid and selective identification and characterization of the oxidative modification of proteins.

Considering the studies performed to investigate HSA- Cys 34 covalent modifications, the application of the method to plasma samples taken from patients undergoing liver resection has made possible to identify Acrolein as the main aldehyde generated by oxidative stress condition.

Considering the analysis performed to study HSA- His 146, we performed a new HSA proteolytic digestion strategy based on the use of chimotrypsin only. This results can be considered the bases for the future studies on the EIARRHPY peptide, in order to identify any covalent modifications of His146 induced by RCS.

Such informations provide an explanation necessary to understand the mechanisms underlying oxidative stress, induced by a condition of ischemia / reperfusion, and also to select biologically active compounds targeted to the detoxification of such cytotoxic oxidation products.

14 Bibliography

62. Rifai, N.; Gillette, M. A.; Carr, S. A. *Nature Biotechnology* **2006,** *24*, 971.
63. Aebersold, R.; Mann, M. *Nature (London, United Kingdom)* **2003,** *422*, 198.
64. Dalle-Donne, I.; Giustarini, D.; Colombo, R.; Rossi, R.; Milzani, A. *Trends in Molecular Medicine* **2003,** *9*, 169.
65. Thannickal, V. J.; Fanburg, B. L. *American journal of physiology. Lung cellular and molecular physiology* **2000,** *279*, L1005.
66. Moldovan, L.; Moldovan, N. I. *Histochemistry and Cell Biology* **2004,** *122*, 395.
67. Beal, M. F. *Free Radical Biology & Medicine* **2002,** *32*, 797.
68. Levine, R. L. *Free Radical Biology & Medicine* **2002,** *32*, 790.
69. Sohal, R. S. *Free Radical Biology & Medicine* **2002,** *33*, 573.
70. Dalle-Donne, I.; Scaloni, A.; Giustarini, D.; Cavarra, E.; Tell, G.; Lungarella, G.; Colombo, R.; Rossi, R.; Milzani, A. *Mass Spectrometry Reviews* **2005,** *24*, 55.
71. Miyata, T.; Van Ypersele de Strihou, C.; Kurokawa, K.; Baynes, J. W. *Kidney International* **1999,** *55*, 389.
72. Loidl-Stahlhofen, A.; Spiteller, G. *Biochimica et Biophysica Acta, Lipids and Lipid Metabolism* **1994,** *1211*, 156.
73. Carini, M.; Aldini, G.; Facino, R. M. *Mass Spectrometry Reviews* **2004,** *23*, 281.
74. Schneider, C.; Tallman, K. A.; Porter, N. A.; Brash, A. R. *Journal of Biological Chemistry* **2001,** *276*, 32392.
75. Esterbauer, H.; Schaur, R. J.; Zollner, H. *Free Radical Biology & Medicine* **1991,** *11*, 81.
76. Zarkovic, N. *Molecular Aspects of Medicine* **2003,** *24*, 281.
77. Petersen, D. R.; Doorn, J. A. *Free Radical Biology & Medicine* **2004,** *37*, 937.
78. Poli, G.; Schaur, R. J. *IUBMB Life* **2000,** *50*, 315.
79. Parola, M.; Bellomo, G.; Robino, G.; Barrera, G.; Dianzani, M. U. *Antioxidants & redox signaling* **1999,** *1*, 255.
80. Uchida, K. *Progress in Lipid Research* **2003,** *42*, 318.
81. Leonarduzzi, G.; Robbesyn, F.; Poli, G. *Free Radical Biology & Medicine* **2004,** *37*, 1694.
82. Kruman, I.; Bruce-Keller, A. J.; Bredesen, D.; Waeg, G.; Mattson, M. P. *Journal of Neuroscience* **1997,** *17*, 5089.

83. Liu, W.; Kato, M.; Akhand, A. A.; Hayakawa, A.; Suzuki, H.; Miyata, T.; Kurokawa, K.; Hotta, Y.; Ishikawa, N.; Nakashima, I. *Journal of Cell Science* **2000,** *113*, 635.
84. Brambilla, G.; Sciaba, L.; Faggin, P.; Maura, A.; Marinari, U. M.; Ferro, M.; Esterbauer, H. *Mutation Research, Genetic Toxicology Testing* **1986,** *171*, 169.
85. Eckl, P. M.; Ortner, A.; Esterbauer, H. *Mutation Research, Fundamental and Molecular Mechanisms of Mutagenesis* **1993,** *290*, 183.
86. Krokan, H.; Grafstrom, R. C.; Sundqvist, K.; Esterbauer, H.; Harris, C. C. *Carcinogenesis* **1985,** *6*, 1755.
87. McCall, M. R.; Tang, J. Y.; Bielicki, J. K.; Forte, T. M. *Arteriosclerosis, Thrombosis, and Vascular Biology* **1995,** *15*, 1599.
88. Nguyen, E.; Picklo, M. J. *Biochimica et Biophysica Acta, Molecular Basis of Disease* **2003,** *1637*, 107.
89. Carbone, D. L.; Doorn, J. A.; Kiebler, Z.; Petersen, D. R. *Chemical Research in Toxicology* **2005,** *18*, 1324.
90. Carbone, D. L.; Doorn, J. A.; Kiebler, Z.; Sampey, B. P.; Petersen, D. R. *Chemical Research in Toxicology* **2004,** *17*, 1459.
91. Carbone, D. L.; Doorn, J. A.; Kiebler, Z.; Ickes, B. R.; Petersen, D. R. *Journal of Pharmacology and Experimental Therapeutics* **2005,** *315*, 8.
92. Chen, J. J.; Bertrand, H.; Yu, B. P. *Free Radical Biology & Medicine* **1995,** *19*, 583.
93. Chen, J.; Robinson, N. C.; Schenker, S.; Frosto, T. A.; Henderson, G. I. *Hepatology (Philadelphia)* **1999,** *29*, 1792.
94. Chen, J.; Henderson, G. I.; Freeman, G. L. *Journal of Molecular and Cellular Cardiology* **2001,** *33*, 1919.
95. Michelet, F.; Gueguen, R.; Leroy, P.; Wellman, M.; Nicolas, A.; Siest, G. *Clinical Chemistry (Washington, D. C.)* **1995,** *41*, 1509.
96. Grace, J. M.; MacDonald, T. L.; Roberts, R. J.; Kinter, M. *Free Radical Research* **1996,** *25*, 23.
97. Siems, W.; Carluccio, F.; Grune, T.; Jakstadt, M.; Quast, S.; Hampl, H.; Sommerburg, O. *Clinical Nephrology* **2002,** *58*, S20.
98. Vander Jagt, D. L.; Hunsaker, L. A.; Vander Jagt, T. J.; Gomez, M. S.; Gonzales, D. M.; Deck, L. M.; Royer, R. E. *Biochemical Pharmacology* **1997,** *53*, 1133.
99. Kuo, C.-L.; Vaz, A. D. N.; Coon, M. J. *Journal of Biological Chemistry* **1997,** *272*, 22611.

100. Del Corso, A.; Dal Monte, M.; Vilardo, P. G.; Cecconi, I.; Moschini, R.; Banditelli, S.; Cappiello, M.; Tsai, L.; Mura, U. *Archives of Biochemistry and Biophysics* **1998,** *350*, 245.

101. Luckey, S. W.; Tjalkens, R. B.; Petersen, D. R. *Advances in Experimental Medicine and Biology* **1999,** *463*, 71.

102. Lauderback, C. M.; Hackett, J. M.; Huang, F. F.; Keller, J. N.; Szweda, L. I.; Markesbery, W. R.; Butterfield, D. A. *Journal of Neurochemistry* **2001,** *78*, 413.

103. Gardner, H. W.; Deighton, N. *Lipids* **2001,** *36*, 623.

104. Musatov, A.; Carroll, C. A.; Liu, Y.-C.; Henderson, G. I.; Weintraub, S. T.; Robinson, N. C. *Biochemistry* **2002,** *41*, 8212.

105. Patel, M. S.; Korotchkina, L. G. *Methods in Molecular Biology (Totowa, NJ, United States)* **2002,** *186*, 255.

106. Crabb, J. W.; O'Neil, J.; Miyagi, M.; West, K.; Hoff, H. F. *Protein Science* **2002,** *11*, 831.

107. Ishii, T.; Tatsuda, E.; Kumazawa, S.; Nakayama, T.; Uchida, K. *Biochemistry* **2003,** *42*, 3474.

108. Ferrington, D. A.; Kapphahn, R. J. *FEBS Letters* **2004,** *578*, 217.

109. Bardag-Gorce, F.; Li, J.; French, B. A.; French, S. W. *Experimental and Molecular Pathology* **2005,** *78*, 109.

110. Uchida, K.; Stadtman, E. R. *Proceedings of the National Academy of Sciences of the United States of America* **1992,** *89*, 4544.

111. Szweda, L. I.; Uchida, K.; Tsai, L.; Stadtman, E. R. *Journal of Biological Chemistry* **1993,** *268*, 3342.

112. Nadkarni, D. V.; Sayre, L. M. *Chemical Research in Toxicology* **1995,** *8*, 284.

113. Sayre, L. M.; Arora, P. K.; Iyer, R. S.; Salomon, R. G. *Chemical Research in Toxicology* **1993,** *6*, 19.

114. Cohn, J. A.; Tsai, L.; Friguet, B.; Szweda, L. I. *Archives of Biochemistry and Biophysics* **1996,** *328*, 158.

115. Anderson, M. M.; Hazen, S. L.; Hsu, F. F.; Heinecke, J. W. *Journal of Clinical Investigation* **1997,** *99*, 424.

116. Sakata, K.; Kashiwagi, K.; Sharmin, S.; Ueda, S.; Irie, Y.; Murotani, N.; Igarashi, K. *Biochemical and Biophysical Research Communications* **2003,** *305*, 143.

117. Sakata, K.; Kashiwagi, K.; Sharmin, S.; Ueda, S.; Igarashi, K. *Biochemical Society Transactions* **2003,** *31*, 371.

118. Uchida, K. *Trends in Cardiovascular Medicine* **1999,** *9*, 109.
119. Furuhata, A.; Nakamura, M.; Osawa, T.; Uchida, K. *Journal of Biological Chemistry* **2002,** *277*, 27919.
120. Cox, R.; Goorha, S.; Irving, C. C. *Carcinogenesis* **1988,** *9*, 463.
121. Ren, S.; Kalhorn, T. F.; Slattery, J. T. *Drug Metabolism and Disposition* **1999,** *27*, 133.
122. Southwell, J. L.; Yeargans, G. S.; Kowalewski, C.; Seidler, N. W. *Journal of Enzyme Inhibition and Medicinal Chemistry* **2002,** *17*, 19.
123. Pocernich Chava, B.; Butterfield, D. A. *Neurotoxicity research* **2003,** *5*, 515.
124. Kehrer, J. P.; Biswal, S. S. *Toxicological Sciences* **2000,** *57*, 6.
125. Tsakadze Nina, L.; Srivastava, S.; Awe Sunday, O.; Adeagbo Ayotunde, S. O.; Bhatnagar, A.; D'Souza Stanley, E. *American journal of physiology. Heart and circulatory physiology* **2003,** *285*, H727.
126. Beauchamp, R. O., Jr.; Andjelkovich, D. A.; Kligerman, A. D.; Morgan, K. T.; Heck, H. d. A. *Critical Reviews in Toxicology* **1985,** *14*, 309.
127. Rindgen, D.; Nakajima, M.; Wehrli, S.; Xu, K.; Blair, I. A. *Chemical Research in Toxicology* **1999,** *12*, 1195.
128. Lee, S. H.; Blair, I. A. *Chemical Research in Toxicology* **2000,** *13*, 698.
129. Lin, D.; Lee, H.-g.; Liu, Q.; Perry, G.; Smith, M. A.; Sayre, L. M. *Chemical Research in Toxicology* **2005,** *18*, 1219.
130. Doorn, J. A.; Petersen, D. R. *Chemico-Biological Interactions* **2003,** *143-144*, 93.
131. Zhang, W.-H.; Liu, J.; Xu, G.; Yuan, Q.; Sayre, L. M. *Chemical Research in Toxicology* **2003,** *16*, 512.
132. Slatter, D. A.; Avery, N. C.; Bailey, A. J. *Journal of Biological Chemistry* **2004,** *279*, 61.
133. Slatter, D. A.; Murray, M.; Bailey, A. J. *FEBS Letters* **1998,** *421*, 180.
134. Slatter, D. A.; Paul, R. G.; Murray, M.; Bailey, A. J. *Journal of Biological Chemistry* **1999,** *274*, 19661.
135. Fu, M.-X.; Requena, J. R.; Jenkins, A. J.; Lyons, T. J.; Baynes, J. W.; Thorpe, S. R. *Journal of Biological Chemistry* **1996,** *271*, 9982.
136. Odani, H.; Shinzato, T.; Usami, J.; Matsumoto, Y.; Brinkmann Frye, E.; Baynes, J. W.; Maeda, K. *FEBS Letters* **1998,** *427*, 381.
137. Shangari, N.; Bruce, W. R.; Poon, R.; O'Brien, P. J. *Biochemical Society Transactions* **2003,** *31*, 1390.

138. Shangari, N.; O'Brien, P. J. *Biochemical Pharmacology* **2004,** *68*, 1433.
139. Nguyen, A. T.; Donaldson, R. P. *Archives of Biochemistry and Biophysics* **2005,** *439*, 25.
140. Cabiscol, E.; Ros, J. *Redox Proteomics* **2006**, 399.
141. Levine, R. L.; Stadtman, E. R. *Redox Proteomics* **2006**, 123.
142. Berlett, B. S.; Stadtman, E. R. *Journal of Biological Chemistry* **1997,** *272*, 20313.
143. Stadtman, E. R.; Levine, R. L. *Amino Acids* **2003,** *25*, 207.
144. Baynes, J. W. *Diabetes* **1991,** *40*, 405.
145. Baynes, J. W.; Thorpe, S. R. *Diabetes* **1999,** *48*, 1.
146. Thorpe, S. R.; Baynes, J. W. *Amino Acids* **2003,** *25*, 275.
147. Ong, W. Y.; Lu, X. R.; Hu, C. Y.; Halliwell, B. *Free Radical Biology & Medicine* **2000,** *28*, 1214.
148. Uchida, K. *Free Radical Biology & Medicine* **2000,** *28*, 1685.
149. Rahbar, S.; Figarola, J. L. *Archives of Biochemistry and Biophysics* **2003,** *419*, 63.
150. Januszewski, A. S.; Alderson, N. L.; Metz, T. O.; Thorpe, S. R.; Baynes, J. W. *Biochemical Society Transactions* **2003,** *31*, 1413.
151. Baynes, J. W. *Clinical Chemistry and Laboratory Medicine* **2003,** *41*, 1159.
152. Baynes, J. W.; Thorpe, S. R. *Free Radical Biology & Medicine* **2000,** *28*, 1708.
153. Uchida, K.; Kanematsu, M.; Sakai, K.; Matsuda, T.; Hattori, N.; Mizuno, Y.; Suzuki, D.; Miyata, T.; Noguchi, N.; Niki, E.; Osawa, T. *Proceedings of the National Academy of Sciences of the United States of America* **1998,** *95*, 4882.
154. Berliner, J. A.; Heinecke, J. W. *Free Radical Biology & Medicine* **1996,** *20*, 707.
155. Slatter, D. A.; Bolton, C. H.; Bailey, A. J. *Diabetologia* **2000,** *43*, 550.
156. Stocker, R.; Keaney, J. F., Jr. *Physiological Reviews* **2004,** *84*, 1381.
157. Shao, B.; O'Brien, K. D.; McDonald, T. O.; Fu, X. Y.; Oram, J. F.; Uchida, K.; Heinecke, J. W. *Annals of the New York Academy of Sciences* **2005,** *1043*, 396.
158. Noiri, E.; Yamada, S.; Nakao, A.; Tsuchiya, M.; Masaki, I.; Fujino, K.; Nosaka, K.; Ozawa, T.; Fujita, T.; Uchida, K. *Free Radical Biology & Medicine* **2002,** *33*, 1651.
159. Calingasan, N. Y.; Uchida, K.; Gibson, G. E. *Journal of Neurochemistry* **1999,** *72*, 751.
160. Lucas, D. T.; Szweda, L. I. *Proceedings of the National Academy of Sciences of the United States of America* **1998,** *95*, 510.
161. Eaton, P.; Li, J.-M.; Hearse, D. J.; Shattock, M. J. *American Journal of Physiology* **1999,** *276*, H935.

162. Mak, S.; Lehotay, D. C.; Yazdanpanah, M.; Azevedo, E. R.; Liu, P. P.; Newton, G. E. *Journal of Cardiac Failure* **2000,** *6*, 108.
163. Miyata, T.; Kurokawa, K.; Van Ypersele De Strihou, C. *Journal of the American Society of Nephrology* **2000,** *11*, 1744.
164. Miyata, T.; Sugiyama, S.; Saito, A.; Kurokawa, K. *Kidney International, Supplement (1974-2011)* **2001,** *78*, S25.
165. Miyata, T.; Saito, A.; Kurokawa, K.; van Ypersele de Strihou, C. *Nephrology, Dialysis, Transplantation* **2001,** *16*, 8.
166. Suzuki, D.; Miyata, T. *Internal Medicine (Tokyo)* **1999,** *38*, 309.
167. Solin, M.-L.; Ahola, H.; Haltia, A.; Ursini, F.; Montine, T.; Roveri, A.; Kerjaschki, D.; Holthofer, H. *Kidney International* **2001,** *59*, 481.
168. Toyokuni, S.; Yamada, S.; Kashima, M.; Ihara, Y.; Yamada, Y.; Tanaka, T.; Hiai, H.; Seino, Y.; Uchida, K. *Antioxid. Redox Signaling* **2000,** *2*, 681.
169. Liu, Q.; Raina, A. K.; Smith, M. A.; Sayre, L. M.; Perry, G. *Molecular Aspects of Medicine* **2003,** *24*, 305.
170. Woltjer Randall, L.; Maezawa, I.; Ou Joyce, J.; Montine Kathleen, S.; Montine Thomas, J. *Journal of Alzheimer's disease : JAD* **2003,** *5*, 467.
171. Aslan, M.; Oezben, T. *Current Alzheimer Research* **2004,** *1*, 111.
172. Picklo, M. J., Sr.; Montine, T. J.; Amarnath, V.; Neely, M. D. *Toxicology and Applied Pharmacology* **2002,** *184*, 187.
173. Barnham, K. J.; Masters, C. L.; Bush, A. I. *Nature Reviews Drug Discovery* **2004,** *3*, 205.
174. McGrath, L. T.; McGleenon, B. M.; Brennan, S.; McColl, D.; Mc, I. S.; Passmore, A. P. *QJM : monthly journal of the Association of Physicians* **2001,** *94*, 485.
175. Lovell, M. A.; Xie, C.; Markesbery, W. R. *Neurobiology of Aging* **2001,** *22*, 187.
176. Dei, R.; Takeda, A.; Niwa, H.; Li, M.; Nakagomi, Y.; Watanabe, M.; Inagaki, T.; Washimi, Y.; Yasuda, Y.; Horie, K.; Miyata, T.; Sobue, G. *Acta Neuropathologica* **2002,** *104*, 113.
177. Selley, M. L. *Free Radical Biology & Medicine* **1998,** *25*, 169.
178. Simpson, E. P.; Henry, Y. K.; Henkel, J. S.; Smith, R. G.; Appel, S. H. *Neurology* **2004,** *62*, 1758.
179. Terman, A.; Brunk, U. T. *International Journal of Biochemistry & Cell Biology* **2004,** *36*, 1400.
180. Esterbauer, H.; Cheeseman, K. H. *Methods in Enzymology* **1990,** *186*, 407.

181. Strohmaier, H.; Hinghofer-Szalkay, H.; Schaur, R. J. *Journal of Lipid Mediators and Cell Signalling* **1995,** *11*, 51.

182. Spies-Martin, D.; Sommerburg, O.; Langhans, C.-D.; Leichsenring, M. *Journal of Chromatography, B: Analytical Technologies in the Biomedical and Life Sciences* **2002,** *774*, 231.

183. Uchida, K.; Osawa, T.; Hiai, H.; Toyokuni, S. *Biochemical and Biophysical Research Communications* **1995,** *212*, 1068.

184. Salomon, R. G.; Kaur, K.; Podrez, E.; Hoff, H. F.; Krushinsky, A. V.; Sayre, L. M. *Chemical Research in Toxicology* **2000,** *13*, 557.

185. Aldini, G.; Gamberoni, L.; Orioli, M.; Beretta, G.; Regazzoni, L.; Facino, R. M.; Carini, M. *Journal of Mass Spectrometry* **2006,** *41*, 1149.

186. Chevion, M.; Berenshtein, E.; Stadtman, E. R. *Free Radical Research* **2000,** *33*, S99.

187. Pupim, L. B.; Himmelfarb, J.; McMonagle, E.; Shyr, Y.; Ikizler, T. A. *Kidney International* **2004,** *65*, 2371.

188. Mera, K.; Anraku, M.; Kitamura, K.; Nakajou, K.; Maruyama, T.; Otagiri, M. *Biochemical and Biophysical Research Communications* **2005,** *334*, 1322.

189. Anraku, M.; Kitamura, K.; Shinohara, A.; Adachi, M.; Suenaga, A.; Maruyama, T.; Miyanaka, K.; Miyoshi, T.; Shiraishi, N.; Nonoguchi, H.; Otagiri, M.; Tomita, K. *Kidney International* **2004,** *66*, 841.

190. Aldini, G.; Vistoli, G.; Regazzoni, L.; Gamberoni, L.; Facino, R. M.; Yamaguchi, S.; Uchida, K.; Carini, M. *Chemical Research in Toxicology* **2008,** *21*, 824.

191. Aldini, G.; Orioli, M.; Carini, M. *Redox Report* **2007,** *12*, 20.

192. Brancatisano, R.; Isla, A.; Habib, N. *American journal of surgery* **1998,** *175*, 161.

193. Jaeschke, H. *Journal of hepatology* **1996,** *25*, 774.

194. Selzner, M.; Clavien, P. A. *Seminars in liver disease* **2001,** *21*, 105.

195. Serracino-Inglott, F.; Habib, N. A.; Mathie, R. T. *Am. J. Surg.* **2001,** *181*, 160.

196. Rosser, B. G.; Gores, G. J. *Gastroenterology* **1995,** *108*, 252.

197. Bronk, S. F.; Gores, G. J. *Hepatology (Philadelphia, PA, United States)* **1991,** *14*, 626.

198. Gasbarrini, A.; Borle, A. B.; Farghali, H.; Bender, C.; Francavilla, A.; Van Thiel, D. *Journal of Biological Chemistry* **1992,** *267*, 6654.

199. Carini, R.; Autelli, R.; Bellomo, G.; Albano, E. *Experimental Cell Research* **1999,** *248*, 280.

200. Jassem, W.; Fuggle, S. V.; Rela, M.; Koo, D. D. H.; Heaton, N. D. *Transplantation* **2002,** *73*, 493.

201. Lentsch, A. B.; Kato, A.; Yoshidome, H.; McMasters, K. M.; Edwards, M. J. *Hepatology (Baltimore, Md.)* **2000,** *32*, 169.

202. Takeuchi, D.; Yoshidome, H.; Kato, A.; Ito, H.; Kimura, F.; Shimizu, H.; Ohtsuka, M.; Morita, Y.; Miyazaki, M. *Hepatology (Hoboken, NJ, United States)* **2004,** *39*, 699.

203. Dalle-Donne, I.; Aldini, G.; Carini, M.; Colombo, R.; Rossi, R.; Milzani, A. *Journal of Cellular and Molecular Medicine* **2006,** *10*, 389.

204. Poli, G.; Schaur, R. J.; Siems, W. G.; Leonarduzzi, G. *Medicinal Research Reviews* **2008,** *28*, 569.

205. O'Brien, P.; Siraki, A.; Shangari, N. *Crit. Rev. Toxicol.* **2005,** *35*, 609.

206. Aldini, G.; Dalle-Donne, I.; Facino, R. M.; Milzani, A.; Carini, M. *Medicinal Research Reviews* **2007,** *27*, 817.

207. Pennathur, S.; Heinecke, J. W. *Antioxid. Redox Signaling* **2007,** *9*, 955.

208. LoPachin, R. M.; Barber, D. S.; Gavin, T. *Toxicological Sciences* **2008,** *104*, 235.

209. Aldini, G.; Dalle-Donne, I.; Colombo, R.; Facino, R. M.; Milzani, A.; Carini, M. *ChemMedChem* **2006,** *1*, 1045.

210. Negre-Salvayre, A.; Coatrieux, C.; Ingueneau, C.; Salvayre, R. *British Journal of Pharmacology* **2008,** *153*, 6.

211. Tallman, K. A.; Kim, H.-Y. H.; Ji, J.-X.; Szapacs, M. E.; Yin, H.; McIntosh, T. J.; Liebler, D. C.; Porter, N. A. *Chemical Research in Toxicology* **2007,** *20*, 227.

212. Perna, A. F.; Acanfora, F.; Luciano, M. G.; Pulzella, P.; Capasso, R.; Satta, E.; Cinzia, L.; Pollastro, R. M.; Iannelli, S.; Ingrosso, D.; De Santo, N. G. *Clinical Chemistry and Laboratory Medicine* **2007,** *45*, 1678.

213. Bar-Or, D.; Heyborne, K. D.; Bar-Or, R.; Rael, L. T.; Winkler, J. V.; Navot, D. *Prenatal Diagnosis* **2005,** *25*, 245.

214. Musante, L.; Candiano, G.; Petretto, A.; Bruschi, M.; Dimasi, N.; Caridi, G.; Pavone, B.; Del Boccio, P.; Galliano, M.; Urbani, A.; Scolari, F.; Vincenti, F.; Ghiggeri, G. M. *Journal of the American Society of Nephrology* **2007,** *18*, 799.

215. Musante, L.; Bruschi, M.; Candiano, G.; Petretto, A.; Dimasi, N.; Del Boccio, P.; Urbani, A.; Rialdi, G.; Ghiggeri, G. M. *Biochemical and Biophysical Research Communications* **2006,** *349*, 668.

216. Papac, D. I.; Shahrokh, Z. *Pharmaceutical Research* **2001,** *18*, 131.